

AN ANALYSIS OF FLOW INDUCED ACOUSTIC  
RESONANCE IN CAVITIES

---

A Dissertation  
Presented to  
the Faculty of the Graduate School  
University of Missouri

---

In Partial Fulfillment  
of the Requirements for the Degree  
Doctor of Philosophy

---

by  
George H. Watson

1970

---

Dr. John B. Miles - Dissertation Supervisor

## ACKNOWLEDGEMENTS

The author is indebted to his parents for their interest and support of his graduate education. Sincere appreciation is expressed to the author's advisor, Dr. John B. Miles, for his continued advice and involvement in this research effort. Special thanks is given to Mr. Charles Montesana for his many discussions with the author concerning acoustic theory. The financial support provided the author by the University of Missouri in the form of research and teaching assistantships, a NASA Dissertation Fellowship, and a grant from the Research Council for the purchase of equipment is sincerely appreciated.

TABLE OF CONTENTS

CHAPTER	PAGE
I. INTRODUCTION . . . . .	1
II. SURVEY OF RELATED LITERATURE . . . . .	5
2.1 Steady-State Flow in Cavities . . . . .	5
2.2 Detection and Influence of Acoustic Resonance on Cavity Flow . . . . .	8
2.3 Effect of the Approaching Boundary Layer on Acoustic Resonance . . . . .	16
III. DESCRIPTION AND SCOPE OF INVESTIGATION . . . . .	19
IV. DESCRIPTION OF EQUIPMENT AND INSTRUMENTS USED IN THE EXPERIMENTAL INVESTIGATION . . . . .	26
V. DISCUSSION OF EXPERIMENTAL RESULTS . . . . .	39
5.1 Orientation of Acoustic Pressure Wave Within Cavity . . . . .	39
5.2 Correlation of Resonant Frequencies . . . . .	51
5.3 Nature of the Approaching Boundary Layer . . . . .	54
5.4 Occurrence of Acoustic Resonance . . . . .	60
5.5 Shear Layer Oscillation . . . . .	73
5.6 Influence of Acoustic Resonance on Cavity Flow Field . . . . .	87
5.7 Effects of Perturbations in Internal and External Flow Fields on Acoustic Resonance . . . . .	93

CHAPTER	PAGE
5.8 Effect of Reducing the Width of the Mixing Region on the Acoustic Response of the Cavity . . . . .	104
VI. CONCERNING METHODS FOR PREDICTING AND CONTROLLING ACOUSTIC RESONANCE . . . . .	107
6.1 Analysis of White's Prediction Theory . . .	107
6.2 Significant Parameters for Improved Prediction Techniques . . . . .	113
6.3 Use of Approaching Boundary Layer to Control Acoustic Resonance . . . . .	118
VII. CONCLUSIONS AND RECOMMENDATIONS . . . . .	121
7.1 Conclusions . . . . .	121
7.2 Recommendations . . . . .	124
BIBLIOGRAPHY . . . . .	125
VITA . . . . .	128

## LIST OF FIGURES

FIGURE	PAGE
3-1. Cavity flow model . . . . .	20
3-2. Photographic record of a stable pressure signal .	22
3-3. Photographic record of a pressure signal with a sinusoidally varying amplitude . . . . .	22
3-4. Photographic record of a pressure signal with a randomly varying amplitude . . . . .	23
3-5. Photographic record of a pressure signal with a non-sinusoidal wave form . . . . .	23
4-1. Schematic of flow generating system, boundary layer removal apparatus, and cavity support structure used during experimental investigation . . . .	27
4-2. Nozzle and cavity used during experimental investigation . . . . .	28
4-3. Ducting and blower used for boundary layer removal . . . . .	30
4-4. Section from boundary layer removal plates (full scale) . . . . .	31
4-5. Schematic of locations of threaded mounting holes for the pressure transducers . . . . .	33
4-6. Columbia and Kistler transducers mounted on cavity wall . . . . .	34

FIGURE	PAGE
4-7. Actuator and track used for positioning the hot-wire anemometer probe . . . . .	34
4-8. System of instruments used to determine the orientation of acoustic pressure waves within the cavity: 1) Kistler charge amplifier, 2) Heathkit power supply, 3) Columbia transducer, 4) C-12 Polaroid camera attachment, 5) Kistler transducer . . . . .	35
4-9. Type 1912 third-octave recording analyzer and Old Gold Model, Type 2-H hot-wire anemometer used during spectral analysis of the velocity fluctuations in the shear layer and freestream flow field . . .	35
4-10. Photographic record of the pressure signals from the Kistler (top) and Columbia (bottom) transducers . . . . .	37
4-11. Sensing instruments used during experimental investigations: Kistler transducer, Columbia transducer, and hot-wire anemometer probe . . .	38
5-1. Photographic record of pressure signals as sensed at different positions on the cavity wall indicating a change in phase angle of the acoustic pressure wave . . . . .	40

FIGURE	PAGE
5-2. Polar plot of acoustic pressure wave within cavity (Helmholtz mode) . . . . .	43
5-3. Polar plot of acoustic pressure wave within cavity (half-wave mode) . . . . .	44
5-4. Polar plot of acoustic pressure wave within cavity (full-wave mode) . . . . .	45
5-5. Polar plot of acoustic pressure wave with nodes along the streamwise and vertical dimensions of the cavity . . . . .	46
5-6. Polar plot of acoustic pressure wave that stands along the vertical dimension of the cavity . .	47
5-7. Strouhal number as a function of freestream Mach number . . . . .	53
5-8. Velocity profiles of boundary layer for several freestream velocities (boundary condition #1, full removal) . . . . .	57
5-9. Data points for boundary layer thickness and corresponding curve-fits . . . . .	58
5-10. Data points for momentum thickness and corresponding curve-fits . . . . .	59
5-11. Range of freestream velocity and mixing length over which a representative resonant mode prevails (boundary layer condition #2, measured frequency - 833 cps) . . . . .	61

FIGURE	PAGE
5-12. Representation of the ranges of freestream velocity and mixing length which sustain resonance for boundary layer condition #1 (full removal) . . . . .	63
5-13. Representation of the ranges of freestream velocity and mixing length which sustain resonance for boundary layer condition #2 (partial removal) . . . . .	64
5-14. Representation of the ranges of freestream velocity and mixing length which sustain resonance for boundary layer condition #3 (no removal) . . . . .	65
5-15. Representation of the ranges of freestream velocity and mixing length which sustain resonance for boundary layer condition #4 (partial augmentation) . . . . .	66
5-16. Amplitude of acoustic pressure as a function of freestream velocity . . . . .	68
5-17. Shift of resonant peak with increasing boundary layer thickness . . . . .	70
5-18. Effect of approaching boundary layer thickness on acoustic intensity . . . . .	72
5-19. Frequency spectrum of the time-dependent, x-component of velocity in the shear layer . . . . .	75



FIGURE	PAGE
5-20. Time-mean velocity profile in shear layer . . . .	77
5-21. Hot-wire signal as monitored in shear layer. (Hot-wire signal-top; Kistler transducer signal bottom) . . . . .	79
5-22. Orientation of hot-wire within shear layer . . .	79
5-23. Uncorrected frequency spectrum of hot-wire anemometer signal . . . . .	81
5-24. Typical calibration curve for the hot-wire anemometer . . . . .	82
5-25. Comparison of velocity profiles along cavity centerline for resonant and non-resonant conditions . . . . .	88
5-26. Orientation of baffles within cavity . . . . .	94
5-27. Kistler transducer signal as monitored when the 4 inch baffle was mounted vertically within the cavity. (U = 121 fps; Mixing Length = 5.5") . . . . .	94
5-28. System used to generate a perturbed freestream .	101
5-29. Comparison of frequency spectrums of hot-wire anemometer signals for perturbed and quiescent freestreams . . . . .	102
6-1. Relative size and position of the characteristic mass with respect to the cavity volume . . . .	116

LIST OF TABLES

TABLE	PAGE
5-1. Summary of boundary layer control conditions. . .	55
5-2. Summary of acoustic energies dissipated at some peak resonant conditions. . . . .	71
5-3. Summary of data from which the shear layer deflection is calculated. . . . .	85
5-4. Effect of baffles on the Helmholtz mode of resonance (U = 121 fps, X = 6.9"). . . . .	97
5-5. Effect of baffles on the half-wave mode of resonance (U = 121 fps, X = 5.5"). . . . .	98
5-6. Effect of baffles on the full-wave mode of resonance (U = 132 fps, X = 1.1"). . . . .	99
5-7. Summary of data which indicates the effect of reducing the width of the mixing region on resonance. . . . .	105
6-1. Comparison of measured acoustic periods with White's characteristic pumping time for the cavity (boundary layer condition #1, full removal). . . . .	112

## LIST OF SYMBOLS

### English

A	area
c	acoustic velocity
$C_r$	Crocco number
D	diameter of cavity
$f_{imp}$	imposed frequency
$f_{meas}$	measured frequency
$g_c$	dimensional constant
H	vertical height of rectangular cavities
I	acoustic intensity
$I_{lj}$	mass flow integral
L	characteristic length
M	Mach number
$M_c$	mass of fluid within cavity
n	integer accounting for multiple waves standing in the cavity opening
N	integer accounting for the acoustic wavelength being a multiple of the cavity diameter
$P_o$	amplitude of acoustic pressure
$Re_\delta$	Reynolds number based on the thickness of the approaching boundary layer
$St_{imp}$	Strouhal number based on imposed frequency
$St_{meas}$	Strouhal number based on measured frequency of the acoustic wave
$t_a$	characteristic time for adjustment to a pressure wave
$t_c$	characteristic time for adjustment to fluid entrainment

T	acoustic period
u	x-component of velocity in boundary layer or shear layer
u'	x-component of spectral velocity
U	freestream velocity
$W_s$	pumping rate of shear layer
x	streamwise coordinate
X	mixing length (length of the cavity opening)
y	vertical coordinate

Greek

$\delta$	boundary layer thickness
$\theta$	momentum thickness
$\lambda$	wave length
$\rho$	fluid density
$\sigma$	single-stream mixing similarity parameter

## CHAPTER I

### INTRODUCTION

Interest in cavity flows originated within the aircraft industry when buffeting in open bomb bays and cockpits of military aircraft became a matter of concern with regard to the structural loading on the aircraft. There were fears that the occurrence of periodic pressure disturbances associated with the buffeting could oscillate at frequencies close to one of the natural frequencies of the aircraft and possibly lead to structural failure of some component. Investigations were subsequently carried out to determine the amplitude and frequencies of the pressure disturbances encountered in such configurations (1,2).

Cavity configurations may also occur in aerodynamic surfaces. An example of such cavities would be the discontinuity in the surface between an airfoil and its flap. The effect of such cavities on the drag of an aircraft is, quite naturally, of major interest. Also, the presence of a cavity in an aerodynamic surface can affect the location of boundary layer separation downstream from the cavity. Cavities in the surfaces of re-entry vehicles have generated interest in the heat transfer mechanisms between the cavity and the freestream. The determination of the influence of a cavity on drag or heat transfer necessitates a study of the flow field within the cavity. It is then possible to predict momentum transfer to the cavity, which provides a means for calculating drag, and to predict flow

velocities induced within the cavity, which allows for determining heat transfer coefficients along the cavity walls.

Mathematical models of cavity flow fields have been formulated which rather accurately predict velocities induced in circular cavities (3,4). To a lesser extent, models of flow fields within rectangular cavities have been suggested (5,6,7,8,9), but these models are necessarily more descriptive than analytical due to the complex nature of the flow fields induced in rectangular cavities. The validity of these models is determined in part by how accurately the mixing process between the freestream and the fluid within the cavity is simulated by the model. The mixing process may be treated with single stream mixing theory (10) or some other form of fluid entrainment modeling. Past investigations have shown that such models produce accurate results provided the flow fields are not subjected to periodic pressure disturbances which may be either self-induced or the result of some external source. However, experiment (3,11) has also shown that the heat transfer rates and drags predicted by such models become inaccurate when the cavity is subjected to periodic pressure fluctuations. These self-induced periodic pressure oscillations appear to be produced by the interaction between the freestream and the cavity. Under proper flow conditions, a sound field of distinct frequency can be heard and a periodic pressure oscillation can be detected within the cavity. Under such conditions the cavity may be said to be acoustically resonating, the acoustic resonance being sustained by energy from the freestream.

The conditions necessary to sustain acoustic resonance in

cavities have not yet been rigorously identified. Investigations (1,2,3,12) in the past have shown that resonance is a function of freestream velocity and cavity geometry. These two basic parameters have been used to express resonant frequencies in non-dimensional form as the Strouhal number ( $St = \frac{L}{U} f$ ), which provides a convenient method for correlating data. Two other parameters may be of significance in defining conditions conducive to resonance; these are the nature of the approaching boundary layer and the length of the region throughout which the mixing processes take place between the free-stream and the fluid within the cavity (the mixing region). An understanding of how these parameters, as well as freestream velocity and cavity geometry, affect the capacity of a cavity to resonate could lead to a method of predicting the flow conditions which must exist in order to achieve a given resonant state.

The research described herein attempts to quantitatively define the effect of the approaching boundary layer on the intensity and frequency of the resonant acoustic field induced in circular cavities. The thickness of the approaching boundary layer is controlled by means of a boundary layer removal unit. The boundary layer thickness and momentum thickness are determined and presented as functions of freestream velocity. The influence of the approaching boundary layer on resonance can then be described in terms of the boundary layer thickness and the momentum thickness. Provisions for observing the influence of mixing length on resonance are provided through the use of a sliding plate extending over the downstream edge of the cavity. The length of the mixing region can then be independently controlled and its influence on resonance identified. The influence

of flow disturbances in the freestream and in the internal cavity flow field on acoustic resonance are investigated. Spectral analyses of the frequencies at which velocity fluctuations occur in the shear layer are made in order to observe the influence of acoustic resonance on velocity distributions in the shear layer. The influence of the approaching boundary layer and mixing length on acoustic resonance is then discussed with regard to techniques for predicting resonance.



## CHAPTER II

### SURVEY OF RELATED LITERATURE

#### 2.1 Steady-State Flow in Cavities

A trend has been established in the past to identify, for individual study, separate regions of flow fields within and about cavities. In general, these regions may be classified as the freestream, the approaching boundary layer, the shear layer spanning the cavity opening and the cavity wake (the flow field induced within the cavity). The cavity wake is often further reduced into specific regions such as the boundary layer along the cavity wall, the vortical flow in the central region of the cavity, as well as the shear layer over the cavity (which is often included in studies of internal cavity flows). Freestream velocity and cavity geometry have been used as the primary parameters and their effects on the cavity flow field are interpreted from how these parameters affect individual regions of the flow. To a lesser extent, the nature of the approaching boundary layer has been used as a parameter.

Roshko (5) was among the first to recognize the vortex-like nature of the flow field within rectangular cavities and assessed that the equilibrium of the vortex flow system was dependent on cavity geometry and parameters of the external flow field such as freestream velocity and approaching boundary layer thickness.

Charwat et al. (6,7) also substantiated the existence of vortical flow in rectangular cavities, although his main effort was directed toward establishing the critical streamwise length of the cavity at which

the shear layer reattached to the cavity floor. Fox (8) studied flow fields in square notches (cavities) and detected the existence of a regular flow pattern within the cavity which he credited to a vortex flow that he described as "being more nearly square than nearly circular along its boundaries". Burggraf (9) recognized the recirculating nature of flow in rectangular cavities and attempted to formulate a mathematical model for the flow field in terms of a quasi-inviscid fluid at high Reynolds numbers.

The awareness of vortex flows being induced in cavity-type configurations led to the use of circular cavities in experimental investigations in order to preserve the vortical nature of the flow. This allowed study of a more continuous flow field which would be more amenable to mathematical analysis. Miles (3) performed one of the earlier investigations into the mechanisms of flow entrainment in and heat transfer from circular cavities with heated walls. The flow field was conveniently broken down into separate regions for isolated study; these regions being the freestream, the approaching boundary layer, the shear layer over the cavity, the boundary layer type flow along the cavity wall, and the vortical flow within the cavity. A heat transfer model was then formulated using regions and mechanisms which were identified as: 1) the thermal boundary layer along the cavity wall where heat was transferred from the heated wall to the fluid, 2) diffusion of the thermal boundary layer into the shear layer at the separation edge (the origin of the shear layer spanning the cavity opening), and 3) heat transfer across the shear layer due to a temperature gradient between the freestream and the cavity fluid. Velocity distributions in the

shear layer where determined through the use of the turbulent mixing theory developed by Korst (10). The diffusion of the thermal boundary layer into the shear layer was simulated as heat transfer from a line source placed at the origin of the shear layer.

Bales (4) conducted a study similar to that of Miles (3) but refined the heat transfer model by accounting for the effect of the velocity and temperature profiles of the freestream and cavity boundary layers approaching the separation edge. This allowed for a more realistic simulation of the diffusion of heat from the thermal boundary layer along the cavity wall into the shear layer than did the concept of diffusion of heat from a line source. A finite-difference numerical technique was used to solve the governing equations (continuity, momentum, energy) of the shear layer. The velocity and temperature profiles of the approaching boundary layer for the freestream and for the boundary layer along the cavity wall were used as initial conditions in the finite-difference scheme. As an incidental advantage, this mathematical model had the flexibility of being able to use the approaching boundary layer thickness as a parameter.

A mathematical model for heat transfer from rectangular cavities formulated by Charwat et al. (7) has as its basic premise the occurrence of a periodic mass pulse being fed into the cavity. This was assumed to be caused by the periodic oscillation of the shear layer about some mean position. The time-mean mass flow was considered to be zero. The momentum associated with this mass pulse was thought to be balanced by the centrifugal force of fluid rotating around a vortex at the recompression (downstream) corner of the cavity. This allowed the

distance that the shear layer deflected from its mean position to be calculated, which in turn provided for the calculation of the amount of mass fed into the cavity during one-half of the pulsation cycle. The heat convected away from the cavity could then be calculated provided that the mean bulk temperature of the fluid in the cavity as well as the freestream temperature were known.

## 2.2 Detection and Influence of Acoustic Resonance on Cavity Flow

The fact that the flow model in Charwat's (7) analysis is assumed to be subjected to a pulsating mass flow suggests that the phenomenon present was close to that of acoustic resonance. Indeed Charwat does mention that measurements of acoustic radiation were made in order to gauge the rotational speed of the vortex system. He evidently equated the time required for one revolution of the vortex to the period of the acoustic radiation in order to calculate the centrifugal force of fluid circulating around the vortex. His interpretation of mass exchange between the freestream and the cavity as being analogous to the cavity "breathing" at ultrasonic frequencies molded the formulation of a model for the flow mechanisms. This may well have been the first attempt to formulate a flow model for cavities that considered the presence of acoustic resonance.

The possibility of the occurrence of acoustic resonance in cavities has been suggested by some other investigators. Roshko (5) noted the presence of sound production in high-speed flows past cavities. He suggested that the production of these sound waves was associated with movements of the vortex system within the cavity, the frequency of the emitted sound being determined by some form of

coupling between the acoustic field and the vortex motion.

Fox (8) measured the surface pressure coefficient along the walls of rectangular cavities. He noticed that the cavity emitted a distinct sound at the highest freestream velocity ( $M = .5$ ) used during the investigation. During this sound emission, the pressure coefficient on the floor of the cavity rose above the values recorded at lower freestream velocities. Fox interpreted this as being due to a standing pressure wave that had the effect of raising the pressure on the bottom of the cavity.

Miles (3) also observed the emission of sound from cavities at a number of subsonic freestream velocities. He was able to control the length of the shear layer through varying the length of the cavity opening by means of a sliding flat plate over the rear edge of the cavity. By moving the sliding plate to different locations, he was able to "tune" the cavity to particular acoustic frequencies while holding the freestream velocity constant. This indicated that the length of the cavity opening was a significant parameter affecting the emission of sound from cavities, which Miles described as acoustic resonance.

Miles noted in his experimental work that the bulk temperature of the fluid within the cavity dropped significantly with the onset of acoustic resonance. This implied that acoustic resonance provided a significant mechanism for heat transfer. The theoretical predictions of the heat transfer rates as calculated from Miles' model were no longer accurate when resonant conditions prevailed, since the model did not account for the periodic pressure oscillations and their influence on

the cavity flow field. The nature of the effect of acoustic resonance on the heat transfer mechanisms was not understood and consequently no provision for it could be made in the mathematical model. Also, the nature of the freestream flow which would be conducive to flow induced acoustic resonance was not known; consequently, the onset of acoustic resonance could not be predicted on the basis of prescribed flow conditions.

McGregor (11) experimentally measured the drag of resonating cavities and found that drag was increased with the onset of acoustic resonance. He postulated that this increase in drag was due to an increase in momentum transfer between the cavity and the freestream caused by an oscillation of the shear layer. Fluid with relatively high velocity was injected into the cavity during one-half of the oscillation and was ejected from the cavity at relatively low velocity during the other half of the oscillation. The resulting change in momentum of the fluid was manifested as an increase in the drag force on the cavity.

It is evident from Miles' study that acoustic resonance ~~was~~ has a decided effect on the heat transfer mechanism between the cavity and the freestream. McGregor has shown that the drag of cavities is strongly influenced by resonance. To date, however, the cause of acoustic resonance is not fully understood. There have been some exploratory investigations into the nature of acoustic resonance and some general trends basic to the occurrence of resonance have been established, as outlined in the following paragraphs.

Krishnamurty (1,2) investigated the pressure field induced in

rectangular cavities by subsonic and supersonic flows and found that strong acoustic radiation could be emitted by cavities under certain flow conditions. He determined that the main parameters affecting the acoustic radiation were the shape of the recompression corner of the cavity, cavity length and depth, freestream velocity, local speed of sound, and approaching boundary layer thickness of the freestream. As an essential conclusion of his investigation, it was found that the most intense acoustic radiation occurred at frequencies which were inversely proportional to the length of the cavity opening.

Krishnamurty also concluded that the vertical position and shape of the downstream edge of the cavity were critical to the occurrence of sound emission from the cavity. He felt that flow visualization studies indicated that it was necessary for the shear layer to impinge and recompress on the downstream edge in order to generate sound waves. The basic mechanism of acoustic resonance was outlined by Krishnamurty as an oscillation of the shear layer resulting in periodic impingement of the shear layer on the downstream corner of the cavity creating a periodic pressure disturbance. The oscillation of the shear layer was thought to be caused by the inherent instability of the shear layer itself which made available a range of frequencies of pressure disturbances at the downstream corner of the cavity. Quoting Krishnamurty, "One may assume that there exists some kind of phase relation between the pressure fluctuation at the back edge and the motion of the shear layer, say at the front edge." Hence, a distinct frequency of oscillation is selected from the band of frequencies originally made available by the instability of the shear layer. Krishnamurty suggests that the coupling between the periodic pressure waves and the

oscillation of the shear layer is similar to the phenomenon of vortex shedding off bluff bodies.

Morse and Ingard (13) attribute cavity resonance to a feedback system similar to that described by Krishnamurty. Their interpretation of acoustic resonance in cavities may be outlined as follows. Vortices are assumed to be shed off the upstream edge of the cavity. When the time of travel of a vortex moving across the cavity opening equals the time required for an acoustic pressure wave to travel to and be reflected back from the surrounding walls of the cavity, strong acoustic resonance may be expected to occur. This concept of acoustic resonance implies that the resonant frequency is a continuous function of the velocity of the fluid passing over the cavity opening.

Chanaud's (14) description of acoustic resonance agrees with Morse's et al. concept insofar as there exists a feedback mechanism necessary to sustain resonance. However, his interpretation of the available resonant frequencies differed from that of Morse. According to Chanaud, any disturbance will cause vortices to be shed off the upstream edge of the cavity, due to the instability of the separated flow at that point. The actual frequency at which these vortices are shed is dependent on the frequency of the disruption. In the case of flow induced acoustic resonance in cavities, the disturbing force is an acoustic pressure wave reflected from the cavity walls to the cavity opening. The frequency of the cavity resonance is then controlled by the normal resonant modes of the cavity.

Rossiter (15) recorded instantaneous pressure measurements within and downstream from rectangular cavities at transonic Mach numbers.



Emission of sound waves was detected at certain combinations of free-stream velocity and cavity lengths. Rossiter attributed this resonance to the shedding of vortices off the leading edge of the cavity. The vortex shedding was thought to have been stimulated by a feedback mechanism similar to that described by Morse (13) and Chanaud (14). A theory was then presented to predict the frequencies of the emitted sound and it was based on previous work by Brown (16) which dealt with the phenomenon of edge-tones. Rossiter's theory is dependent on an experimentally determined constant of proportionality between the freestream velocity and the translational velocity of the vortices. Rossiter was satisfied with the agreement of this theory with his experimental results.

Spee (17) conducted an experimental investigation into the nature of the interaction of a shock-free transonic flow with sound waves generated by a resonating cavity. The cavity model used by Spee had an adjustable opening similar to that used by Miles (3) and the length of the cavity opening was used to adjust the resonant frequency. Spee used Rossiter's model for vortex shedding off the upstream edge of the cavity as an explanation for the occurrence of acoustic resonance. He also found that it was possible to rather accurately predict the shape of streamlines in the shear layer by making use of Nyborg's (18) work which dealt with formulating an equation of motion of a fluid particle placed in a jet that was subjected to self-maintained pressure oscillations. Some data regarding resonant frequencies as a function of Mach number are presented.

Torda and Patel (12) studied the flow field induced in cavities with a triangular planform by a steady flow passing over the cavity. The cavities were mounted such that the apex of the triangular cavity was directed in the upstream direction. They found that it was possible to induce acoustic resonance in these cavities. The frequency of the resonant acoustic field was conveniently correlated with a Strouhal number based on the streamwise height of the cavity and the freestream velocity.

Plumbee et al. (19) developed a theory for predicting resonant frequencies and pressure amplification of an acoustic pressure field induced in rectangular cavities by supersonic and subsonic flow fields. Using classical acoustic theory (13), he presented a method for calculating the acoustic response of cavities subjected to a freestream flow field. The cavities were assumed to respond in the traditional manner of a resonator; that is, with a pressure anti-node at the base of the cavity and a pressure node at the cavity opening, although no experimental data was presented to confirm this mode of resonance. Plumbee incorporated the turbulence (noise) of the approaching boundary layer as the forcing function in the acoustic formulation used to calculate the intensity of the resonant acoustic field. The frequencies of the measured turbulence in the boundary layer which correspond to the maximum intensity were found to agree favorably with the theoretically calculated resonant frequencies. Plumbee then concluded that acoustic resonance in cavities is due to the ability of the cavity to acoustically respond to the noise spectrum of the approaching boundary layer. In addition to the acoustic response, Plumbee noted a pressure

fluctuation of much lower frequency than the acoustic field, which he attributed to the inherent instability of the shear layer spanning the cavity opening.

White et al. (20) has presented a theory for predicting the freestream velocities at which resonance will occur based on the ability of the turbulent shear layer spanning the cavity opening to pump fluid into the cavity. White experimentally verified the existence of pressure waves moving along the cavity opening parallel to the direction of the freestream. According to White, the reattachment of the shear layer at the downstream edge of the cavity is modified as the pressure wave approaches and then recedes from the edge, causing an inflow and outflow of mass. Resonance is thought to occur when the period of the pressure wave (the time required for the wave moving at acoustic velocity to traverse twice the length of the cavity opening) matches a characteristic time for pumping fluid into the cavity. The characteristic time is defined as the mass flow rate into the cavity, caused by the turbulent mixing processes in the shear layer (19), divided into the mass of the fluid within the cavity. Other investigators (21,22) have considered the characteristic time as defined above to be characteristic of the time required to establish steady flow conditions in a region where initially stagnant fluid is put into motion by viscous mixing with constant velocity flow. As of this date, White has not verified his theory with experimental data.

### 2.3 Effect of the Approaching Boundary Layer on Acoustic Resonance

Many investigators have indicated that the thickness of the approaching boundary layer may be a significant parameter affecting acoustic resonance in cavities. Krishnamurty (1,2) was able to obtain data related to the effect of laminar and turbulent approaching boundary layers on acoustic resonance in cavities. He noted that the resonant frequency was reduced and the acoustic intensity was halved by the presence of a thick turbulent approaching boundary layer as compared to the resonant frequency and intensity occurring when the approaching boundary layer was laminar and probably much thinner. The thickness of the laminar boundary layer was calculated from an expression for the thickness of a developing boundary layer. No attempt was made to obtain thicknesses of the turbulent boundary layer. Krishnamurty suggested that an experimental program should be conducted to determine the effect of parameters such as  $L/\delta$  and  $Re_\delta$  on the resonant acoustic frequencies and intensities.

Charwat et al. (6) probably utilized the approaching boundary layer as a parameter more extensively than any other investigator. He studied the effects of the parameter  $\delta/H$  on the static pressure distribution within the cavity. The approaching boundary layer in these tests was turbulent and relatively thick.  $\delta$  was fixed by the freestream velocity so the parameter  $\delta/H$  was varied by controlling the depth of the cavity. Charwat noted that a thick boundary layer tended to damp out pressure gradients within the cavity. This result

can also be inferred from Rossiter's work (15), insofar as it was found that the acoustic resonance could be completely suppressed by affixing a small spoiler upstream of the cavity, effectively creating a thick boundary layer ahead of the cavity. Conversely, Rossiter found that a laminar approaching boundary layer would induce acoustic resonance in cavities.

The heat transfer model proposed by Charwat et al. (7) indirectly accounts for the effect of the approaching boundary layer because of the fact that the amount of fluid fed into the cavity during each pulse was considered to be proportional to the thickness of the shear layer at reattachment. Charwat thought it likely that the thickness of the shear layer would increase as the thickness of the approaching boundary layer increased. Consequently, this model predicts higher mass flow rates and, consequently, higher heat transfer rates between the cavity and the freestream as the approaching boundary layer becomes thicker.

Roshko (5) expected that the pressures induced in cavities due to freestream flows passing over them would depend on the state of the approaching boundary layer, although his investigation did not explore this possibility. Fox (8) also suggested that the approaching boundary layer might be an important factor in governing the nature of flow fields induced in cavity configurations. Spee (17) mentioned that the effect of the approaching boundary layer on the pressure field emitted by the cavity was an uncertain factor in interpreting the measured intensities of the acoustic field.

Plumbee (19) used the turbulence spectrum, or as he calls it the noise spectrum, of the approaching boundary layer as the driving force for acoustic resonance.

White's (20) prediction technique for resonance is indirectly dependent upon the nature of the approaching boundary layer, inasmuch as the mixing theory from which the pumping rate for the free shear layer is calculated assumes the approaching boundary layer thickness to be zero. Consequently, accurate results from White's prediction theory can reasonably be expected only for the case of very thin approaching boundary layers.

## CHAPTER III

### DESCRIPTION AND SCOPE OF INVESTIGATION

The cavity flow system depicted in Figure 3-1 may be described as follows. The freestream and its boundary layer approach the cavity opening along a flat plate. At the upstream edge of the cavity, the approaching boundary layer detaches from the plate. The upstream edge is therefore referred to as the separation edge. Fluid in the freestream and cavity wall boundary layer interact with one another at the separation edge forming a free shear layer resulting from a velocity difference between the two streams. The length of the shear layer is often referred to as the mixing length. The downstream edge of the cavity will be called the recompression edge. The flow field sustained in the cavity by the mixing processes in the free shear layer is referred to as the cavity wake.

In this work acoustic resonance is said to exist if there is present any periodic pressure disturbance which cannot be attributed to random flow perturbations. Thus, by definition, acoustic resonance is said to be present whenever a periodic pressure disturbance can be detected within the cavity regardless of the wave form or the stability of the amplitude of the pressure fluctuation. If the cavity is well "tuned", the acoustic pressure wave form is sinusoidal and has a stable (constant) amplitude (see Figure 3-2). However, analysis of the data from this investigation has shown that

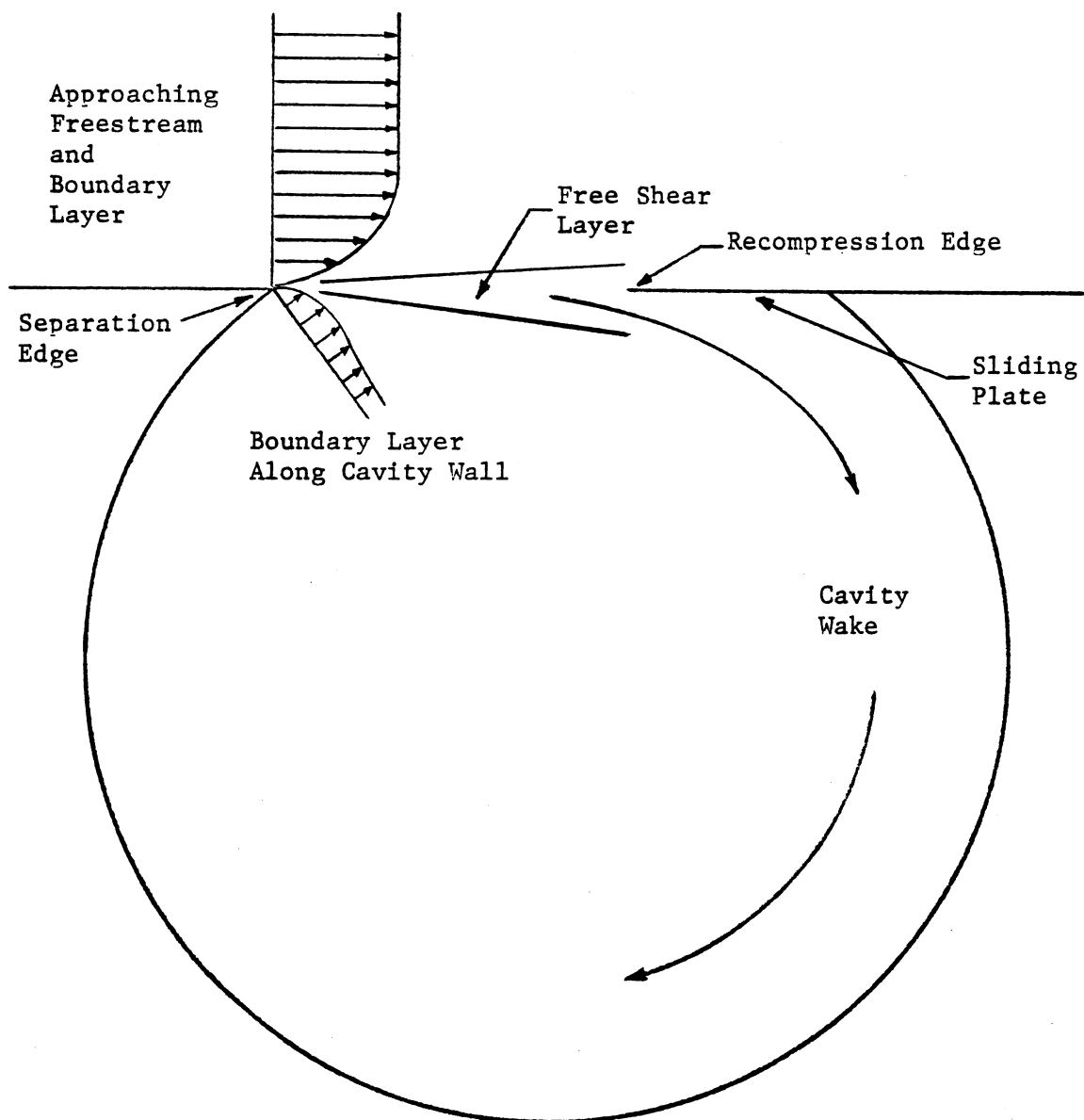


Figure 3-1. Cavity flow model.



there exist relatively broad ranges of velocity and mixing length that produce resonant pressure signals whose amplitudes may vary in a sinusoidal or in a random manner. A relatively long sweep time was used when the photographic record of the Kistler transducer signal shown in Figure 3-3 was taken and as a result a large number of acoustic periods are shown. It is evident that the amplitude of the pressure signal in Figure 3-4 varies randomly. Pressure signals have also been recorded whose wave forms are not sinusoidal, but none the less are periodic (see Figure 3-5). All of these described pressure disturbances are considered to be the result of acoustic resonance.

As mentioned in Chapter II, investigators have attempted to identify the effect of the approaching boundary layer thickness on acoustic resonance in cavities. These investigations have been handicapped by the fact that the nature of the boundary layer was controlled by the freestream velocity and the degree to which the boundary layer was allowed to develop while advancing toward the cavity opening. Only Rossiter (15) attempted to arbitrarily control the state of the boundary layer by placing a spoiler in the boundary layer upstream of the cavity, and Rossiter apparently did not extensively use this technique of boundary layer control. Thus, the effect of boundary layer thickness on acoustic resonance could only be interpreted as a side effect of other more controlled parameters such as freestream velocity. No previous attempts have been made at isolating the approaching boundary layer thickness as a free parameter.

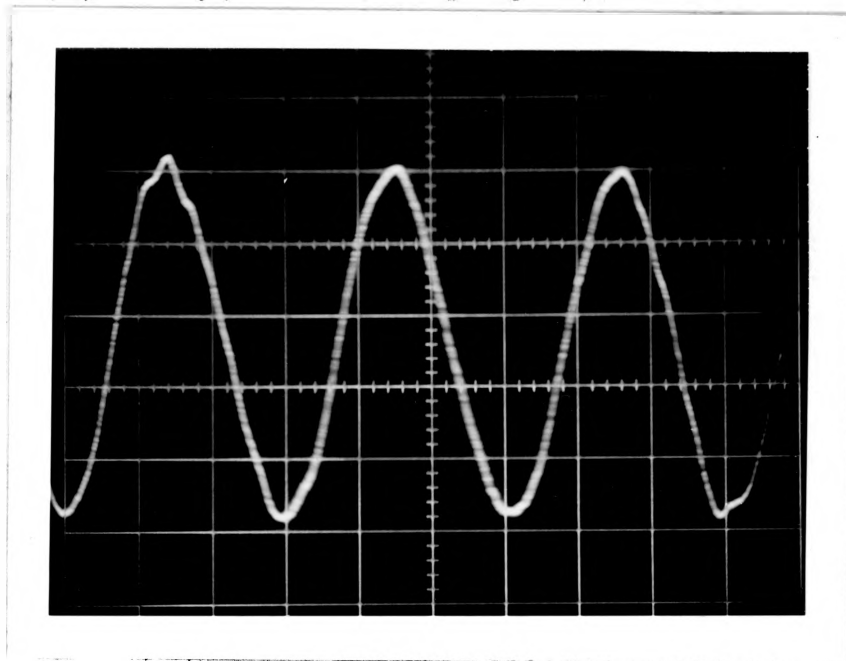


Figure 3-2. Photographic record of a stable pressure signal.

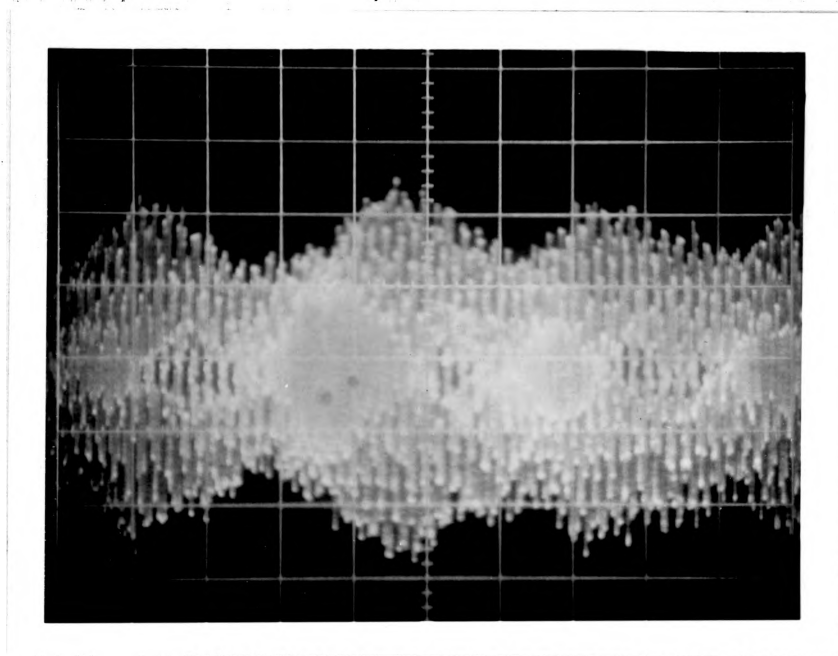


Figure 3-3. Photographic record of a pressure signal with a sinusoidally varying amplitude.

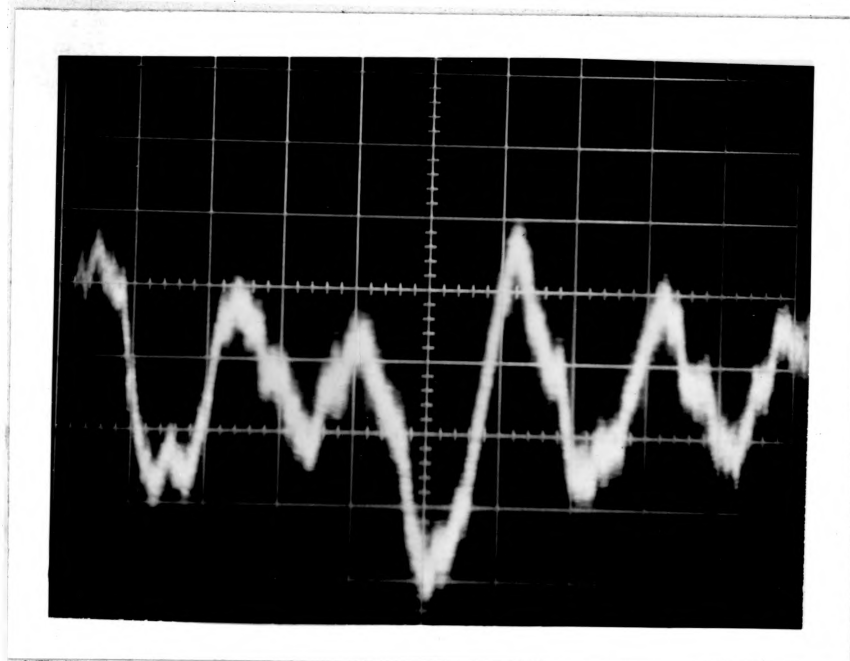


Figure 3-4. Photographic record of a pressure signal with a randomly varying amplitude.

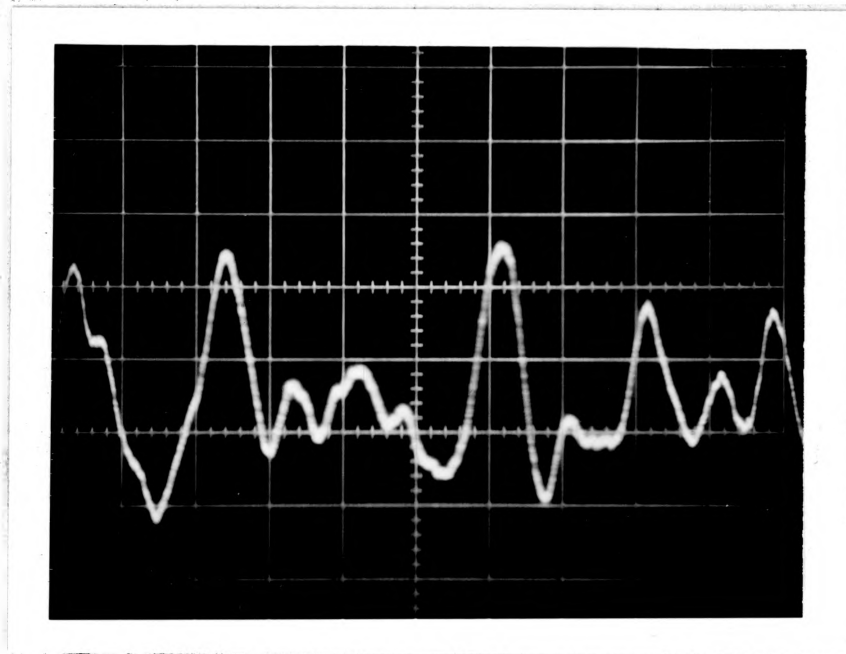


Figure 3-5. Photographic record of a pressure signal with a non-sinusoidal waveform.

A salient feature of the present investigation is the capability to control the thickness of the approaching boundary layer independently of the freestream velocity. This capability is provided by means of a boundary layer removal unit placed in the flow channel slightly upstream of the cavity. The boundary layer can therefore be varied as a free parameter and its effect on acoustic resonance can be studied more rigorously.

Most of the previous investigations that studied the effect of cavity length on acoustic resonance dealt with rectangular cavities in which the length was varied in finite steps. No effort was made to continuously vary the cavity length during these tests. Therefore, it is not certain that data taken in previous investigations were taken at the cavity length required to provide maximum acoustic resonance at a given freestream flow condition. The cavity used in this investigation is equipped with a movable plate which may be used to continuously vary the length of the cavity opening, thereby controlling the length of the mixing region. This made it possible to investigate the ranges of freestream velocity and mixing length over which acoustic resonance might occur.

As a further refinement in studying the acoustic field, in this investigation acoustic intensity was recorded as a continuous function of freestream velocity. The mixing length and boundary layer thickness were used as parameters. Also, the dependence of acoustic resonance on the continuity of the cavity flow field was investigated by disturbing the cavity flow field with baffles. The influence of random perturbations in the freestream flow field on the

intensity and occurrence of acoustic resonance was investigated by disturbing the freestream with a flap, hinged on one side, which was allowed to oscillate due to interaction with the freestream.

Investigations prior to this time have made measurements of the periodic pressures induced in cavities; however, most of these measurements have been made external to the cavity. Provisions were made in this investigation to determine the presence and distribution of periodic pressure disturbances over the volume of the cavity. Analysis of this data points out any dependence of the wavelength of the acoustic field on the dimensions of the cavity.

In addition to studying the nature of acoustic resonance and the parameters that affect it, White's theory for predicting resonance is analyzed and modifications to the theory are proposed. The definition of the characteristic pumping time (21,22) used by White is modified to make it more applicable to and descriptive of acoustic resonance.

## CHAPTER IV

### DESCRIPTION OF EQUIPMENT AND INSTRUMENTS USED IN THE EXPERIMENTAL INVESTIGATION

The freestream flow field was generated by a Sturtevant series 400 centrifugal fan driven by a 75 hp electric motor. The fan was rated at 16,000 CFM and 18 inches of water. The air was discharged from the fan through a diffuser and into a 4' x 4' x 8' settling chamber. Mounted within the settling chamber was a 1.4 inch thick layer of aluminum honeycomb with .25 inch hexagonal mesh and a set of circular turning vanes mounted along the full height of the settling chamber which turned the flow through an angle of 90°. Air discharged from the settling chamber immediately into the nozzle entrance. A set of 20 mesh screens, furnace filters, and a second layer of honeycomb were mounted at the interface between the settling chamber and the nozzle. The nozzle reduced the flow area by a factor of 4 forming a 1' by 1' flow channel. The velocity profile at the nozzle exit was uniform with the exception of the boundary layers along the four walls. A schematic and photograph of the flow generating system appear in Figures 4-1 and 4-2, respectively.

The boundary layer removal unit consisted of a series of perforated plates placed in the floor of the nozzle. The boundary layer above the perforated plates was removed by creating a partial vacuum under the plates. This was accomplished in the following manner.

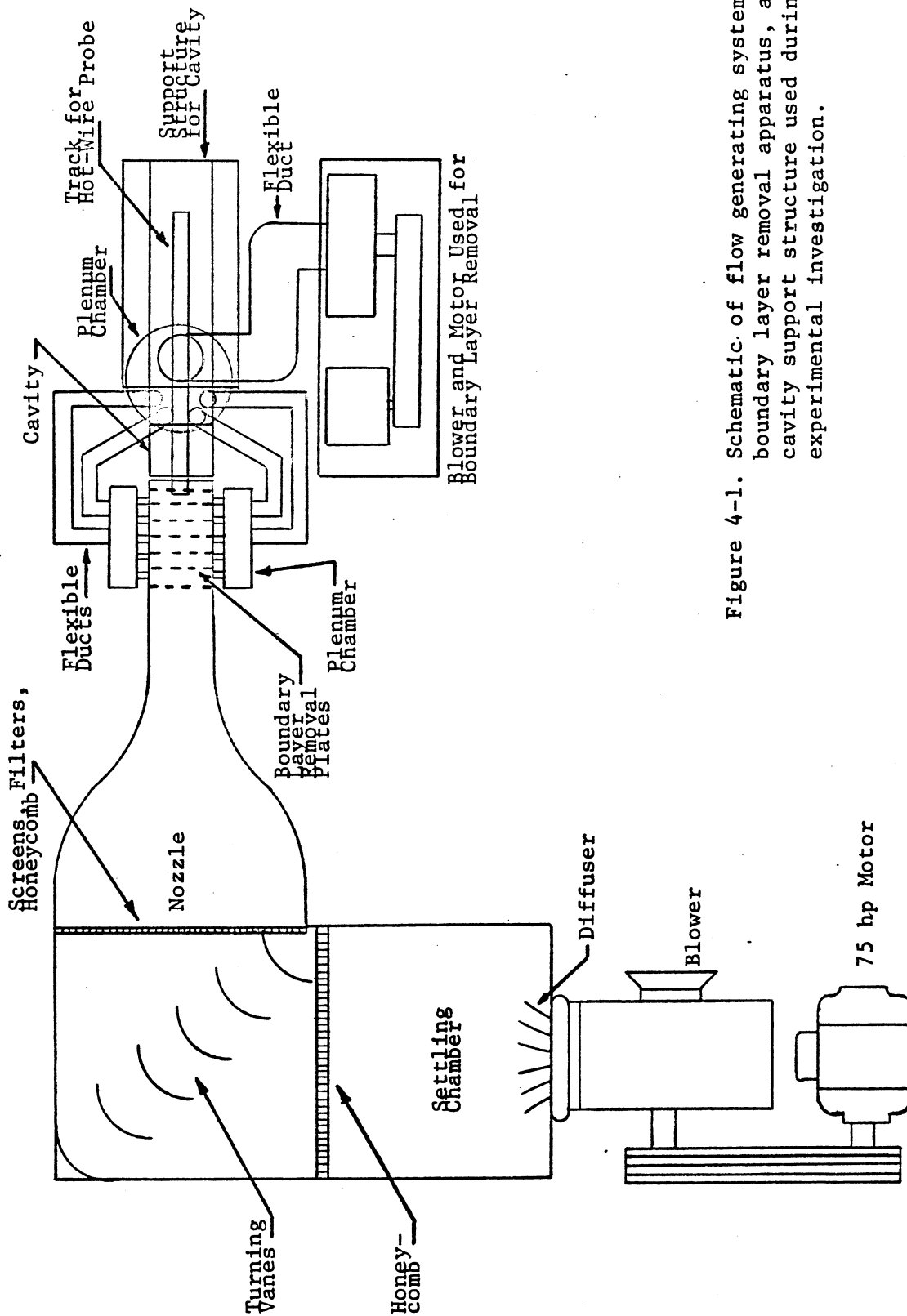


Figure 4-1. Schematic of flow generating system, boundary layer removal apparatus, and cavity support structure used during experimental investigation.

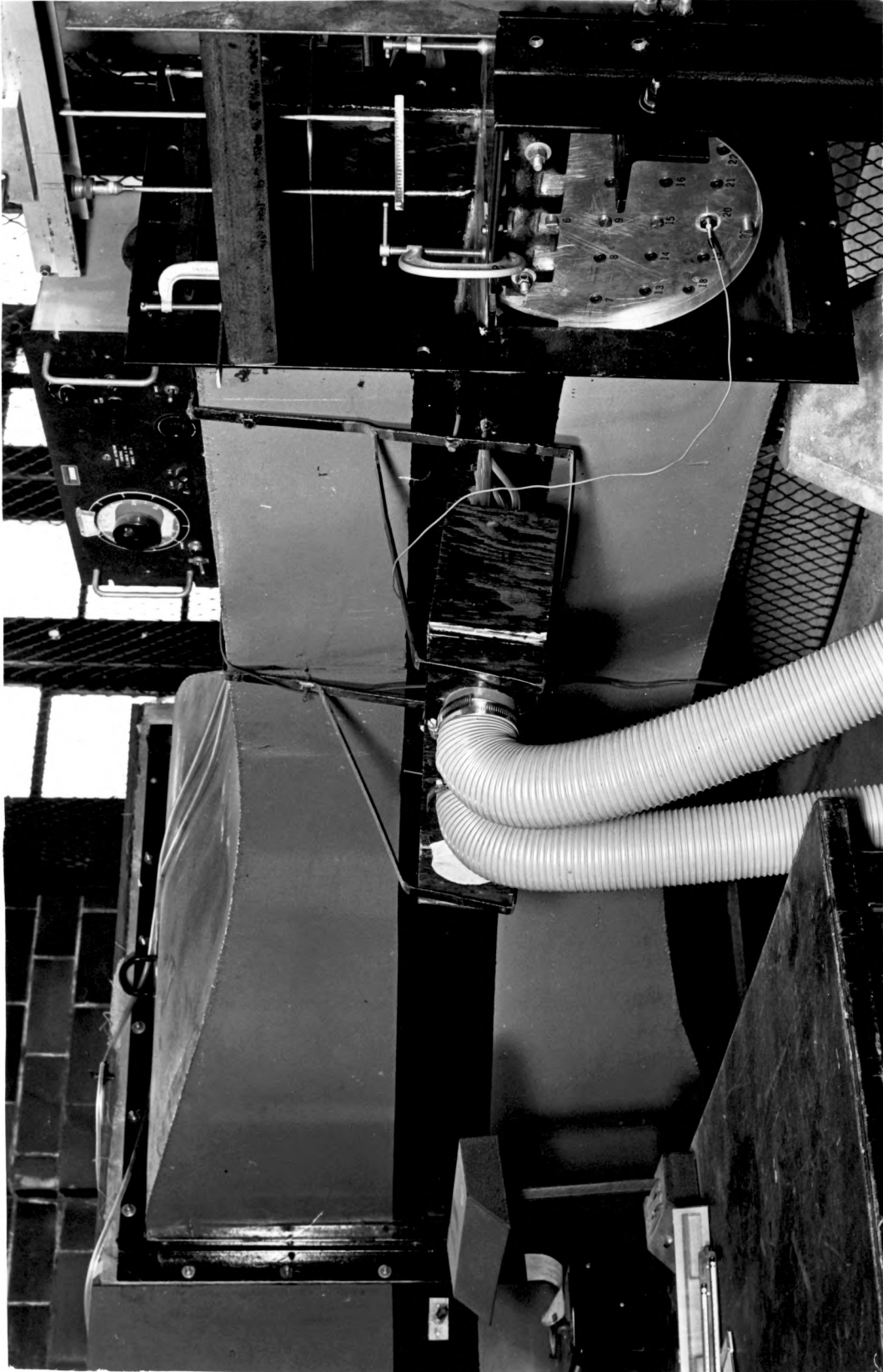


Figure 4-2. Nozzle and cavity used during experimental investigations.



The inlet to a small centrifugal blower was connected to plenum chambers on either side of the nozzle by means of flexible rubber hoses, 3" in diameter (see Figure 4-3). Aluminum tubing was directed from the plenum chambers into the space under the perforated plates. The depths to which the aluminum tubes protruded under the plates were staggered in order to develop a more uniform pressure gradient across the plates, thereby enhancing uniform boundary layer removal. A schematic of the boundary layer removal plates is shown in Figure 4-4.

The degree to which the boundary layer was removed could be controlled by adjusting the opening of a by-pass flow area and allowing ambient air to be drawn into the blower inlet. This reduced the partial vacuum at the inlet of the blower and subsequently reduced the pressure gradient across the perforated plates through which the boundary layer was removed. It was also possible to "augment" the boundary layer by blowing ambient air into the boundary layer. This was accomplished by simply connecting the outlet of the blower to the plenum chambers.

The cavity was mounted at the exit plane of the nozzle. The type of cavity used has been described in current literature (4) as a nearly circular cavity. It is a circular cylinder with a 12 inch diameter and a 9 inch dimension normal to the freestream. The maximum length of the mixing region, or cavity opening, is 8.75 inches. The sliding plate used to control the length of the cavity opening was fabricated from 1/16 inch stainless steel sheeting. The recompression edge of the dividing plate was machined to a 4

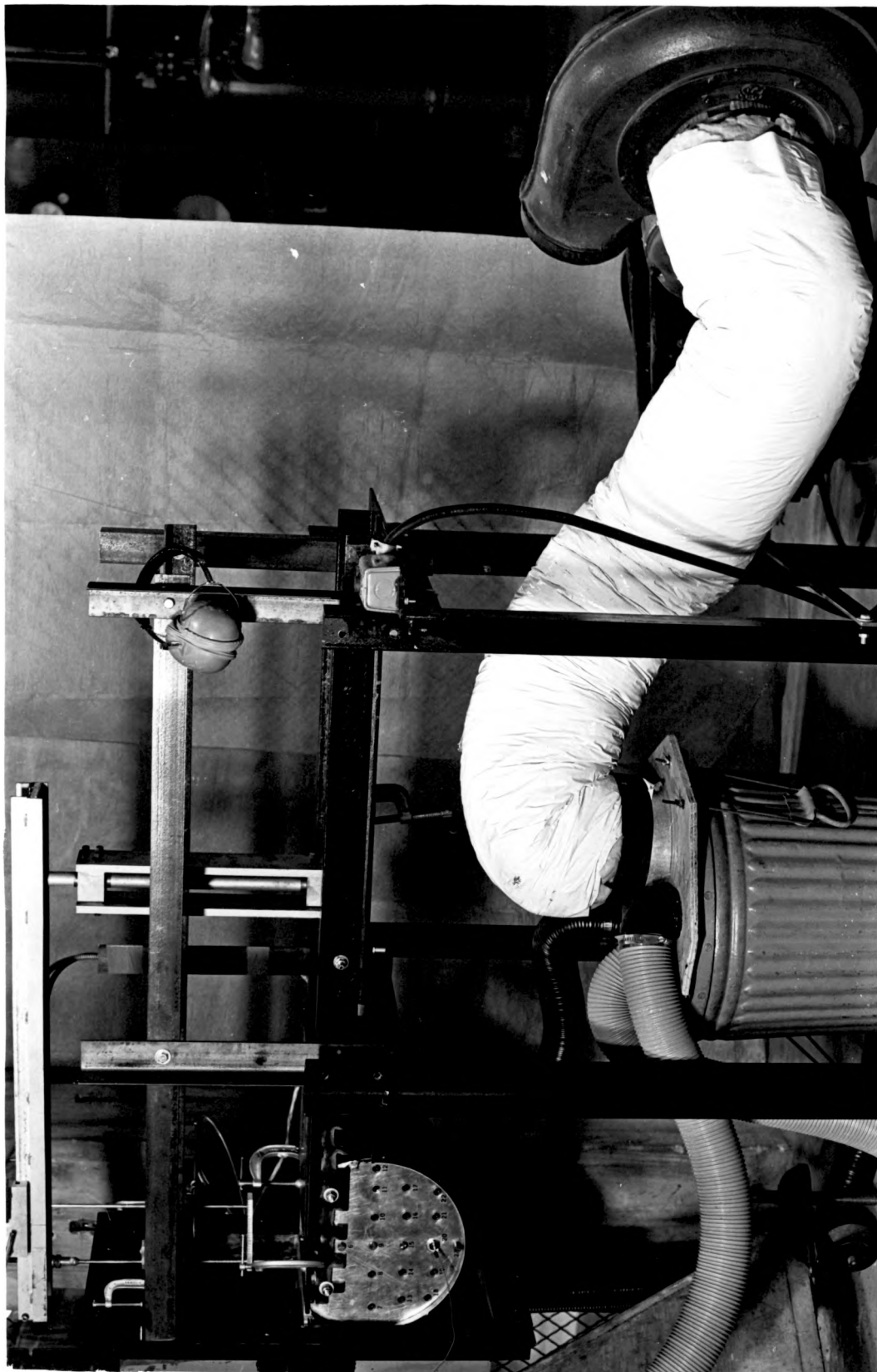


Figure 4-3. Ducting and blower used for boundary layer removal.

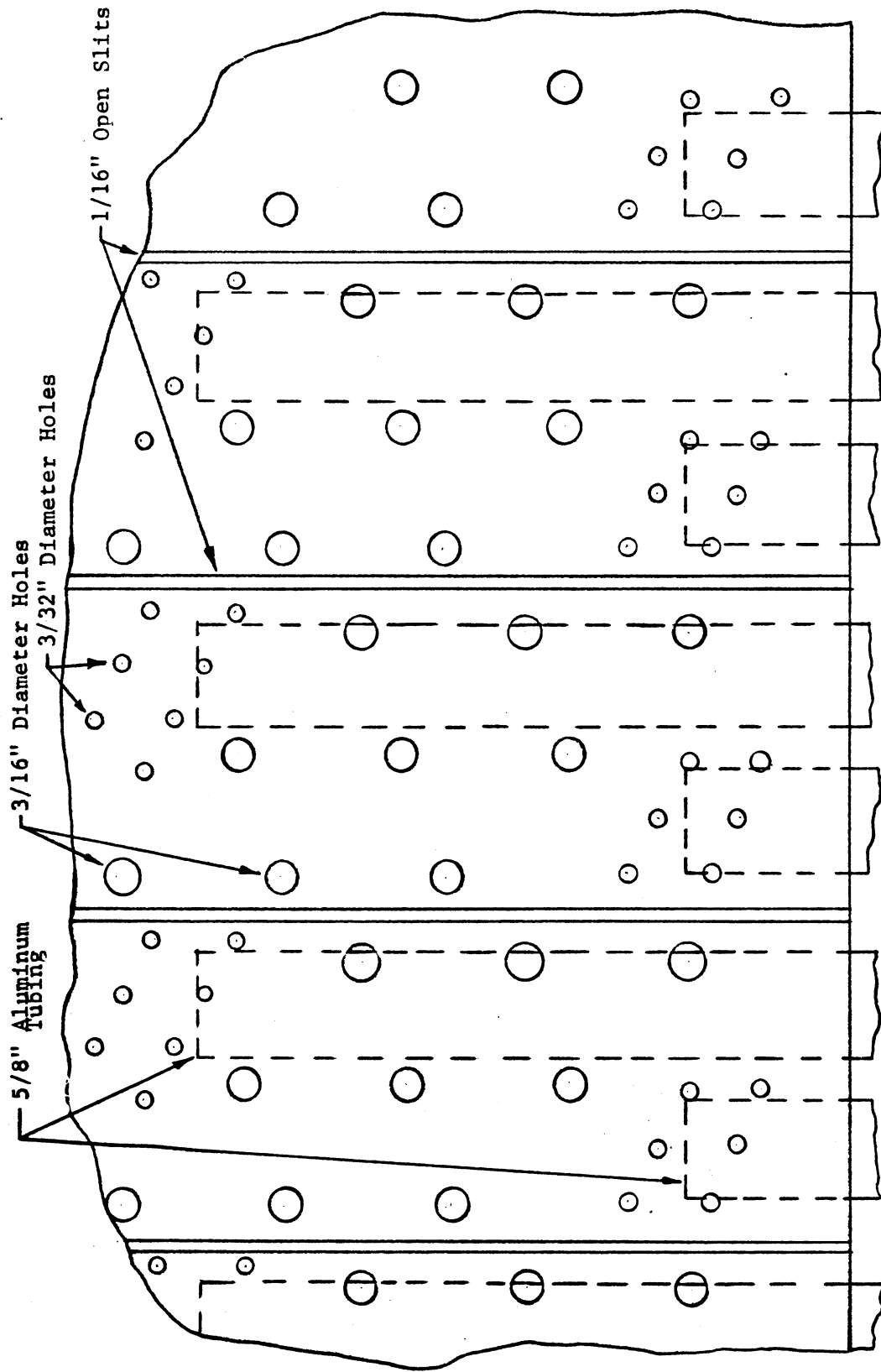


Figure 4-4. Section from boundary layer removal plates (full scale).

to 1 slope in order to reduce the plate's interference with the flow field. Twenty-three threaded mounting holes for a pressure transducer were machined through the wall of the cavity. A schematic drawing showing the locations of the transducer mounting holes is shown in Figure 4-5. Photographs of the cavity system are shown in Figures 4-6 and 4-7.

A track was mounted over the cavity for the purpose of supporting a L. C. Smith & Company Type BBM Actuator used to position a hot-wire anemometer probe. The anemometer was used to measure velocity profiles of the approaching boundary layer and velocity profiles within the cavity. The track allowed the actuator and the hot-wire probe to be positioned at any point downstream from the nozzle exit plane. The actuator was used to position the probe along the vertical axis (see Figure 4-7). An Old Gold Model, Type 2-H Hot-Wire Anemometer was used to make the velocity measurements. This is a constant temperature anemometer with a digital read-out. Tungsten wire, .00015 inch diameter, was used as the sensing element in the hot-wire probes.

During one phase of the experimental investigation, the signal from the hot-wire anemometer was fed into a spectrum analyzer in order to check the frequencies at which turbulent energy was being dissipated. The wave analyzer used was a General Radio Type 1912 Third-Octave Recording Analyzer (see Figure 4-9).

The pressure transducer used to make measurements of the acoustic pressure field within the cavity was a Kistler Quartz Microphone, Model 717. The transducer consists of a piezoelectric sensing ele-

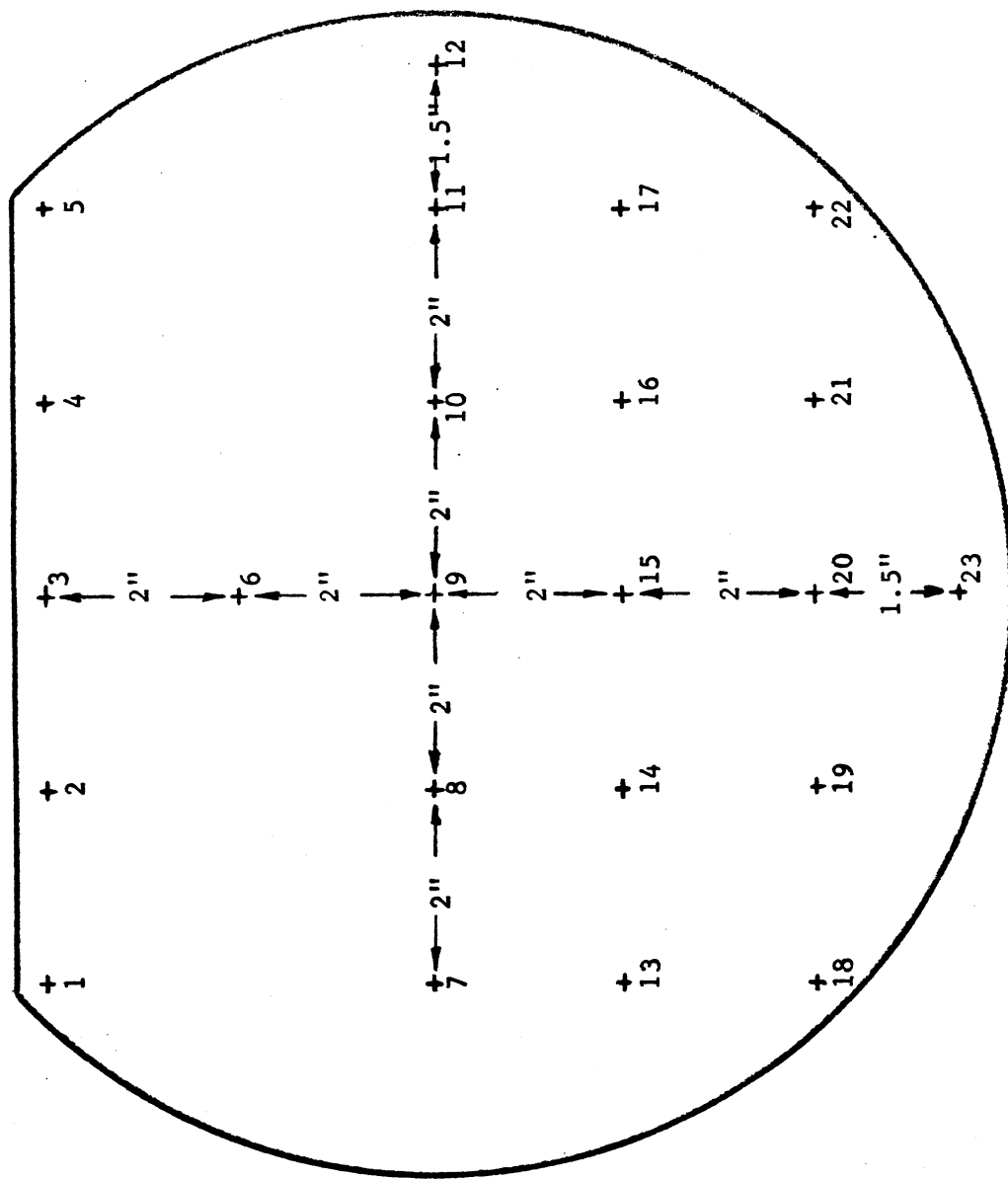


Figure 4-5. Schematic of locations of treaded mounting holes for the pressure transducers.

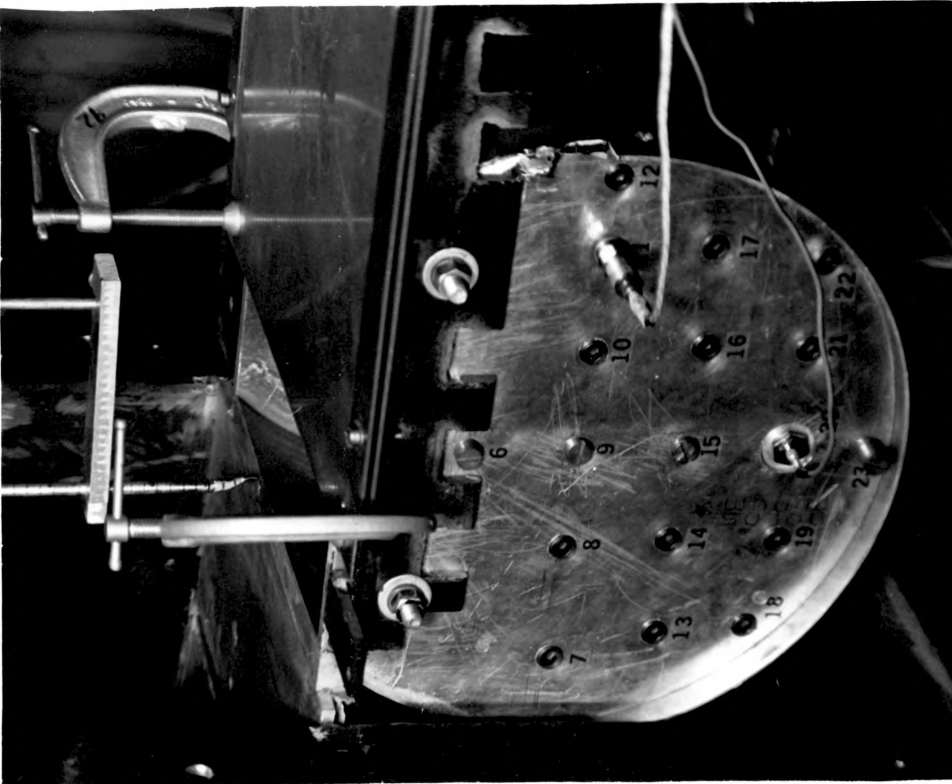


Figure 4-6. Columbia and Kistler transducers mounted on cavity wall.

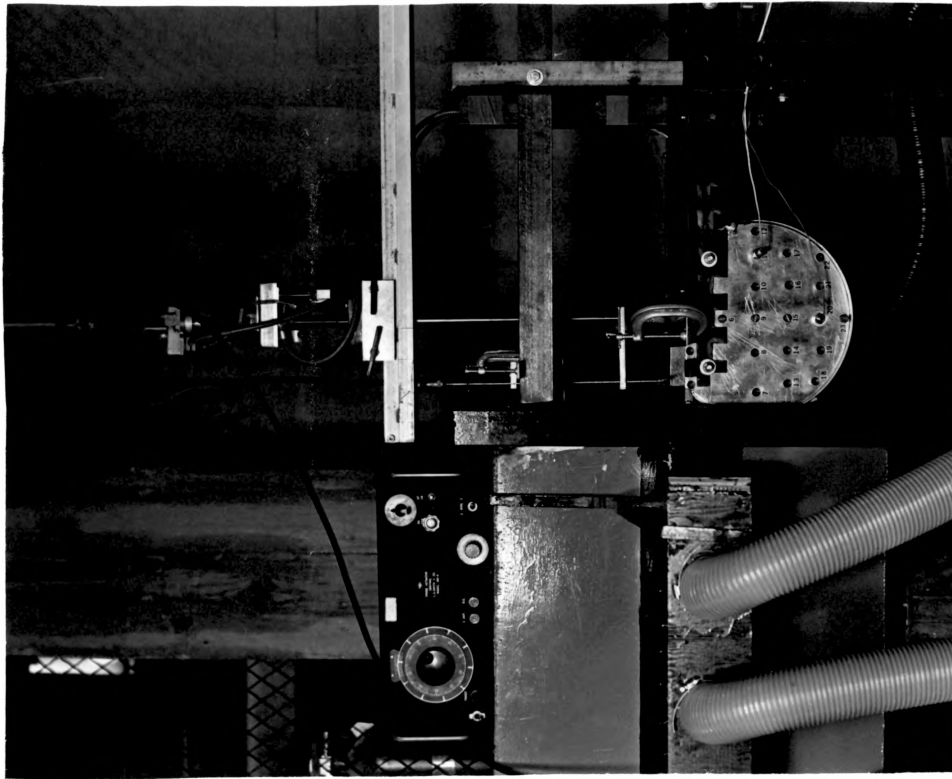


Figure 4-7. Actuator and track used for positioning the hot-wire anemometer probe.

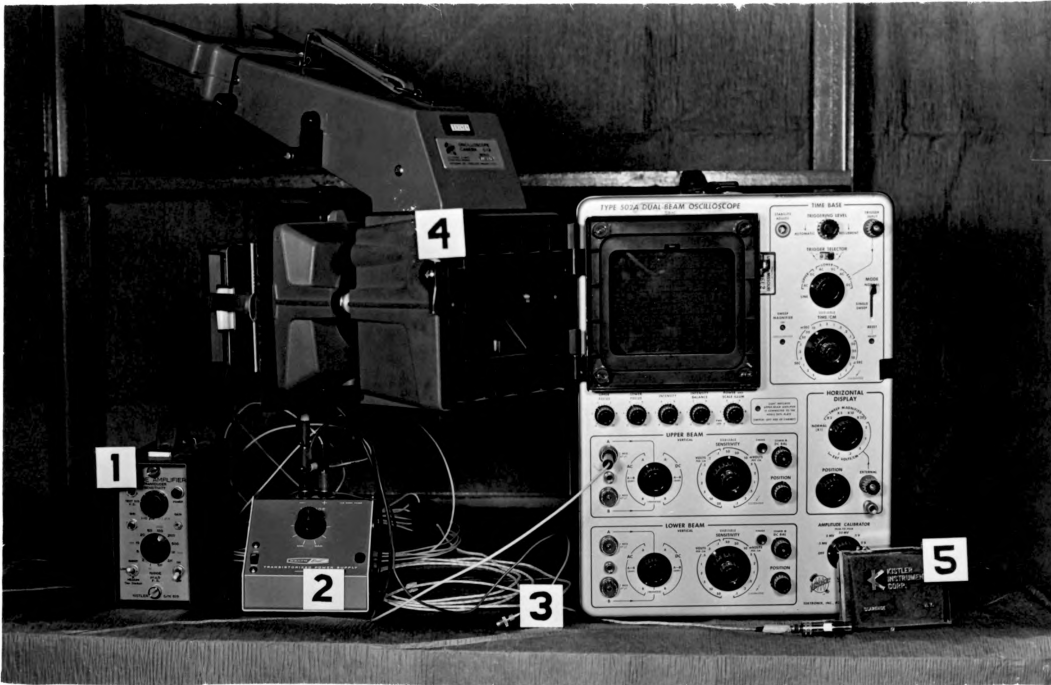


Figure 4-8. System of instruments used to determine the orientation of acoustic pressure waves within the cavity: 1) Kistler charge amplifier, 2) Heathkit power supply, 3) Columbia transducer, 4) C-12 Polaroid camera attachment, 5) Kistler transducer.

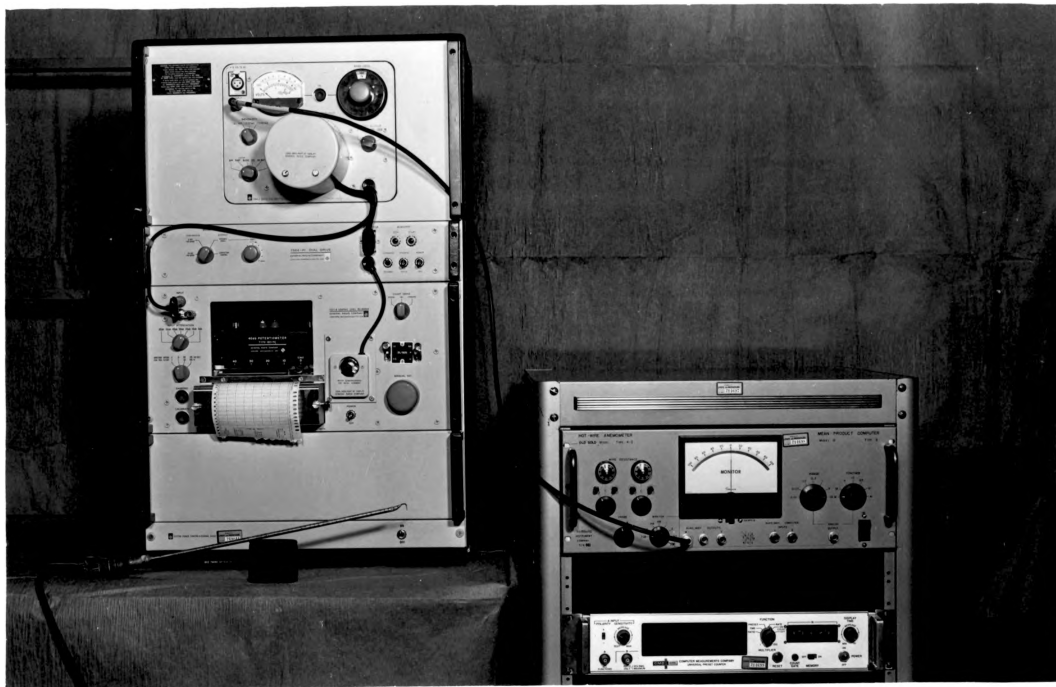


Figure 4-9. Type 1912 Third-Octave Recording Analyzer and Old Gold Model, Type 2-H Hot-Wire Anemometer used during spectral analysis of the velocity fluctuations in the shear layer and freestream flow fields.

ment, the signal of which is immediately amplified by a miniaturized charge amplifier contained within the casing of the microphone itself. Thus, an amplified, low impedance output is provided which connects directly to a recording device. The transducer was sensitive to a time varying signal with an amplitude as low as .00092 psi, rms.

The Kistler transducer was used in conjunction with a Columbia Research Laboratories transducer in order to determine the phase of the acoustic pressure wave throughout the cavity. The signal from the Columbia Transducer was amplified by a Kistler Model 503 Charge Amplifier. However, the capacitance of the Columbia transducer was not within the range for which the Kistler amplifier could provide a calibrated signal. Consequently, the Columbia transducer could not provide reliable data on the amplitude of the acoustic pressure. This was of no concern, however, since the Columbia transducer was used only as a reference to compare the phase shifts of the pressure wave at various locations within the cavity.

The signals from the Kistler and Columbia transducers were monitored simultaneously on a Tektronic 502A dual-beam oscilloscope. The signals could be photographically recorded with the aid of a C-12 Polaroid camera oscilloscope attachment. A representative photograph of the measured pressure signals is shown in Figure 4-10. A photograph of the entire system of instruments used in making measurements to determine the orientation of acoustic pressure waves within the cavity is shown in Figure 4-8.



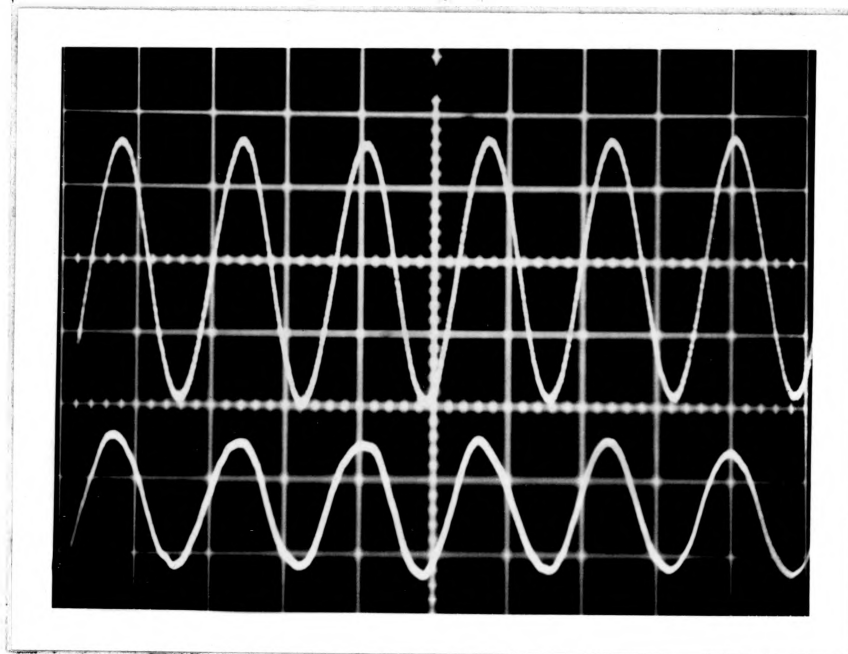


Figure 4-10. Photographic record of the pressure signals from the Kistler (top) and Columbia (bottom) transducers.

The velocity of the freestream was measured by a pitot-static tube used in conjunction with a Meriam model 34FB2 TM Micromanometer.

A composite photograph of the sensing instruments used in this investigation (the Kistler and Columbia transducers and the hot-wire probe) is shown in Figure 4-11.

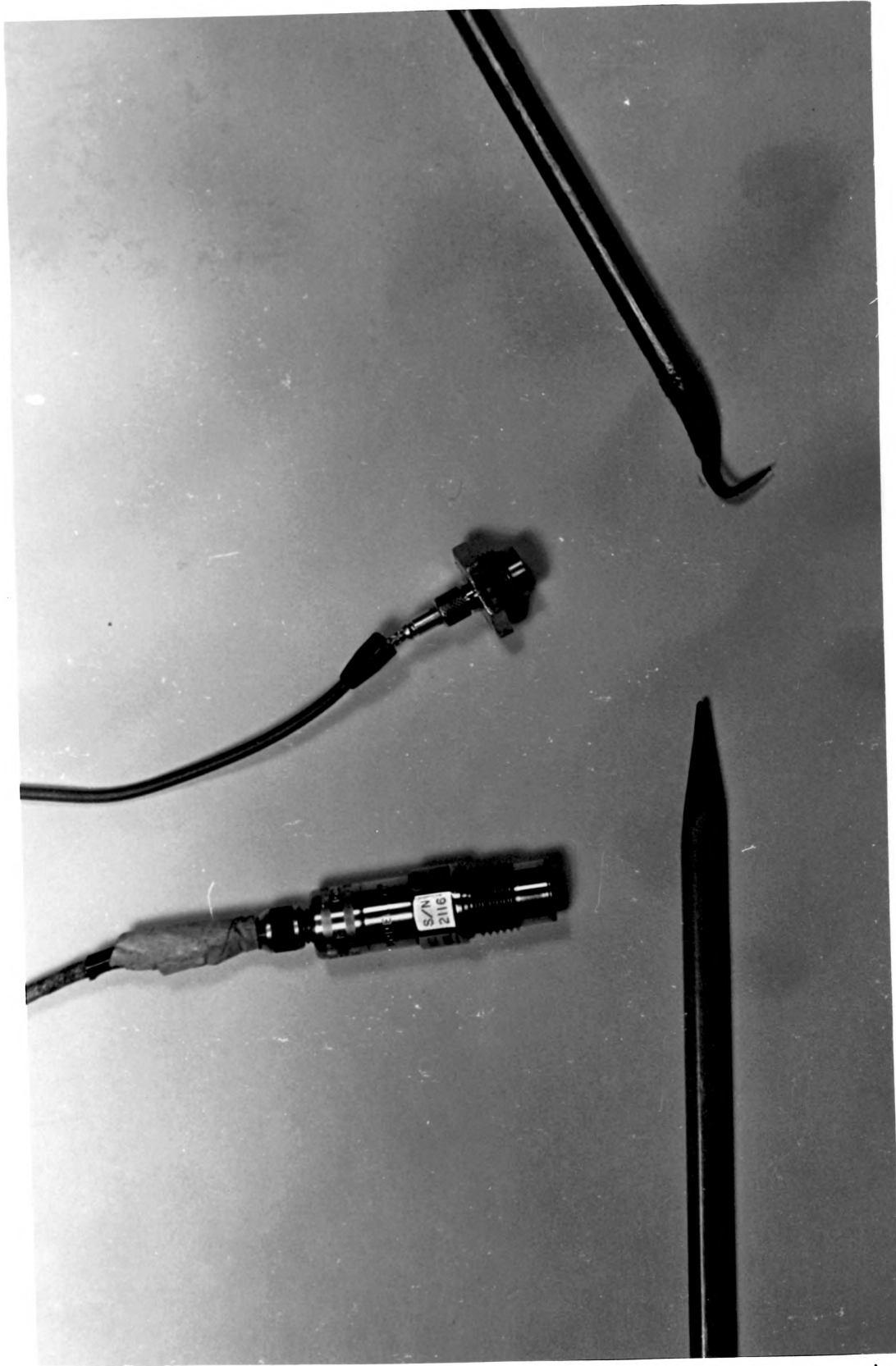


Figure 4-11. Sensing instruments used during experimental investigations: Kistler transducer, Columbia transducer, and hot-wire anemometer probe.

## CHAPTER V

### DISCUSSION OF EXPERIMENTAL RESULTS

#### 5.1 Orientation of Acoustic Pressure Wave Within Cavity

Krishnamurty (2) discarded the notion that standing pressure waves are set up within cavities with the onset of acoustic resonance. White (20) on the other hand, has argued that acoustic radiation from cavities is accompanied by the presence of a pressure wave moving back and forth along the cavity opening. This concept implies that a standing pressure wave may be expected to be present at the cavity opening or, possibly, within the cavity itself. Fox (8) felt that portions of his experimental data suggested the possibility of the presence of standing pressure waves within cavities during the emission of sound from cavities.

An experiment was designed to determine if a standing wave was present within the cavity during acoustic resonance and, if so, to determine the orientation of the wave within the cavity. The experiment may be outlined as follows. The Columbia transducer was placed at a reference position, generally position 20 as shown in Figure 4-5. The Kistler transducer was then mounted in turn at each of the remaining positions and its signal compared with the signal from the Columbia transducer. The signals from the two transducers were monitored simultaneously on an oscilloscope.

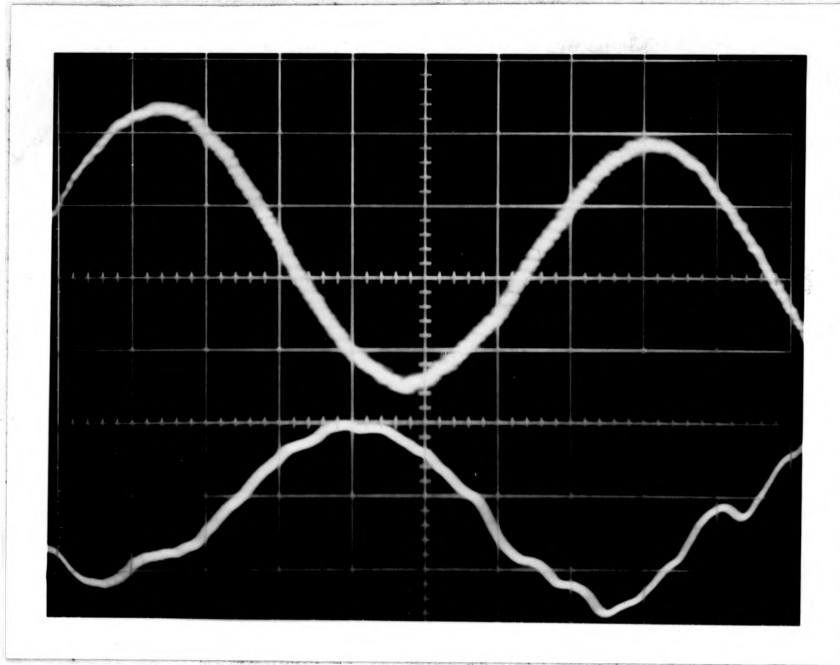


Figure 5-1. Photographic record of pressure signals as sensed at different positions on the cavity wall indicating a change in phase angle of the acoustic pressure wave.

The phase angle of the signal at the Columbia transducer was arbitrarily assigned a value of zero (on a scale going from  $-180^{\circ}$  to  $+180^{\circ}$ ). By monitoring the signals from the Columbia and Kistler transducers simultaneously, the phase angle between the two signals could be determined by measuring the distance between successive peaks of the two signals. The amplitude of the acoustic pressure was measured at each position by the Kistler transducer. A photograph of the traces from the Columbia and Kistler transducers as monitored for a typical resonant condition is shown in Figure 5-1. It is noted that the two signals are approximately  $180^{\circ}$  out of phase.

The phase angle and amplitude of the pressure signal as measured at the various positions were plotted on a schematic of the cavity wall in order to clearly display the spatial variation of these quantities. These "polar" plots are shown in Figures 5-2 through 5-6 for representative resonant conditions. Numerical values for the peak-to-peak acoustic pressure in units of pounds per square inch are indicated at each position on these plots. The arrows emanating from each position indicate the phase angle as referenced to position number 20; zero phase angle being represented as lying along the positive abscissa. The length of the arrows in each plot is drawn to scale in order to represent the magnitude of the acoustic pressure fluctuation at each point.

Analysis of the polar plots showed that acoustic resonance can be rather broadly classified into "modes" of resonance. The most predominant of these modes are referred to as the Helmholtz mode, the half-wave mode, and the full-wave mode.

Figure 5-2 is a polar plot of a typical Helmholtz resonant mode. This mode is characterized by the fact that there is relatively little variation in the phase and amplitude of acoustic pressure throughout the cavity. In other words, the wave length of the acoustic field is large compared with the cavity dimensions, which is characteristic of a Helmholtz resonator (23,24).

Figure 5-3 is representative of the half-wave mode of resonance. It is noted that there is a distinct pressure node along the

vertical diameter of the cavity. The amplitude of the acoustic pressure increases as distance away from the vertical diameter increases and the pressure signal on opposite sides of the cavity in the streamwise direction are  $180^\circ$  out of phase. This suggests that one-half of a pressure wave is standing along the horizontal cavity diameter; that is, parallel to the direction of the freestream. The computed wave length (based on frequency and acoustic velocity) for this particular resonant mode is 1.7 ft, which is approximately twice the cavity diameter.

Figure 5-4 represents the full-wave mode of resonance. It is again noted that the variation in the phase of the acoustic pressure wave is more pronounced in the streamwise direction. Two pressure nodes can be approximately located by extrapolation of the data. These nodes are indicated on the plot. In this case, it appears that a full wave is standing along the cavity diameter, parallel to the direction of the freestream. The wave length calculated from experimental data for this resonant condition was .925 feet, which is approximately equal to the 1 foot diameter of the cavity.

A less frequent mode of resonance is depicted in Figure 5-5. Here distinct pressure nodes of the wave are noted along both the streamwise and vertical cavity diameters. This mode of resonance is evidently strongly influenced by both streamwise and vertical dimensions of the cavity. Figure 5-6 shows a polar plot of an

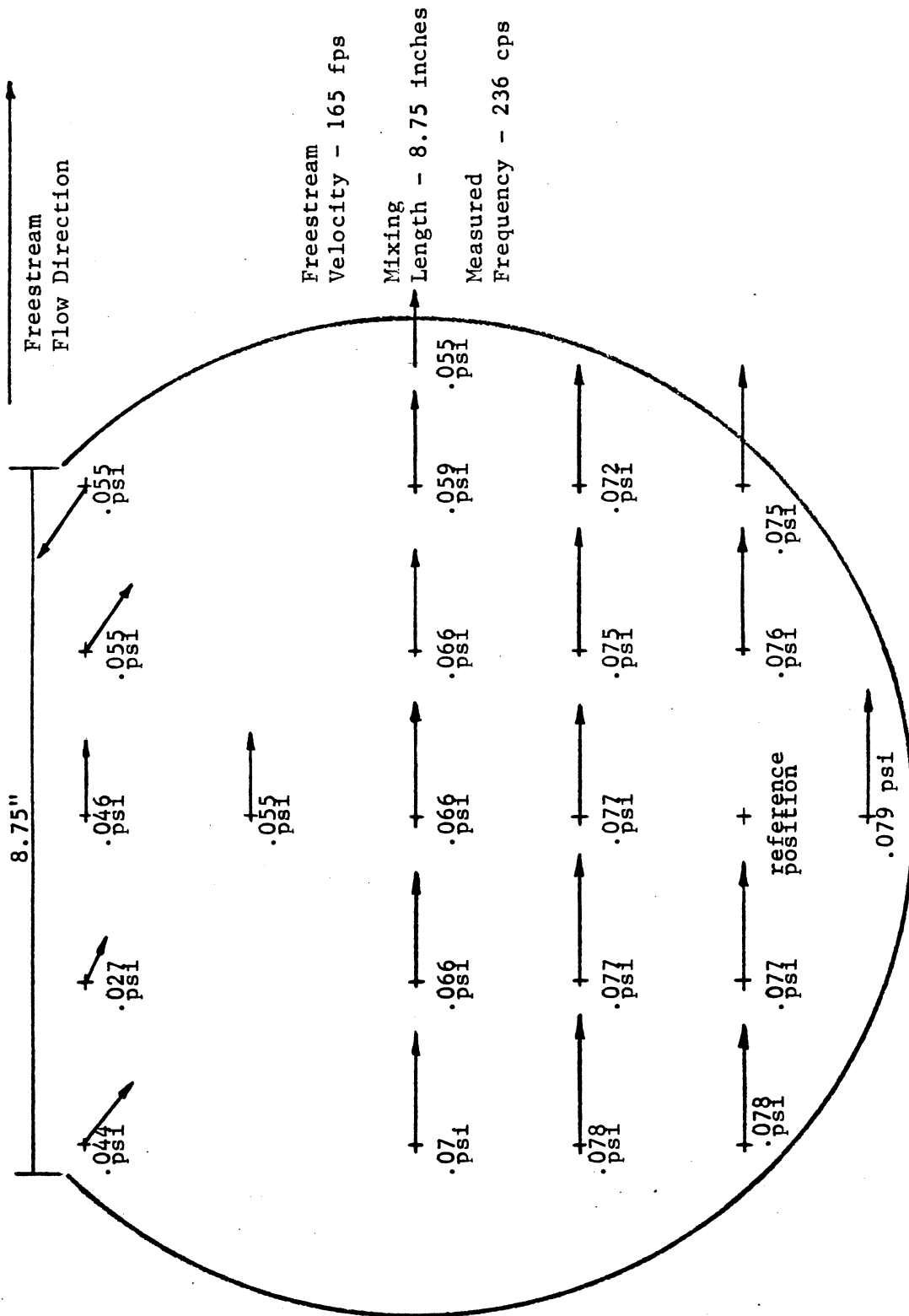


Figure 5-2. Polar plot of acoustic pressure wave within cavity (Helmholtz mode).

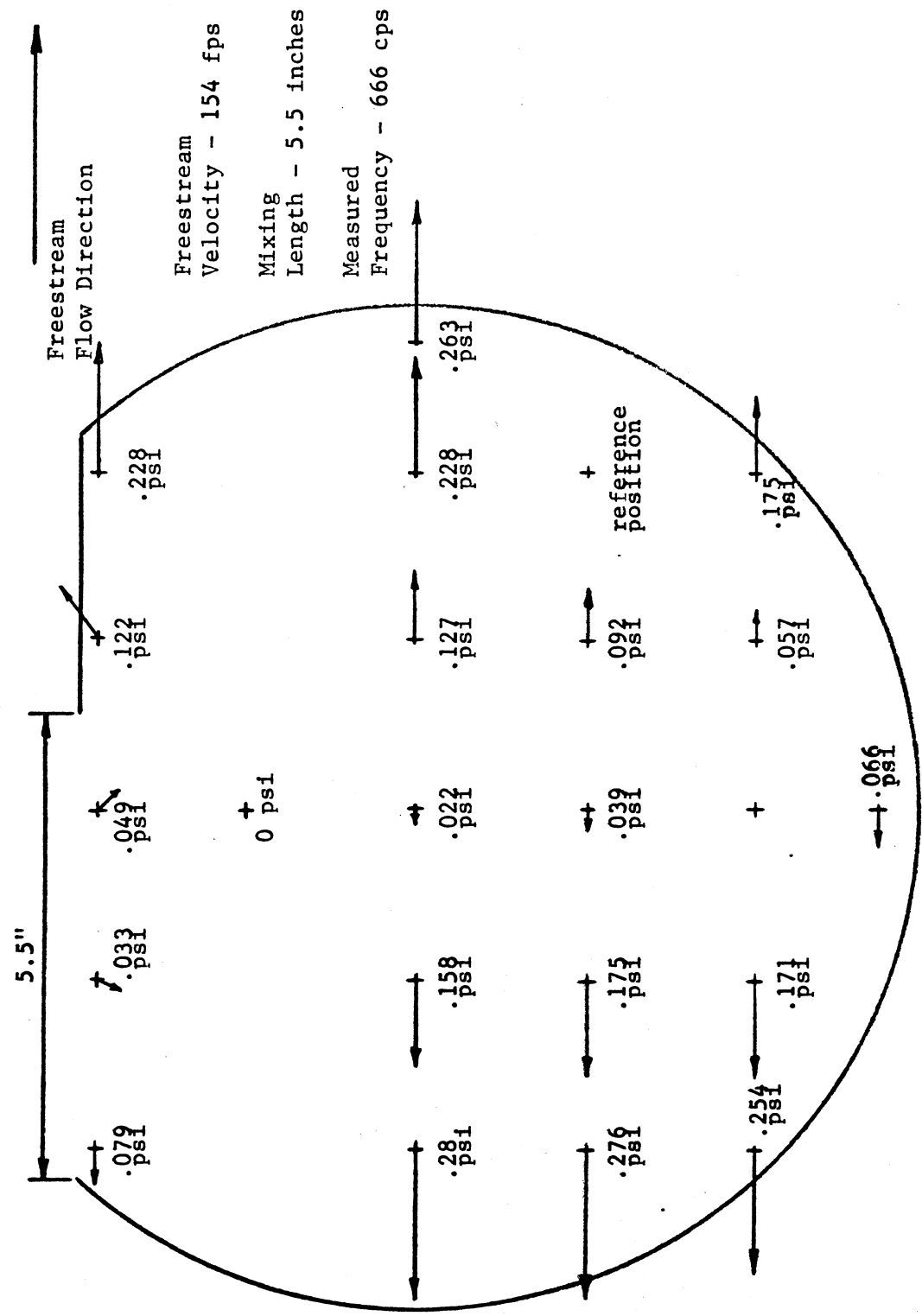


Figure 5-3. Polar plot of acoustic pressure wave within cavity (half-wave mode).



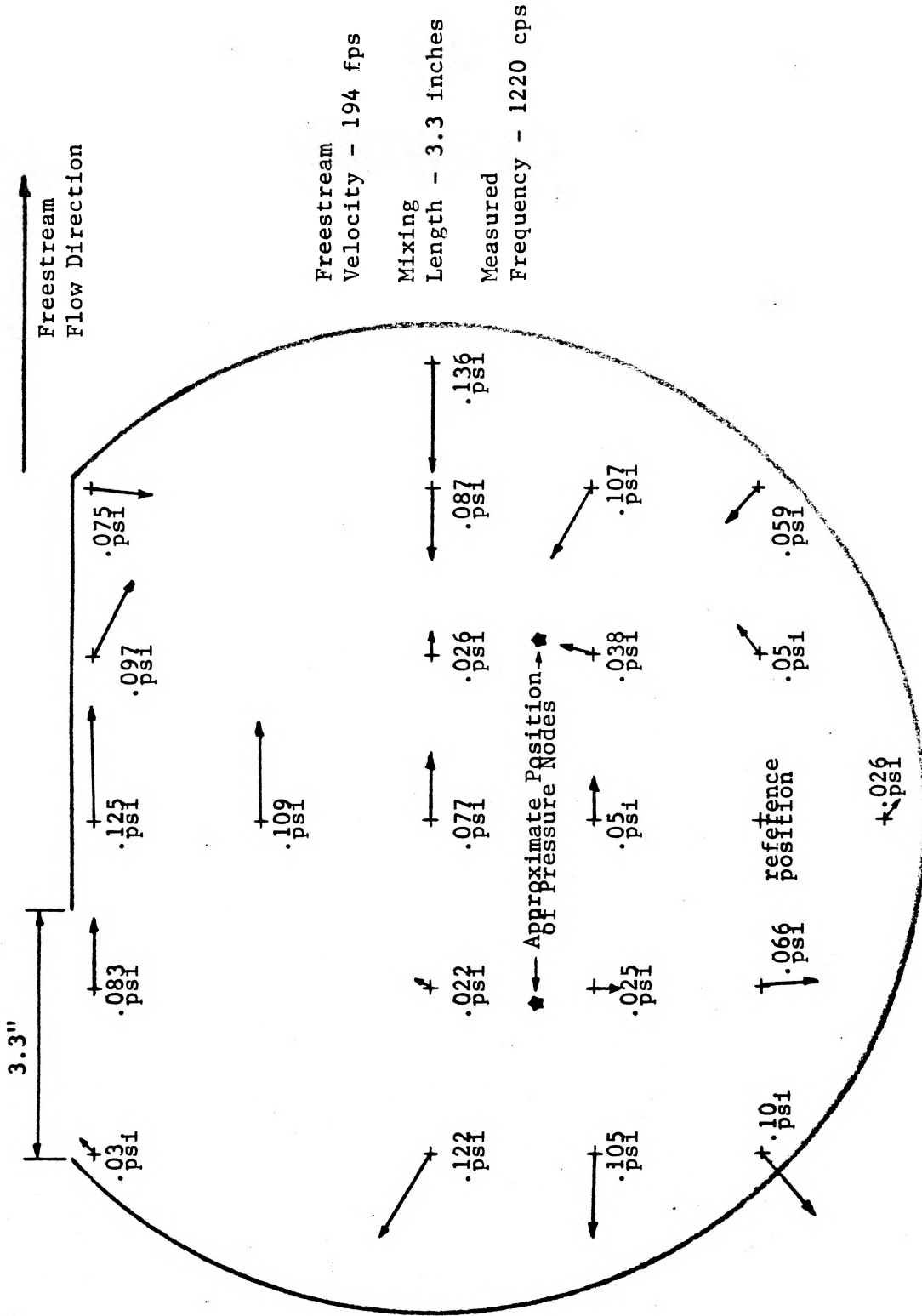


Figure 5-4. Polar plot of acoustic pressure wave within cavity. (full-wave mode).

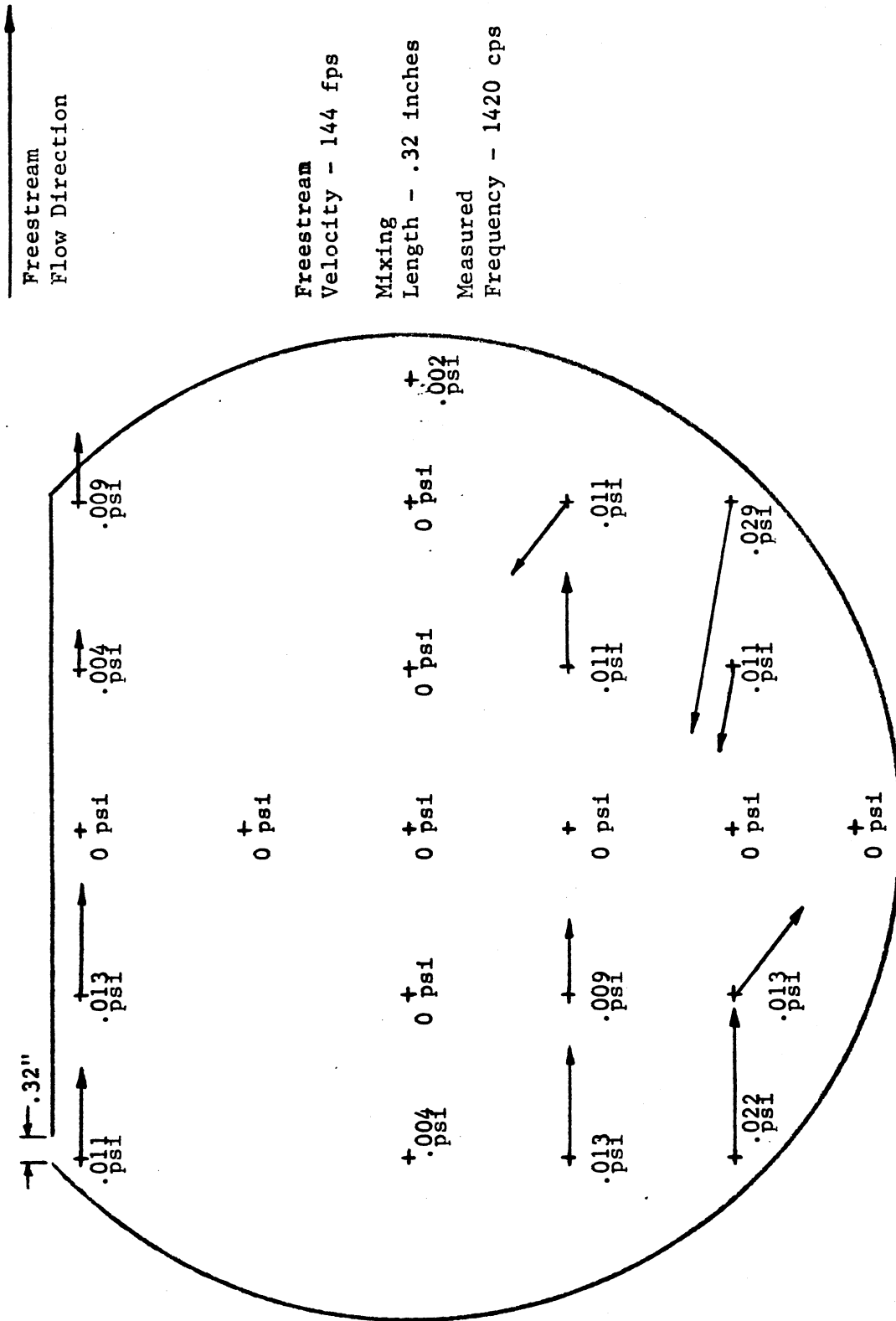


Figure 5-5. Polar plot of acoustic pressure wave with nodes along the streamwise and vertical dimensions of the cavity.

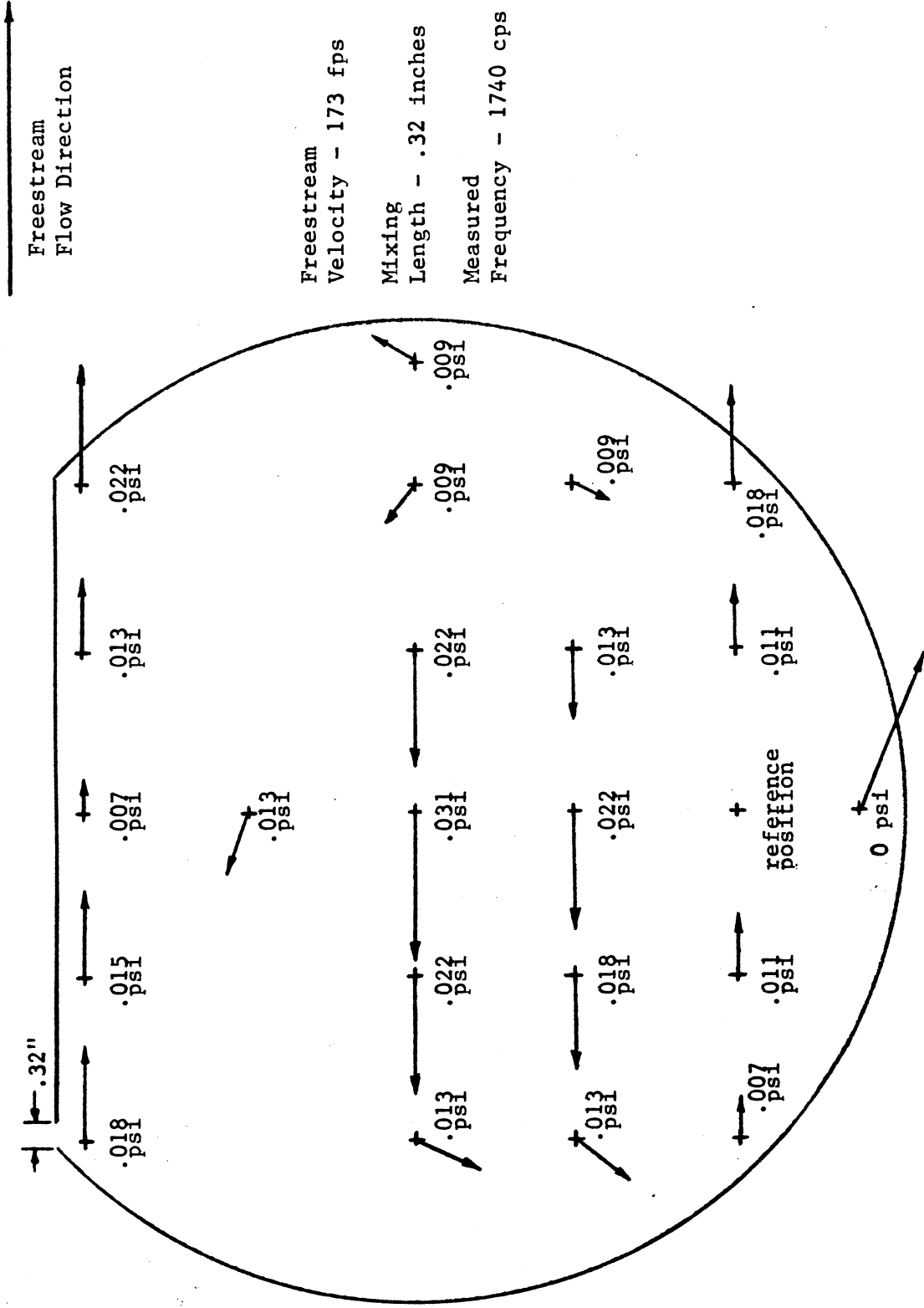


Figure 5-6. Polar plot of acoustic pressure wave that stands along the vertical dimension of the cavity.

acoustic pressure wave with marked variation in amplitude and phase only along the vertical cavity diameter.

It would appear from analysis of the polar plots that White's (20) hypothesis concerning the existence of a pressure wave oriented parallel to the freestream, is usually correct. The half-wave and full-wave modes of resonance, as defined above, are dominate at relatively large mixing lengths. It is interesting to note that there is significant variation of the acoustic pressure wave along the vertical diameter only for those resonant conditions which occur at relatively small mixing lengths. These two observations imply that White's hypothesis holds when there is a large degree of "contact" between the freestream and the cavity flow field. This might be expected because White's interpretation of the driving force for resonance was based on the nature of the mass exchange between the cavity and the freestream. Also, in his experimental work which led to the formulation of his prediction technique for resonance, White apparently did not consider the effect of varying the ratio of mixing length to cavity breadth. In the experimental work which White performed, the streamwise cavity breadth was at all times equal to the mixing length. Thus, at the larger mixing lengths the nature of the flow fields induced within the cavity in the present investigation approaches the character of the flow fields induced in the cavities used in White's investigation.

The Helmholtz mode of resonance has no dependence on the width of the cavity (the horizontal dimension normal to the freestream).

However, the acoustic pressure waves classified within the half-wave and full-wave resonant modes do exhibit some dependence on the cavity width. This is evidenced by the fact that the signals from the Kistler and Columbia transducer when mounted similarly on opposite faces of the cavity are out of phase for a number of the higher resonant modes. The acoustic wave is more strongly influenced by the width of the cavity at the smaller mixing lengths; the acoustic wave becoming more two-dimensional as the mixing length becomes larger. No effort was made to rigorously investigate the distribution of acoustic pressure along the cavity width as was done for the other two dimensions of the cavity. The wave lengths of flow induced acoustic waves do appear to be more strongly influenced by the streamwise dimension of the cavity than by the cavity width, particularly at the larger mixing lengths where the influence of the freestream flow field is greater. This might be expected since all parameters affecting acoustic resonance, such as freestream velocity, approaching boundary layer thickness and mixing length, are all uniform along the width of the cavity. However, in spite of the two-dimensional nature of the flow field that induces acoustic resonance, the occurrence of three-dimensional acoustic waves within the cavity cannot be discounted.

The driving force for the resonant modes observed for relatively small mixing lengths used in this investigation might be a phenomenon similar to that which Brown (16) observed in his experiment on edge-tones. Edge-tones refer to the sound fields

generated by the impingement of a jet of air on the apex of a rigid wedge placed along the centerline of the jet. As fluid within the jet arrives at the wedge, it is alternately deflected to either side of the wedge when the flow conditions and the geometry of the system are such that edge-tones are produced. Brown studied the edge-tones generated by a thin, two-dimensional jet, the thickness of which he considered to be an important parameter with regard to its influence on the frequencies of the edge-tones generated by the interaction between the jet and the wedge. In spite of his suspicion that the jet's thickness, which he referred to as the slit width, might be an important parameter, Brown made no effort to identify its effect on the frequencies of the acoustic fields generated by the edge-tone phenomenon. A parameter that Brown did extensively investigate was the length of the jet as defined by the distance between the wedge and the exit plane from which the jet emanated. This jet length was found to have a significant effect on the frequencies that could be excited. A second influential parameter was the jet velocity.

The smaller mixing lengths which were associated with the generation of the higher frequency modes observed in the present investigation are within the range of the jet lengths which Brown used during his investigation. The boundary layer thickness might be construed as being similar to the slit width used by Brown. Thus, it is possible that a phenomenon related to edge-tones is the

sustaining force during resonance at the smaller mixing lengths used in the present investigation.

## 5.2 Correlation of Resonant Frequencies

The polar plots of the acoustic waves that are present within the cavity during resonance indicate that the resonant frequency, or more precisely the resonant wave length, is dependent on the cavity diameter which may be considered the characteristic dimension of the cavity. It is, therefore, reasonable to attempt to correlate the experimentally measured frequencies in terms of the cavity diameter. This has been done by employing a Strouhal number based on the cavity diameter.

$$St_{\text{meas}} = \frac{D}{U} f_{\text{meas}}$$

The resonant frequencies may be expected to occur predominately in the Helmholtz, half-wave, or full-wave modes; the resonant frequencies being imposed by the dimensions of the cavity. The "imposed" frequencies for half-wave and full-wave modes may be formulated as

$$f_{\text{imp}} = \frac{c}{\lambda} = \frac{c}{D} \frac{1}{N}$$

where  $N$  is a parameter accounting for half-wave resonance ( $N = 2$ ) or full-wave resonance ( $N = 1$ ). These values for  $N$  are assigned as such because the wave length for the acoustic field is equal to the cavity diameter in the full-wave mode and twice that in the half-wave mode. No intuitive value may be assigned to the parameter

N for the Helmholtz mode except to say that the predicted wave length for the acoustic field should be large compared to the characteristic cavity dimension.

The Strouhal number for the imposed resonant frequencies is

$$St_{imp} = \frac{D}{U} f_{imp} = \frac{D}{U} \frac{c}{D} \frac{1}{N} = \frac{1}{M} \frac{1}{N}$$

It is seen in Figure 5-7 that when the Strouhal number for the imposed resonant frequencies is plotted against Mach number, the Strouhal number so formulated follows the trend of the experimental data rather well. The experimental data separates into three distinct groupings representing the Helmholtz, half-wave, and full-wave modes. As expected, values of 2 and 1 for the parameter N provide imposed Strouhal numbers that match the experimental data for the half-wave and full-wave resonant modes. A value of 6 for the parameter N allows the imposed Strouhal number to match the experimental data for the Helmholtz mode. The wave length of the Helmholtz resonant mode is about 5 to 6 times as large as the cavity diameter. Since N is a parameter which accounts for the fact that the acoustic wavelength is expected to be a multiple of the cavity diameter, it is not surprising that a value of 6 for N allows the imposed Strouhal number to match the Strouhal number based on experimental data for the Helmholtz mode.

The use of the cavity diameter as being the characteristic dimension for determining resonant frequencies is in direct opposition to Krishnamurty's (2) conclusion that the resonant frequency



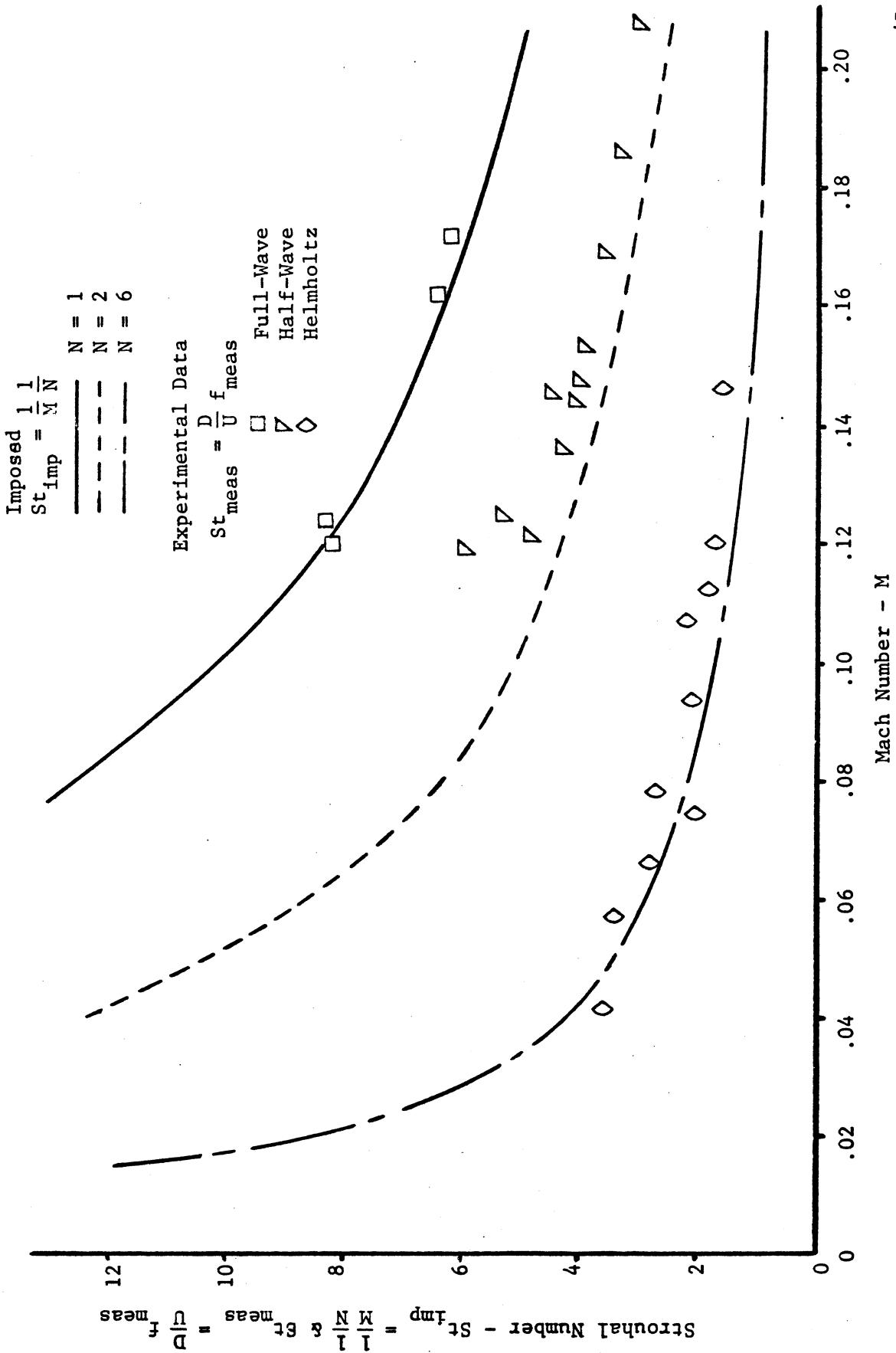


Figure 5-7. Strouhal number as a function of freestream Mach number.

is principally governed by the length of the cavity opening and not by the internal dimensions of the cavity. This conclusion by Krishnamurty may have been encouraged by the fact that he disregarded the possibility that standing waves may have been present within the cavity.

The evidence compiled in this investigation substantially indicates that standing pressure waves within cavities do occur during resonance and that the internal dimensions of the cavity, therefore, significantly affect the wave length of the acoustic field. Spee's (17) data supports this concept of the effect of the cavity dimensions on the frequency of the acoustic field.

### 5.3 Nature of the Approaching Boundary Layer

In order to make use of the thickness of the approaching boundary layer as a parameter, the boundary layer thickness had to be controlled and its magnitude defined. Control of the boundary layer thickness was effected by the use of the boundary layer removal unit described in Chapter IV. The degree of boundary layer removal had to be reproducible in order to assure that the data taken at different times would reflect the influence of a known boundary layer thickness. It was felt that consistent results could best be achieved by using an easily reproduced by-pass flow area in order to effect different magnitudes of partial vacuums under the perforated plate. By using a by-pass flow area of 40 square inches a significant change in the degree of boundary layer removal could be accomplished. With the aid of the

by-pass flow area, four reliably reproducible boundary layer conditions could be effected. These conditions are summarized in Table 5-1 below.

Table 5-1. Summary of Boundary Layer Control Conditions

Boundary Layer Condition	Description	Pressure Difference across Perforated Plates in Inches of Water
1	Full Removal	-5.75
2	Partial Removal	-0.2
3	No Removal	0
4	Partial Augmentation	+0.18

Boundary layer condition #1, full removal, makes no use of the by-pass flow area. All the flow generated by the removal blower is drawn through the perforated plates, thus achieving maximum boundary layer removal. In condition #3, the boundary layer is allowed to develop undisturbed by the boundary layer removal unit. Conditions #1 and #4 make use of the by-pass flow area. Condition #2 is a removal condition while condition #4 augments the approaching boundary layer by blowing ambient air into the boundary layer, thereby causing the boundary layer to thicken.

The pressure gradient listed in Table 5-1 is the difference between the static pressure of the freestream and the pressure within the plenum chambers through which fluid in the boundary

layer is either removed or augmented. Assuming that there is a negligible pressure drop through the tubes extending from the plenum chambers into the space below the perforated plates in the flow channel, the measured pressure difference listed in Table 5-1 is representative of the pressure gradient across the perforated plates which ultimately effects the removal or augmentation of the boundary layer. The minus sign on the pressure difference for boundary layer conditions #1 and #2 indicate that the pressure below the perforated plates is less than the static pressure of the freestream. The pressure difference for condition #4 is positive indicating that the pressure under the perforated plates is greater than the static pressure of the freestream. The existence of no pressure difference across the perforated plates for condition #3 reflects the fact that there is no removal or augmentation of the boundary layer.

The velocity profiles of the approaching boundary layers were measured at selected velocities by use of a hot-wire anemometer. The dependence of the boundary layer on the freestream velocity could then be determined. Figure 5-8 shows the effect of freestream velocity on the nature of the approaching boundary layer for conditions of maximum boundary layer removal (condition #1).

The thickness of the approaching boundary layer was taken as that vertical distance from the plate at which 90% of the freestream velocity was recovered. This definition of boundary layer thickness

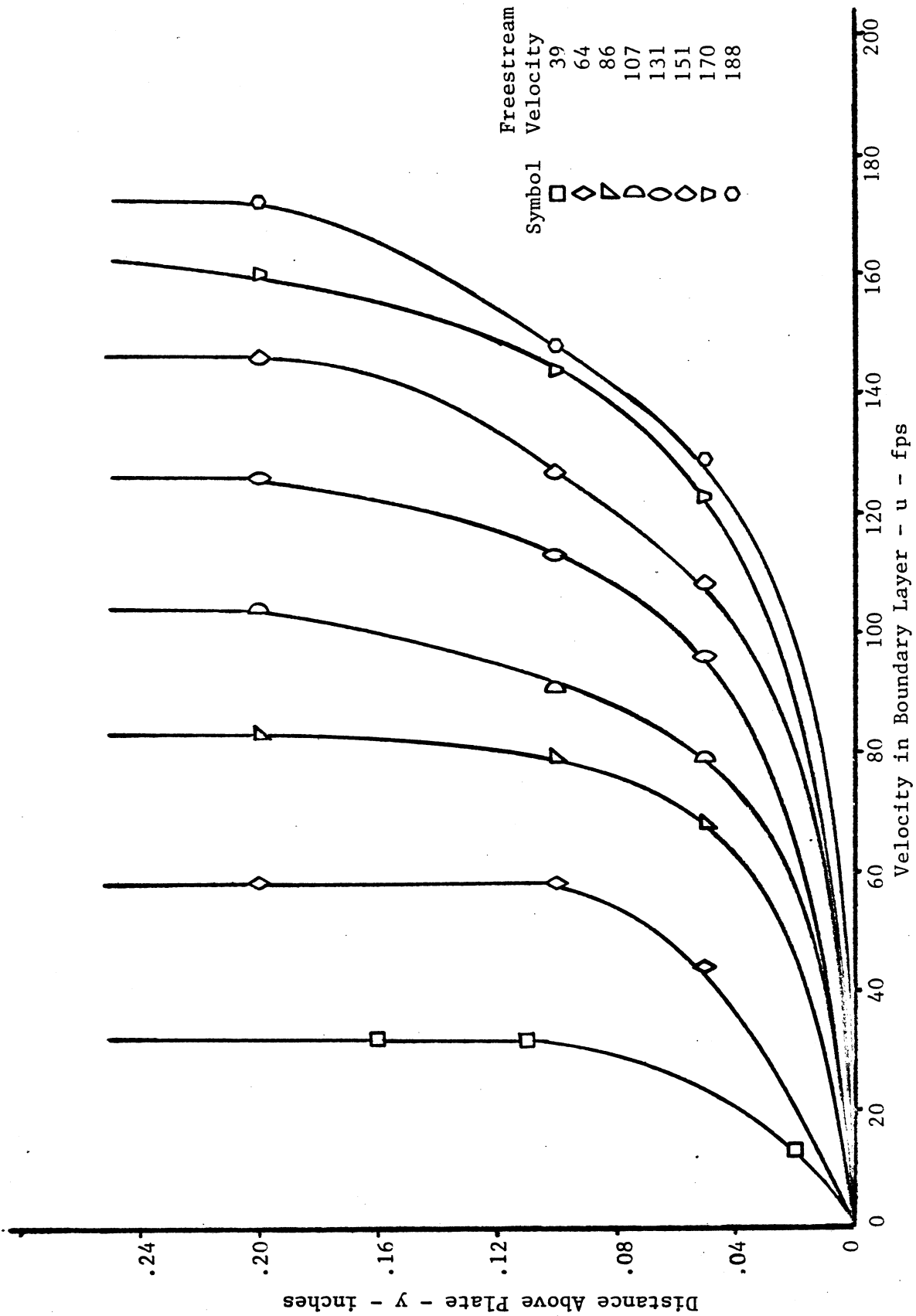


Figure 5-8. Velocity profiles of boundary layer for several freestream velocities (boundary layer condition #1, full removal).

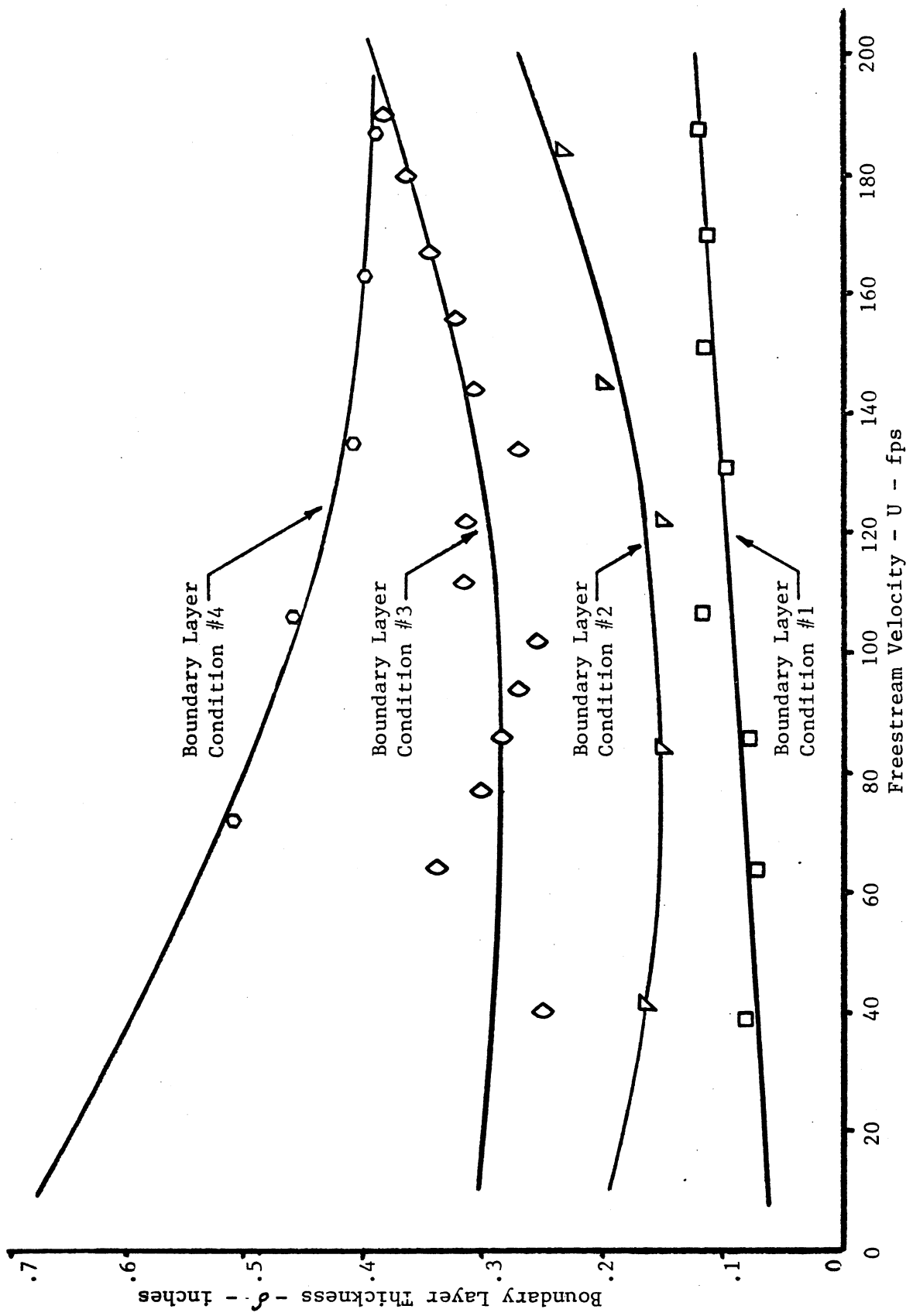


Figure 5-9. Data points for boundary layer thickness and corresponding curve-fits.

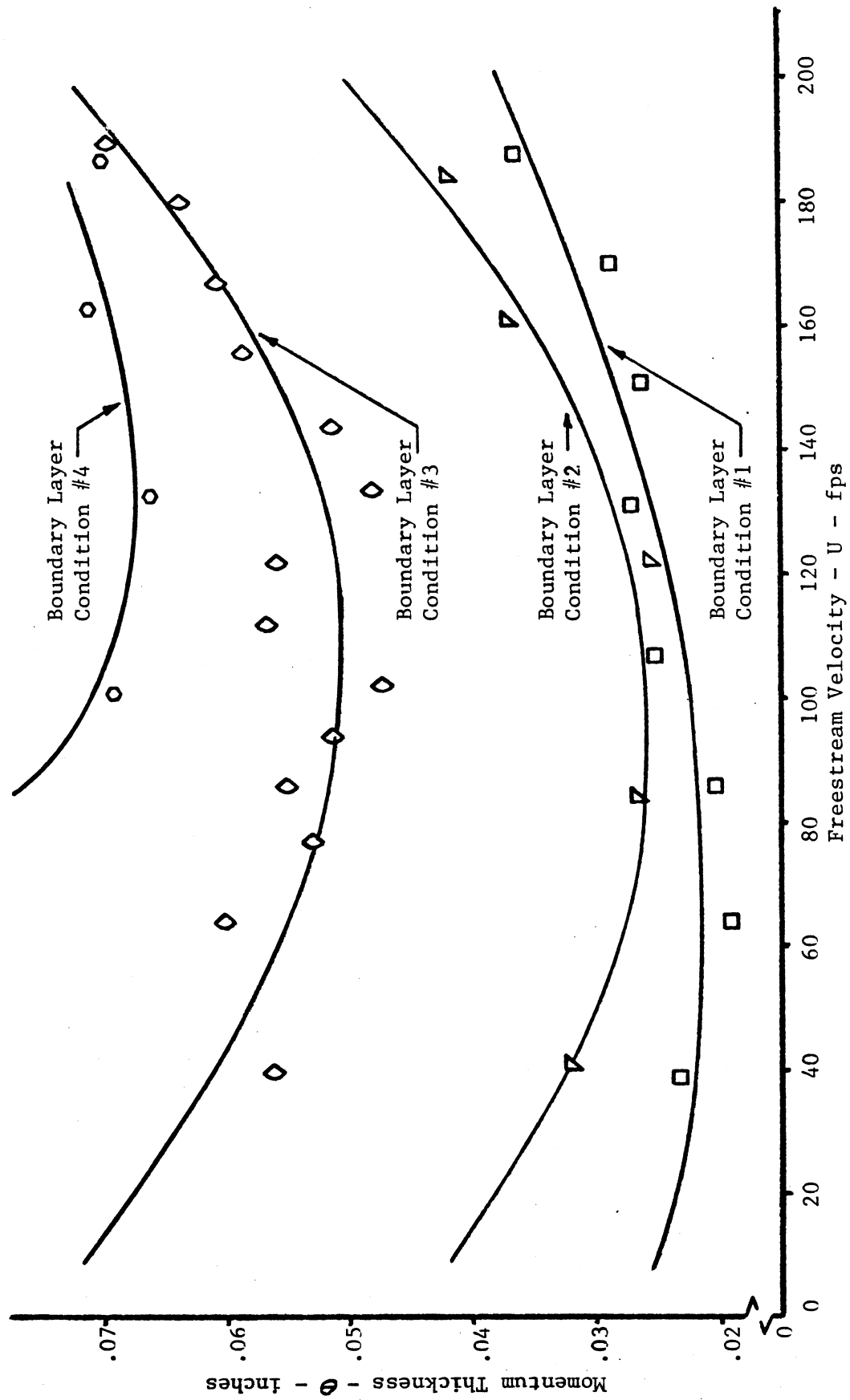


Figure 5-10. Data points for momentum thickness and corresponding curve-fits.

was chosen because it could be easily determined experimentally. Figure 5-9 shows the effect of the freestream velocity on boundary layer thickness. This data was fitted to second degree polynomials by use of a least-square curve-fitting routine. The curve fitted to the data is also shown in Figure 5-9.

The momentum thickness of the approaching boundary layer was calculated by integrating the boundary layer velocity profiles in the manner dictated by the definition of momentum thickness (25) using Simpson's integration method. The effect of freestream velocity on the momentum thickness is shown in Figure 5-10. This data was also fitted to second degree polynomials.

#### 5.4 Occurrence of Acoustic Resonance

Two parameters which have been observed to have a significant effect on acoustic resonance in cavities are the freestream velocity and the mixing length. The amplitude of the acoustic pressure is affected continuously by these parameters while the resonant frequency changes abruptly resulting from a shift from one mode of resonance to another as velocity and mixing length are varied. The frequency remains nearly constant within a given mode of resonance. A resonant mode may prevail over a range of mixing lengths and freestream velocities. Figure 5-11 shows the region defined by mixing length and velocity over which one of the resonant modes of the cavity prevails for boundary layer condition #2. Lines representing constant acoustic pressure are indicated on the plot. These lines of constant pressure are



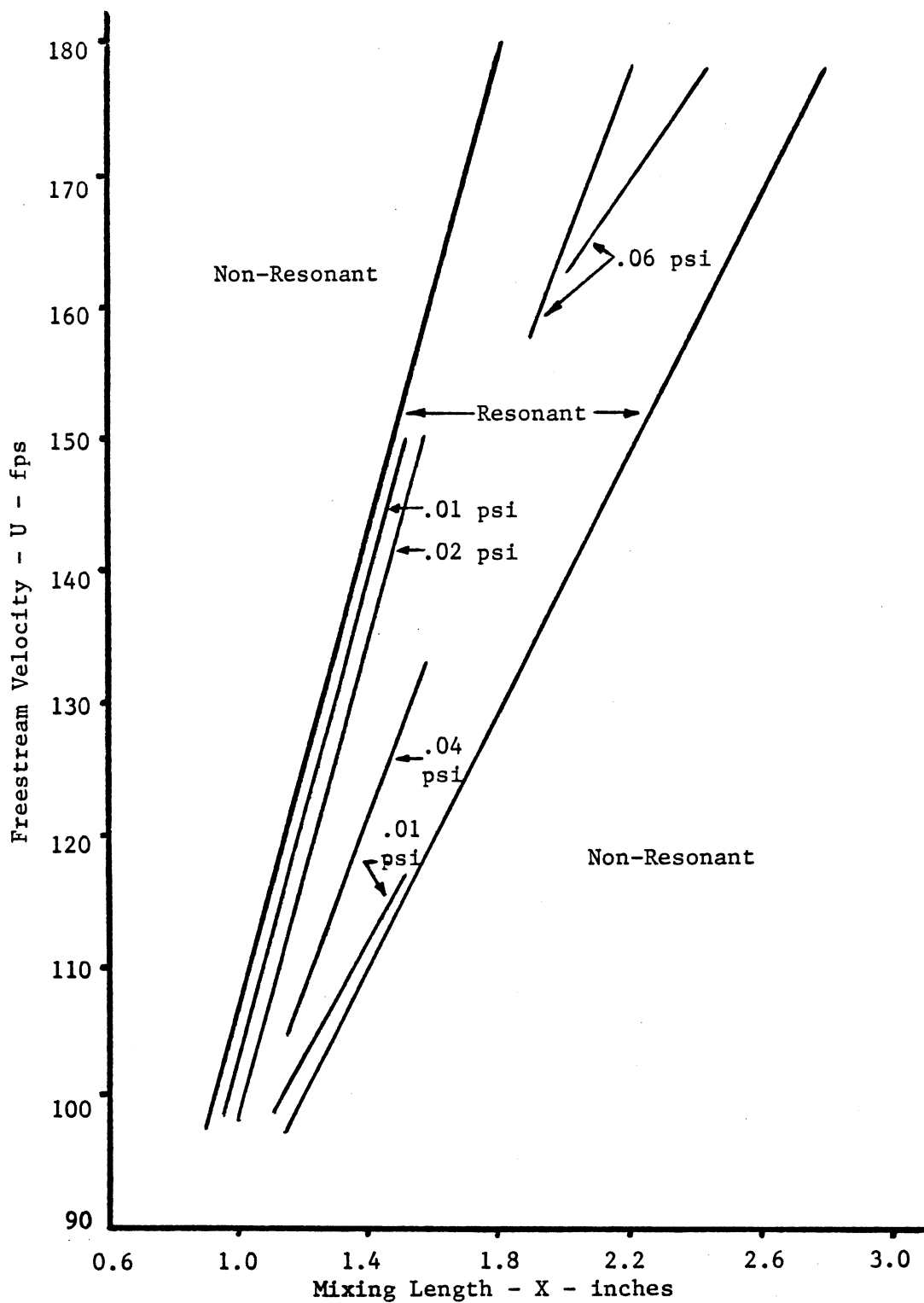


Figure 5-11. Range of freestream velocity and mixing length over which a representative resonant mode prevails (boundary layer condition #2; measured frequency - 833 cps)

approximate fairings between data points for acoustic pressures measured at a pressure anti-node within the cavity. Thus, these lines are only a rough guide to the amplitude of acoustic pressure throughout the mapping. A more accurate representation of the amplitude of acoustic pressure as a function of freestream velocity is shown in Figure 5-16 described later. The data from Figure 5-11 are also included in Figure 5-13.

The approaching boundary layer has a significant effect on the intensity and the occurrence of acoustic resonance. To a lesser extent, the mode of resonance which can be sustained is also affected by the approaching boundary layer. A thick approaching boundary layer tends to suppress the occurrence of resonance, particularly the higher frequencies. This can be ascertained from Figures 5-12 through 5-15. The data in these figures were obtained by recording the frequency and intensity of the acoustic field at several velocities, usually at increments of approximately 5 fps, while holding the mixing length constant. The regions of resonance, as defined by the combinations of freestream velocity and mixing length at which resonance occurs, tend to diminish as the approaching boundary layer thickens. For instance, with few exceptions, the full-wave mode of resonance occurs only for conditions at full boundary layer removal. When the approaching boundary layer is thin, the cavity is resonant at nearly any combination of velocity and mixing length and few regions of non-resonance exist.

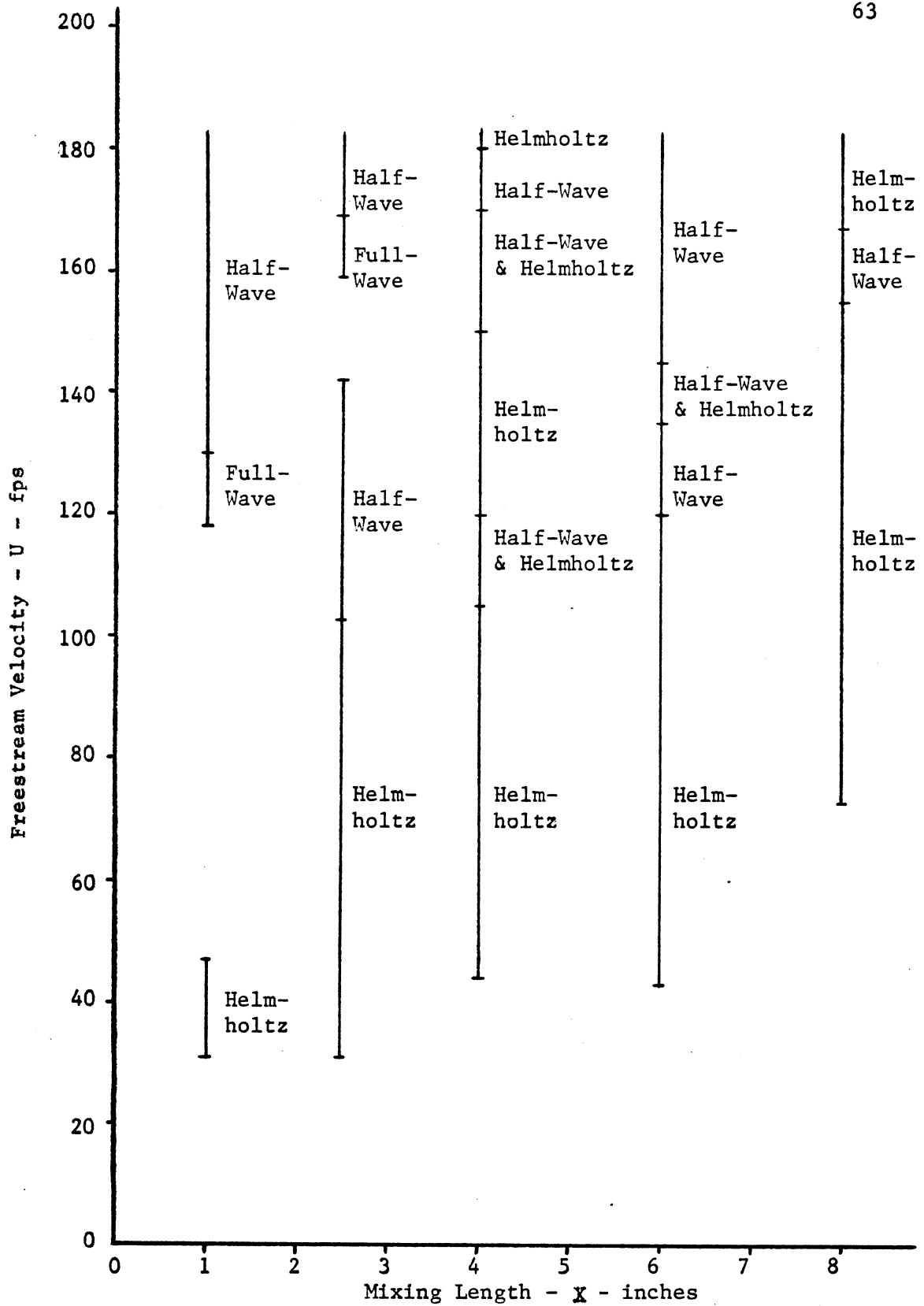


Figure 5-12. Representation of the ranges of freestream velocity and mixing length which sustain resonance for boundary layer condition #1 (full removal).

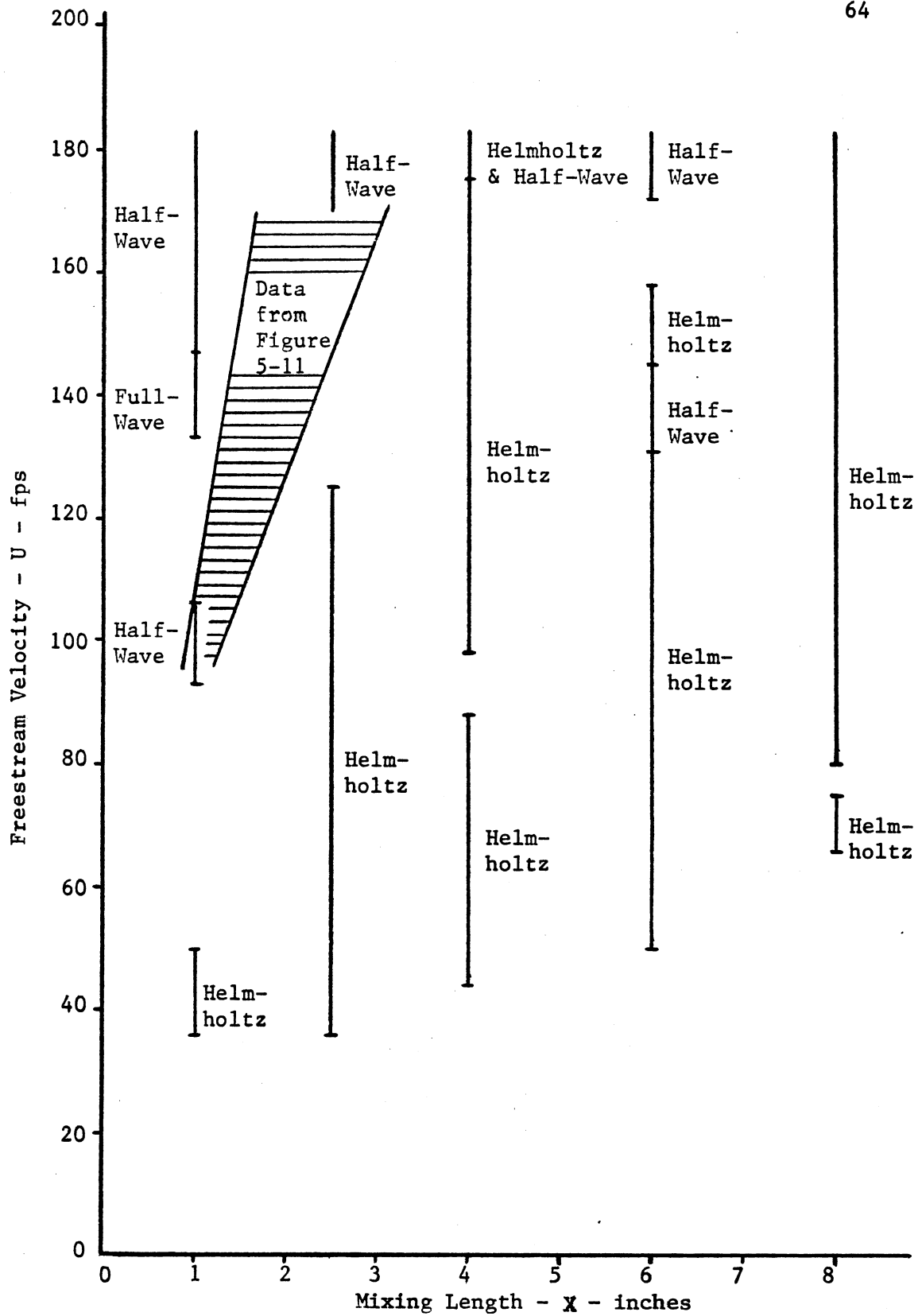


Figure 5-13 Representation of the ranges of freestream velocity and mixing length which sustain resonance for boundary layer condition #2 (partial removal).

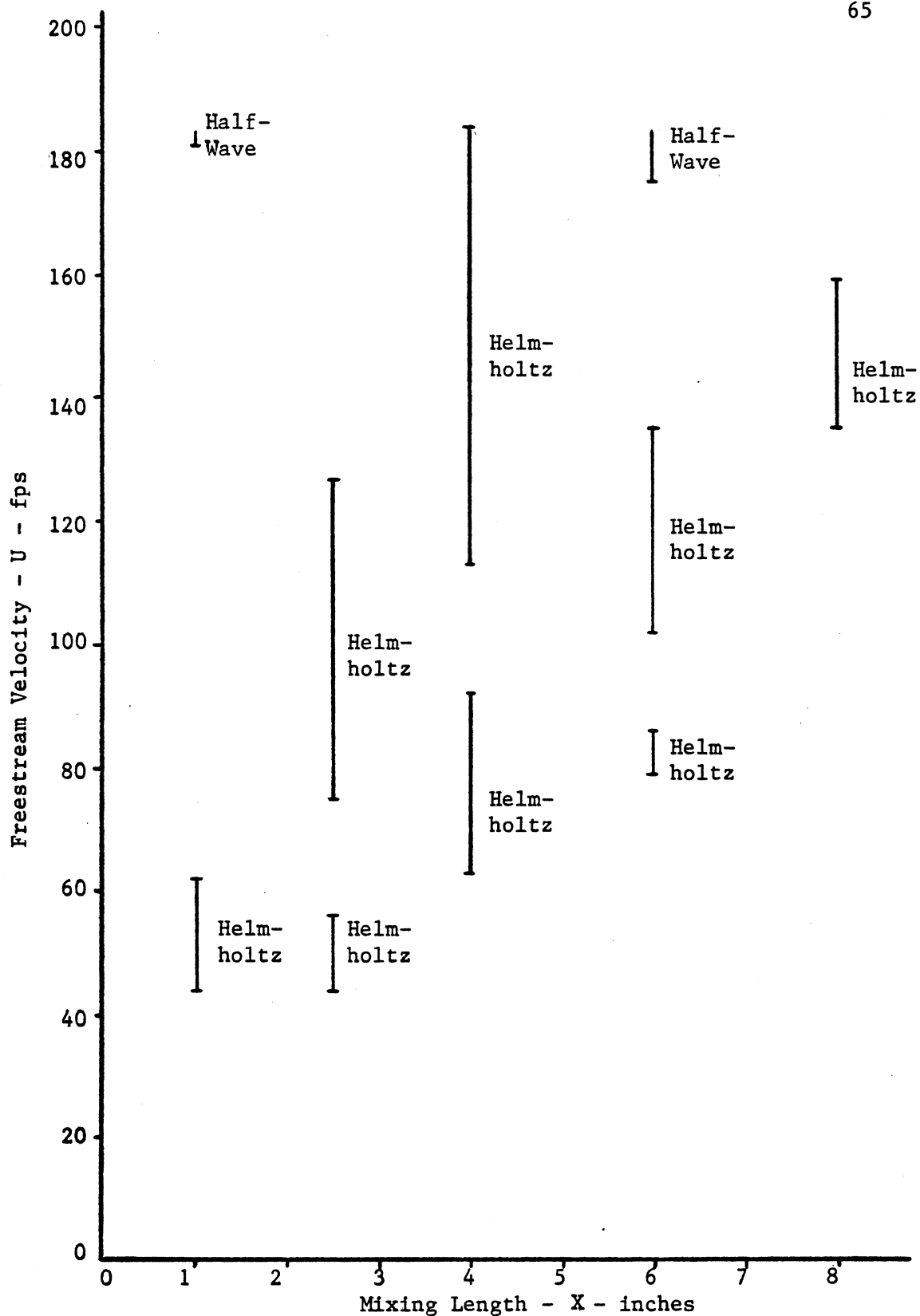


Figure 5-14 Representation of the ranges of freestream velocity and mixing length which sustain resonance for boundary layer condition #3 (no removal).

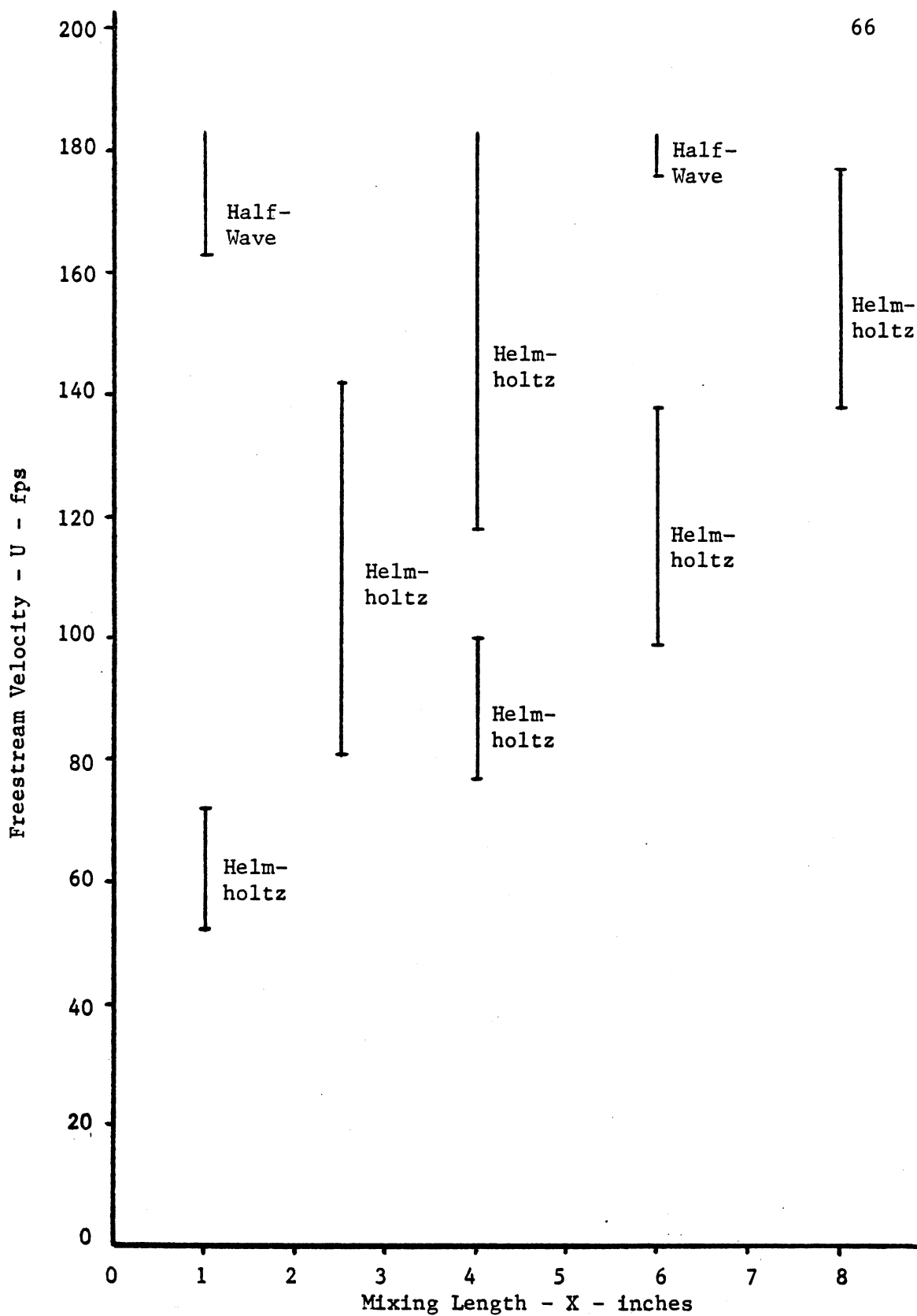


Figure 5-15 Representation of the ranges of freestream velocity and mixing length which sustain resonance for boundary layer condition #4 (partial augmentation).

Records of the acoustic pressure measured at an anti-node within the cavity for a wide range of velocities with constant mixing length provided data which reflected the dependence of acoustic pressure on freestream velocity. This data was taken at the four aforementioned boundary layer conditions in order that the influence of the approaching boundary layer thickness on the level of the acoustic resonance could also be analyzed. Care was taken to place the Kistler transducer at the position within the cavity where the maximum acoustic pressure occurred for a given mode of resonance. The recording of this maximum pressure is critical to calculating the acoustic intensity. Acoustic intensity is the rate at which acoustic energy is transmitted across a unit area of a plane parallel to the wave front. For a simple harmonic wave the acoustic intensity  $I$  is given by the relation

$$I = \frac{g_c P_o^2}{2 \rho c}$$

where  $P_o$  is the amplitude of the acoustic pressure. In the case of a standing pressure wave, as occurs within a resonating cavity,  $P_o$  must be measured at an anti-node.

Figure 5-16 shows these acoustic pressures as a function of freestream velocity with the boundary layer condition used as a parameter. It is evident from this figure that the approaching boundary layer thickness depresses the magnitude of the acoustic

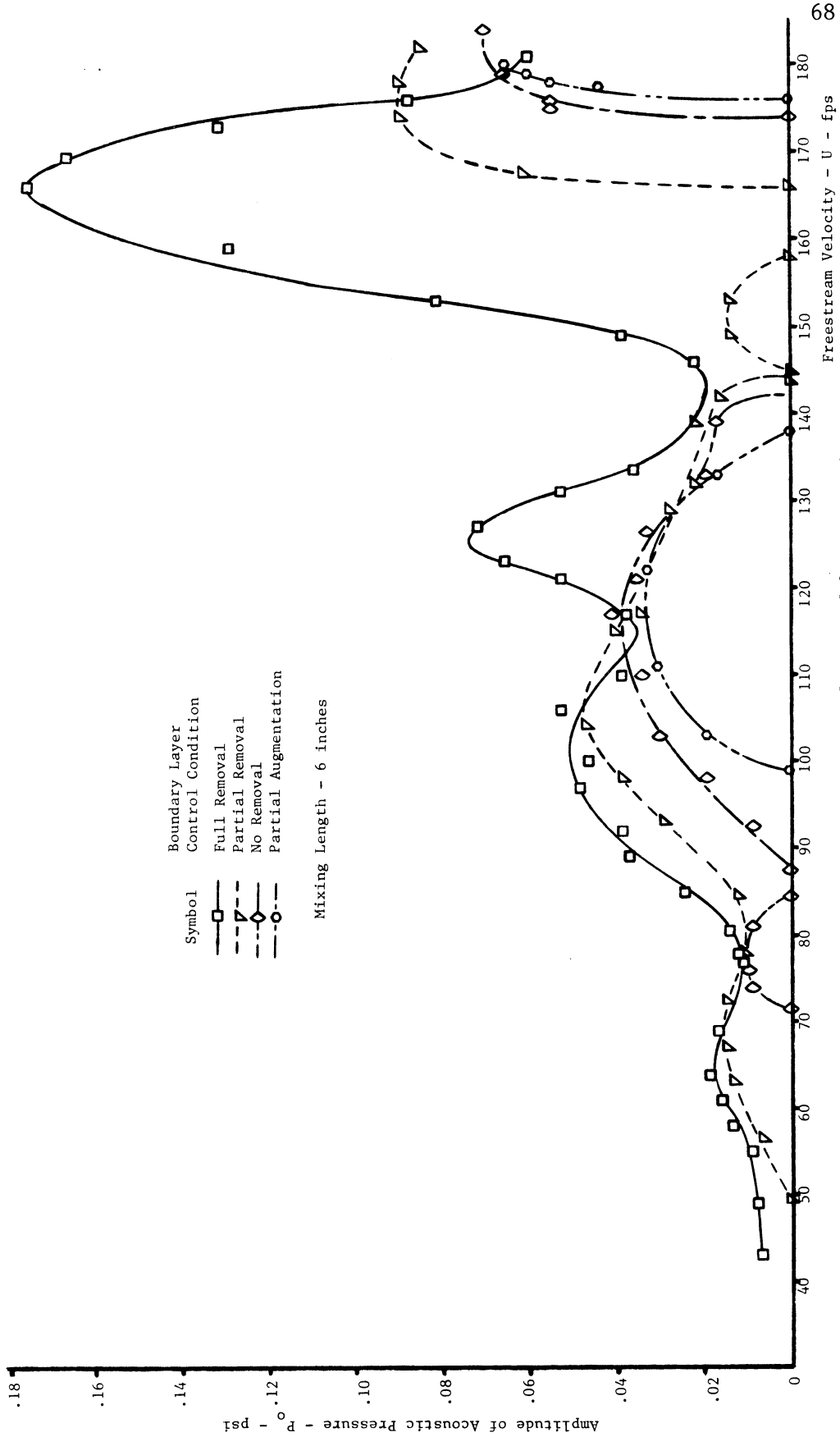


Figure 5-16. Amplitude of acoustic pressure as a function of freestream velocity



pressure. It also appears that the resonant peaks are shifted to higher velocities as the boundary layer thickens. Resonant peaks refer to the maximum acoustic pressure recorded within a given velocity range. For instance, the data recorded at a mixing length of 6 inches as displayed in Figure 5-16 shows a resonant peak at 166 fps for the condition of full boundary layer removal. It is seen that the resonant peak is shifted to higher velocities as the boundary layer is allowed to thicken. This shift of the resonant peaks was also present with similar data recorded at mixing lengths of 1, 2.5, 4, 6, and 8 inches. The shift in one set of the resonant peaks recorded for a mixing length of 2.5 inches is particularly evident as is shown in Figure 5-17.

The amplitude of the acoustic pressure at the resonant peaks is quite high. Intensity levels as high as 150 db re  $2.9 \times 10^{-9}$  psi have been recorded. Table 5-2 shows the power dissipated in acoustic energy at some representative peaks. The peaks represented by Table 5-2 are generally the most intense acoustic pressures recorded at each of the four boundary layer conditions for mixing lengths of 2.5, 4, 6, and 8 inches. In each case the cavity was tuned by adjusting the velocity to obtain the most intense (highly tuned) resonance. The acoustic power is calculated by multiplying the acoustic intensity by the streamwise area of the cavity, defined by the vertical height of the cavity and the width of the cavity. This area is used in the calculation because the acoustic wave

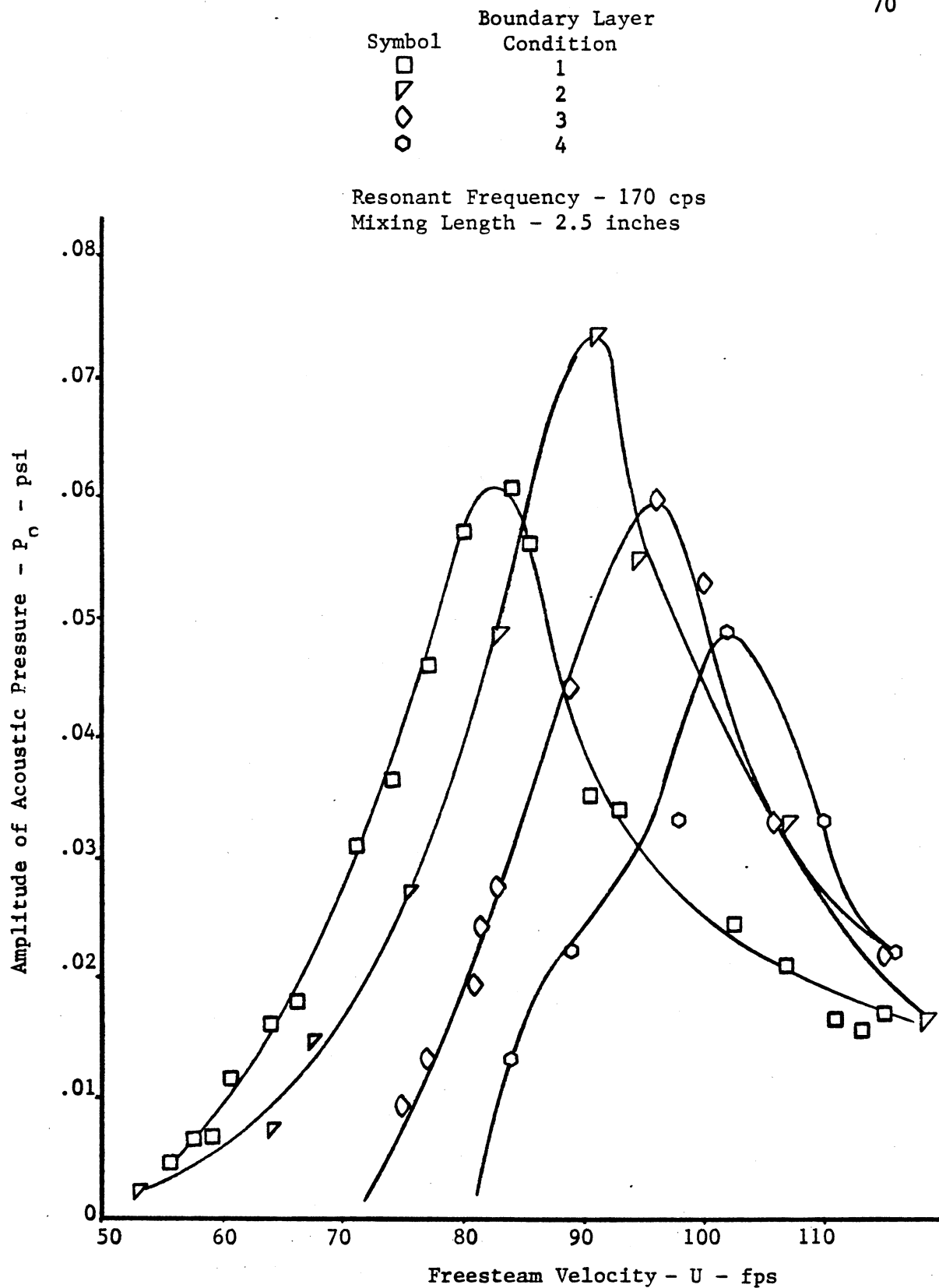


Figure 5-17. Shift of resonant peak with increasing boundary layer thickness

Table 5-2. Summary of acoustic energies dissipated at some peak resonant conditions.

Freestream Velocity	Mixing Length	Boundary Layer Condition	Boundary Layer Thickness	Acoustic Intensity	Power Dissipated
fps	inches	#	inches	$\frac{\text{ft-lbf}}{\text{ft}^2\text{-sec}}$	horse-power
84	2.5	1	.09	57	.065
91	2.5	2	.15	85	.100
95	2.5	3	.29	56	.066
102	2.5	4	.46	38	.042
170	4.0	1	.12	396	.450
159	4.0	2	.20	93	.110
172	4.0	3	.35	51	.058
173	4.0	4	.39	47	.054
166	6.0	1	.11	488	.560
174	6.0	2	.22	128	.140
184	6.0	3	.37	78	.092
178	6.0	4	.39	58	.067
159	8.0	1	.11	69	.075
146	8.0	2	.18	35	.042
154	8.0	3	.33	17	.017
158	8.0	4	.40	8	.009

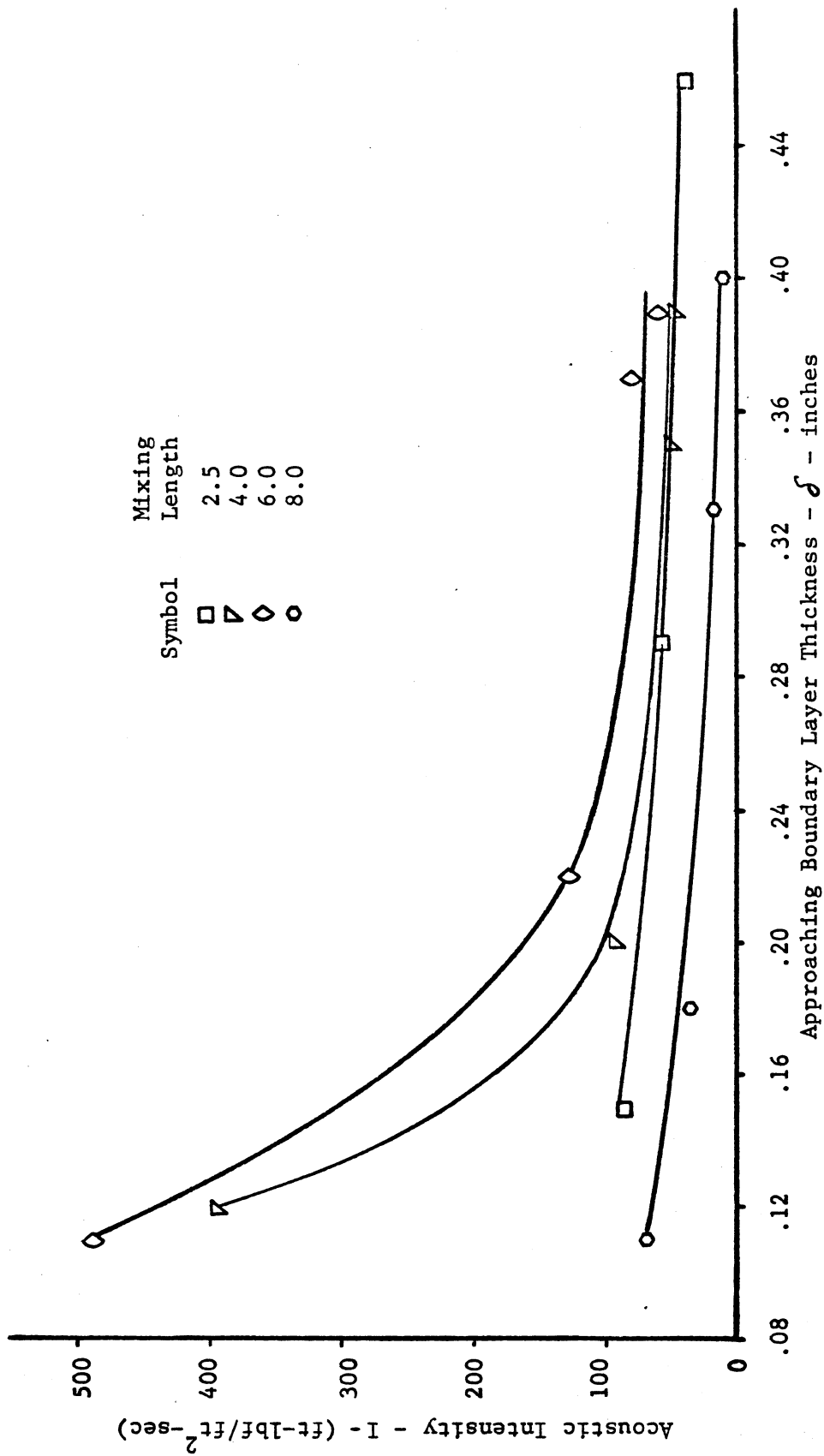


Figure 5-18. Effect of approaching boundary layer thickness on acoustic intensity.

generally stands normal to the surface so defined; thus, the acoustic energy which is generated is transmitted across this surface.

As indicated in Table 5-2, significant amounts of energy can be dissipated due to acoustic resonance. The energy which sustains acoustic resonance must necessarily be drawn from the freestream. Thus, it would be desirable from the standpoint of conserving the energy of the freestream to suppress the intensity of acoustic resonance, if not to completely eliminate its occurrence. It is interesting to note in Table 5-2 that a slight increase in the thickness of the approaching boundary layer can result in a sizable drop in the power dissipated as acoustic energy. This tendency of the boundary layer thickness to suppress resonance is graphically displayed in Figure 5-18, in which the acoustic intensities and the approaching boundary layer thicknesses from Table 5-2 are plotted against one another.

### 5.5 Shear Layer Oscillation

A phenomenon related to edge-tones has been suggested by Rossiter (8) as a possible driving mechanism for acoustic resonance in cavities. Alternatively, a number of investigators have suggested vortex shedding off the forward edge of the cavity as the cause of resonance; hence, there is interest in Roshko's (26) work on vortex shedding off cylinders. Brown's (16) work concerning edge-tones has shown that acoustic frequencies generated by this phenomenon vary with jet velocity and jet length. Roshko's

analysis of vortex shedding off cylinders has demonstrated that the frequency of shedding varies in a linear fashion with velocity. Hence, if either edge-tones or a phenomenon related to vortex shedding off cylinders were the sole cause of acoustic resonance in cavities, it would be expected that the frequency of the acoustic field would vary continuously with velocity. However, the present experiments have shown that the resonant frequency remains essentially constant throughout a range of freestream velocities. The insensitivity of the resonant frequency to freestream velocity implies that the acoustic response of the cavity controls the frequency of the acoustic field as has been concluded by Chanaud (14) rather than any perturbations in the freestream flow field.

A number of investigators (13, 14, 15, 17) have suggested that a feedback mechanism involving the free shear layer spanning the cavity opening and a reflected pressure wave from within the cavity is responsible for acoustic resonance in cavities. Their concept proposes that a perturbation in the flow field over the cavity initiates acoustic resonance. The shedding of vortices off the forward edge of the cavity is generally resorted to as an explanation for the perturbations. The perturbations cause an excess of mass to be fed into the cavity. The excess mass either stagnates on the rear wall of the cavity or isentropically recompresses within the cavity giving rise to an increase in

pressure within the cavity. When flow conditions are conducive to acoustic resonance, the influence of the reflected pressure waves on the shear layer over the cavity sustains the shedding of vortices (perturbations in the shear layer), which in turn sustain the periodic injection of fluid into the cavity.

Charwat (7) and Krishnamurty (2) proposed similar concepts of the driving force for resonance which are analogous to that described above. However, Charwat and Krishnamurty have suggested that oscillations of the shear layer itself, rather than perturbations in the shear layer, initiate and sustain resonance. As the shear layer oscillates about some mean position, fluid is alternately injected into and drawn out of the cavity, sustaining the pressure fluctuations within the cavity, which in turn induces the oscillation of the shear layer. Data taken in the present investigation supports the concept that shear layer oscillation is the sustaining force for acoustic resonance.

A hot-wire probe was mounted in the shear layer over a resonating cavity. The freestream velocity and mixing length was 66 fps and 1.9 inches, respectively. The signal from the hot-wire anemometer was fed into a 1/3-octave spectrum analyzer (General Radio Type 1912 Third-Octave Recording Analyzer) and a spectral analysis was carried out over a frequency range from 3 cps to 2500 cps. A typical distribution of the time-dependent (fluctuating) velocity component over this frequency range is shown in Figure 5-19. The velocity spectrum was measured at different y-coordinates in the

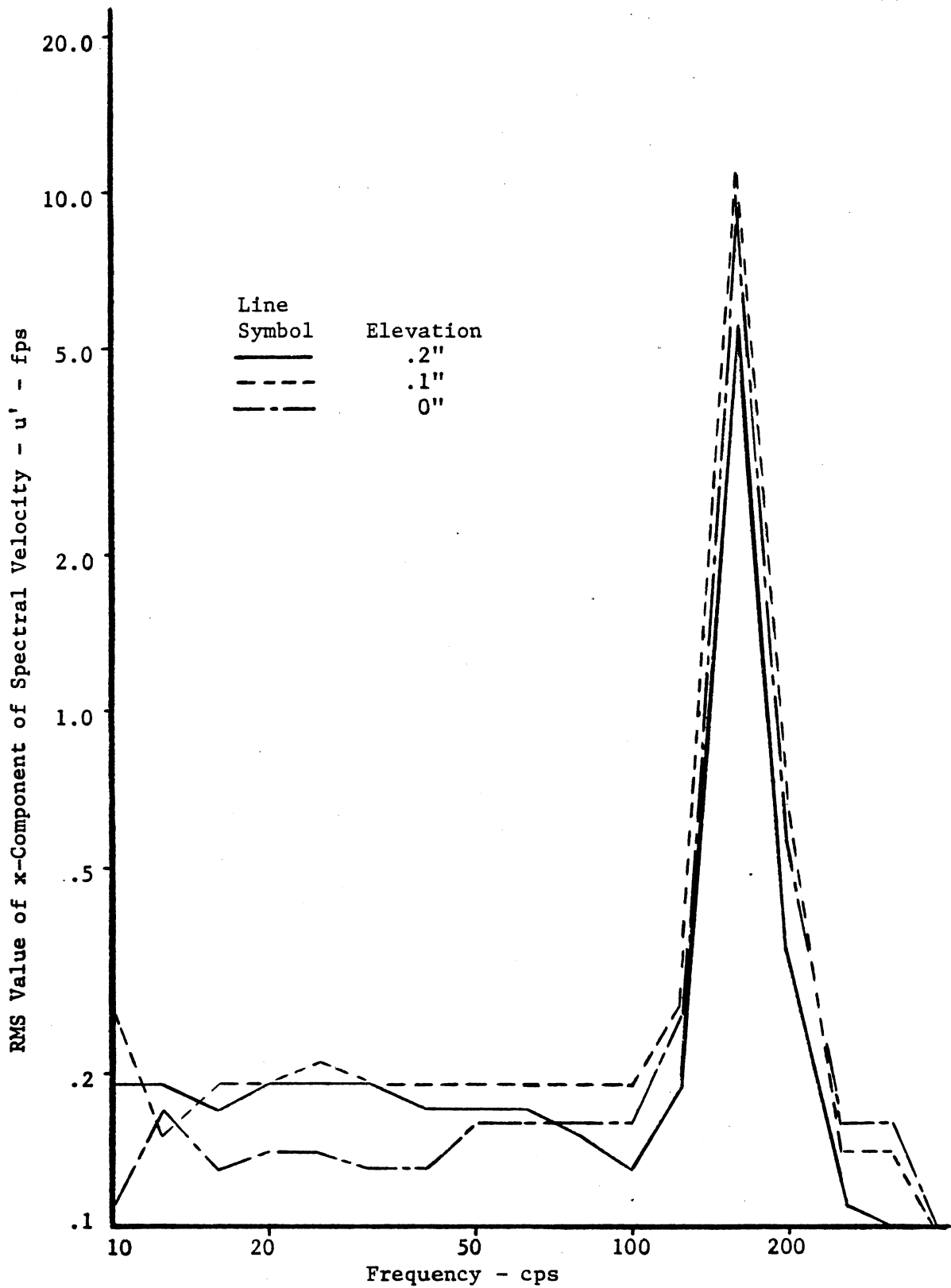


Figure 5-19. Frequency spectrum of the time-dependent, x-component of velocity in the shear layer.



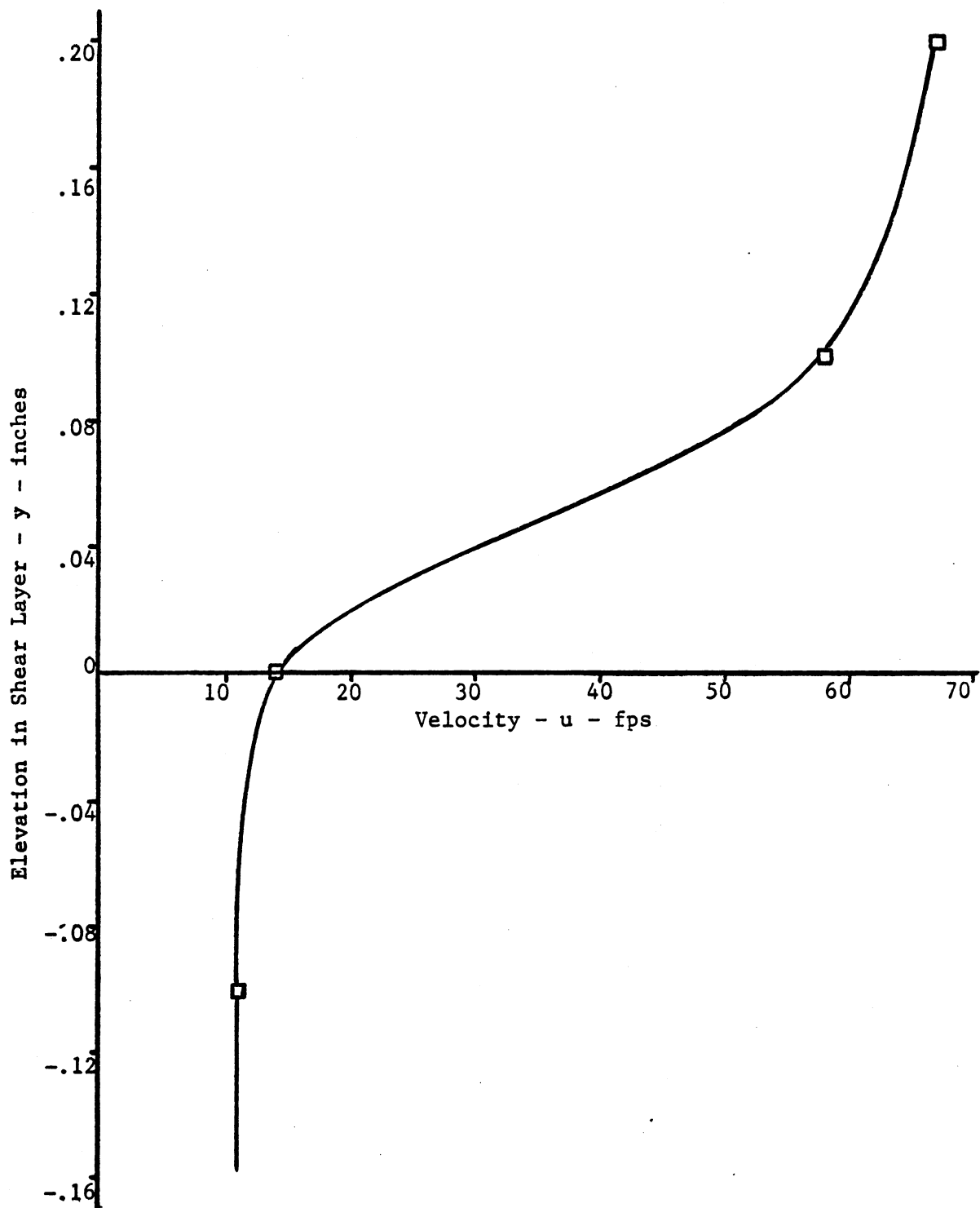


Figure 5-20. Time-mean velocity profile in shear layer.

shear layer while holding the x-coordinate constant. The time-mean velocity profile of the shear layer, shown in Figure 5-20, was also measured by the hot-wire anemometer.

The information presented in Figure 5-19 is the frequency spectrum of the fluctuating velocity component in the x-direction ( $u'$ ). A photographic record of the hot-wire signal as monitored on an oscilloscope is shown in Figure 5-21. Isolation of the stream-wise velocity component as the monitored signal was assured because the hot-wire was mounted horizontally at right angles to the freestream flow direction. Therefore, only fluctuations in the x-component of velocity produce a significant change in the magnitude of the resultant velocity vector across the hot-wire (27). It is noted in Figure 5-19 that the frequency spectrum is rather even-valued except for an abrupt jump centered at 160 cps. The magnitude of the jump varies with the height at which the hot-wire was mounted in the shear layer. However, the disturbance is entirely due to fluctuations in the streamwise velocity component. Evidently, what has happened is that the shear layer was set into oscillation during resonance. Due to the velocity gradient in the shear layer, the hot-wire anemometer monitored a fluctuating signal as the shear layer oscillated across the hot-wire (see Figure 5-22). The magnitude of the sharp increase in the frequency spectrum would be dependent on the magnitude of the mean velocity gradient at the particular elevation at which the hot-wire was mounted in the

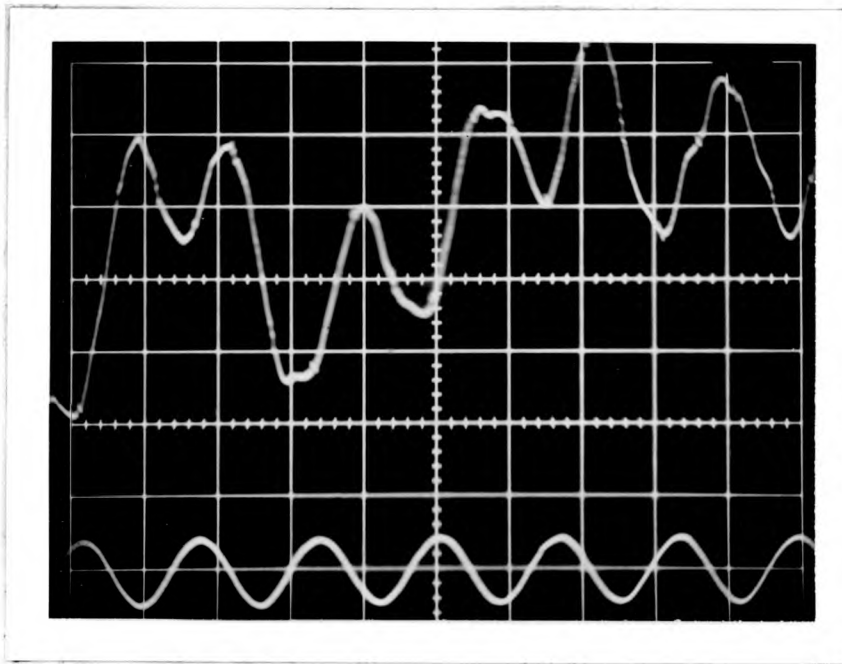


Figure 5-21. Hot-wire signal as monitored in shear layer.  
(Hot-wire signal - top; Kistler transducer  
signal - bottom)

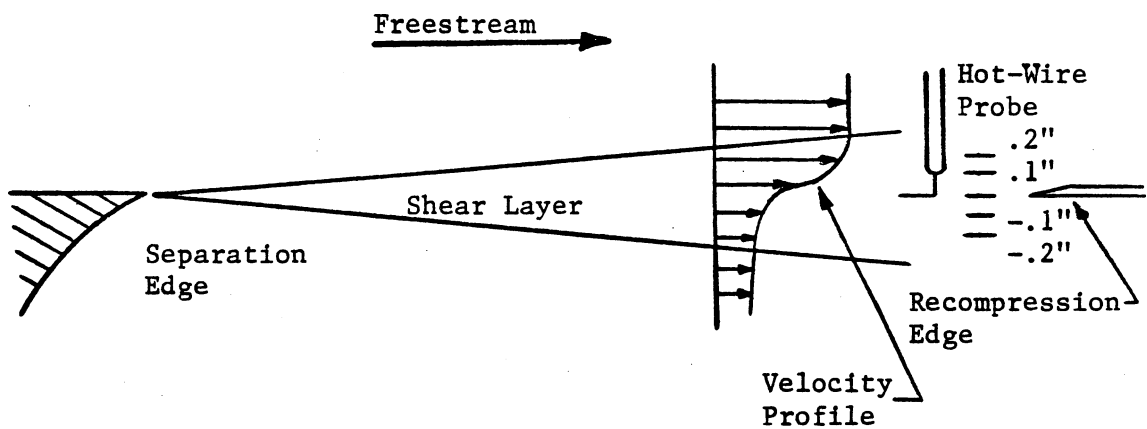


Figure 5-22. Orientation of hot-wire within shear layer.

shear layer. It is expected that the magnitude of this jump would increase as the velocity gradient in the shear layer increased. That this is the case can be seen in Table 5-3 which lists the peak-to-peak spectral velocities, for the center frequency at which the jump occurs, and the mean velocity gradients for the elevations at which data was taken in the shear layer.

The spectral velocities refer to the magnitude of the velocity fluctuation within the bandwidth centered around each center frequency used during the spectral analysis of the hot-wire signal. The actual "raw" data obtained from the analyzer is a rms voltage signal related to the fluctuating velocity component within the particular bandwidth. Raw data for the frequency spectrums taken at elevations of +.2, +.1, and 0 inches in the shear layer are depicted in Figure 5-23. The voltage in each bandwidth is related to the magnitude of the velocity fluctuation within that given bandwidth. The magnitude of the spectral velocity within each bandwidth may be calculated by referring to the calibration curve for the hot-wire anemometer, one of which is shown in Figure 5-24, for the particular hot-wire used during the spectral analysis. The slope of the calibration curve is graphically determined at the mean velocity for each elevation in the shear layer at which a spectral analysis was carried out. These slopes are then multiplied by the corresponding spectral voltage in each bandwidth in order to obtain the spectral velocity for each bandwidth.

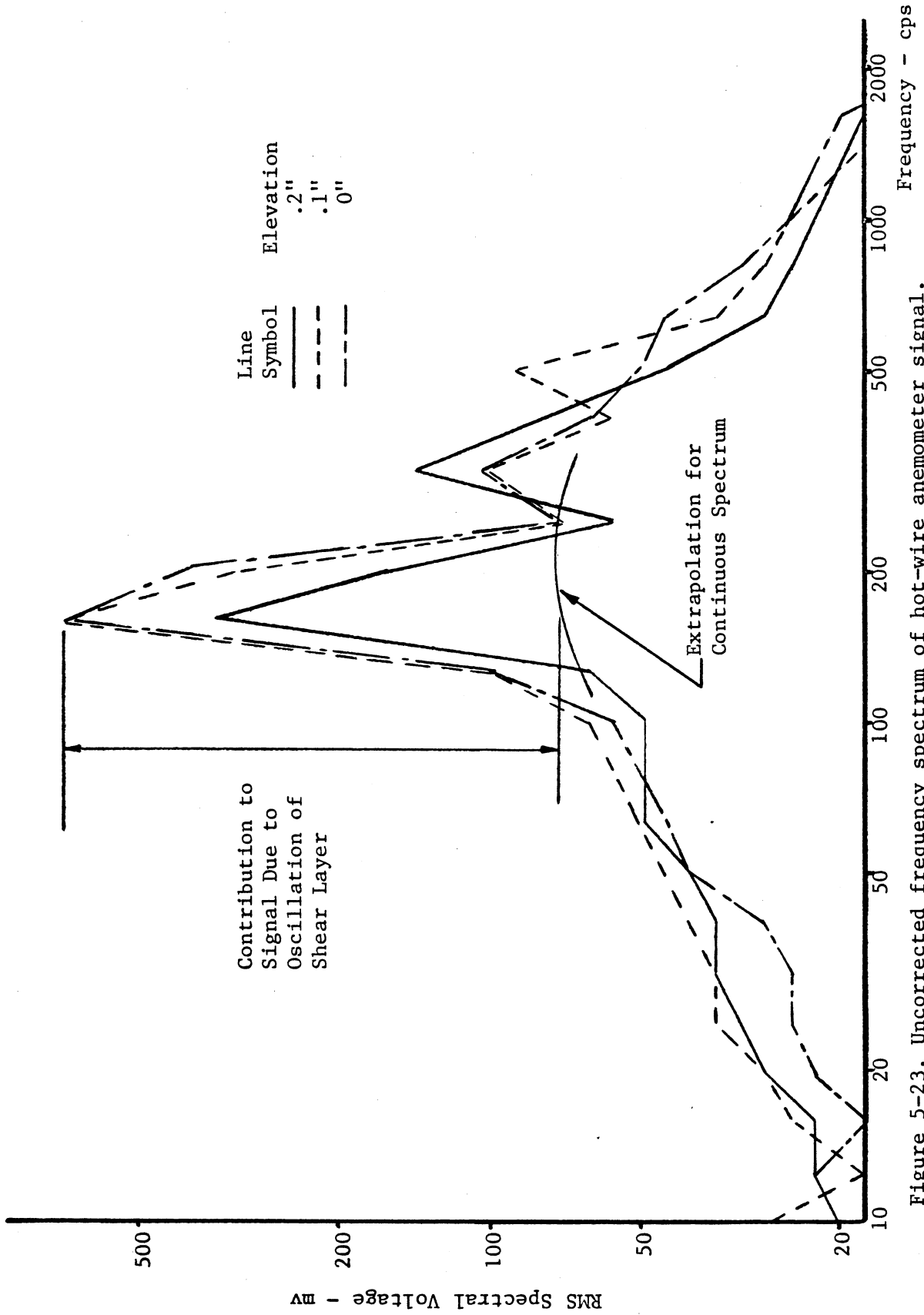


Figure 5-23. Uncorrected frequency spectrum of hot-wire anemometer signal.

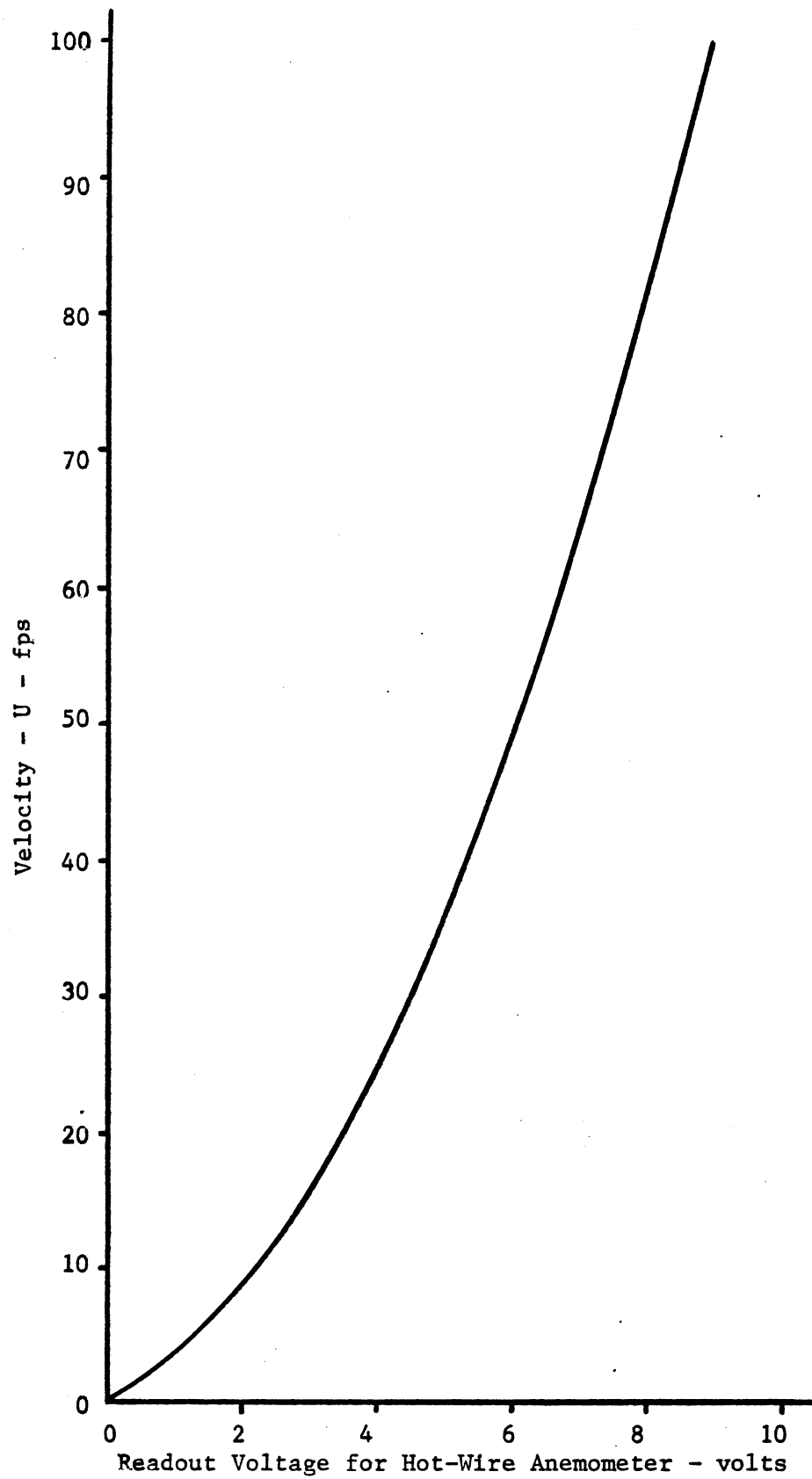


Figure 5-24. Typical calibration curve for the hot-wire anemometer.

$$\text{spectral velocity (u'-fps)} = \left[ \begin{array}{l} \text{slope of} \\ \text{calibration} \\ \text{curve} \end{array} \left( \frac{\text{fps}}{\text{volt}} \right) \right] \times \left[ \begin{array}{l} \text{spectral} \\ \text{voltage} \end{array} \text{ (volts)} \right]$$

Since the bandwidth for a 1/3 octave analyzer increases linearly with the magnitude of the center frequency, a correction must be applied to the raw data to account for the relative increase in the strength of the signal passed through the analyzer at the wider bandwidths centered around the higher frequencies (28). However, this correction is to be applied only to a signal which is continuous and contains no prominent pure-tone components. The raw data depicted in Figure 5-23 has an abrupt jump at the bandwidth centered around 160 cps. It is interesting to note that the frequency of the acoustic field for the particular resonant condition present during the spectral analysis, as recorded by the Kistler transducer, was 172 cps which is within the bandwidth centered at 160 cps. It is then reasonable to assume that the nature of the jump in the raw data spectrum as depicted in Figure 5-22 was effected by the acoustic resonance and that the larger magnitude of the spectral voltage at the center frequency of 160 cps is due to a signal of large amplitude being passed through the analyzer at a frequency of 172 cps.

The continuous velocity spectrum is due to the turbulent nature of the flow in the shear layer. The contribution of turbulence to the time-dependent velocity component cannot be neglected at the frequency at which the peak signal is monitored.

Consequently, the magnitude of the turbulent contribution is subtracted from the peak signal in order to isolate the contribution to the signal induced by the oscillation of the shear layer. The contribution to the spectral voltage centered at 160 cps due to flow turbulence is approximated by an extrapolation of the frequency spectrum as indicated in Figure 5-23. The voltage signal reflecting the influence of the oscillation of the shear layer caused by acoustic resonance is also indicated.

Since the contribution due to oscillation of the shear layer to the spectral voltage centered at 160 cps is passed through the analyzer at a known frequency (the resonant frequency of 172 cps), the aforementioned correction accounting for changes in bandwidth is not applied to that portion of the spectral voltage caused by oscillation of the shear layer. However, the continuous frequency spectrum, which is due to turbulence in the flow, as monitored by the analyzer as well as the extrapolated curve through the bandwidth centered around 160 cps are corrected in the manner discussed by Peterson and Gross (28). The above interpretation of the spectral voltages was used to calculate the spectral velocities appearing in Figure 5-19.

The magnitude of the deflection of the oscillating shear layer was calculated as being equal to the spectral velocity divided by the velocity gradient taken at the elevation at which the spectral velocity was measured. The velocity gradient at the various elevations in the shear layer was taken as being equal to the slope



of a tangent to the velocity profile as represented in Figure 5-20. The deflection of the shear layer as calculated from the following formula is included in Table 5-3.

$$\text{deflection of shear layer (inches)} = \frac{\text{spectral velocity (fps)}}{\text{velocity gradient (fps/inch)}}$$

Table 5-3. Summary of data from which the shear layer deflection is calculated.

Elevation in Shear Layer	Spectral Velocity at 160 cps (peak-to-peak)	Velocity Gradient from Mean Velocity Profile	Deflection of Shear Layer
inches	fps	fps/inch	inches
.2	27.2	46.	.5
.1	27.2	250.	.1
0	10.4	167.	.07

At this time a second correction applied to the spectral velocity monitored at the resonant frequency during the spectral analysis must be mentioned. The voltage output of the analyzer is an rms signal. However, the peak-to-peak signal is of interest in calculating the peak-to-peak oscillation of the shear layer. Assuming the waveform of the spectral velocity monitored at the resonant frequency to be sinusoidal, one can easily calculate the peak-to-peak signal from the rms output of the analyzer.

It is encouraging that the shear layer deflection as calculated for the elevations  $y = 0$  and  $y = .1$  inches are approximately equal. This means that the above method of calculating shear layer deflection provides for equal deflections in the vertical direction as would be expected. If this were not the case the shear layer would be compressed or rarefied as it oscillated. The deflection calculated for the elevation  $y = .2$  inches is much larger than the deflections calculated for  $y = 0$  and  $y = .1$  inches. However, it is evident from the shear layer deflections of  $.1$  and  $.07$  inches calculated for the elevations  $y = .1$  and  $0$  inches, that the steep portion of the velocity gradient will at times be deflected up to the elevation of the hot-wire when the hot-wire is mounted at an elevation of  $.2$  inches. As has been pointed out by McGregor (11), the shear layer must deflect farther toward the freestream than it does into the cavity in order to satisfy conservation of mass. Thus, it is probable that the velocity gradient as obtained from the mean velocity profile underestimates the actual variations in mean velocity monitored by the hot-wire at an elevation of  $.2$  inches. This would lead to the calculation of shear layer deflections for that elevation which are much too large.

Krishnamurty (2) suggested as a possible driving force for acoustic resonance in rectangular cavities a feedback coupling between the resonant acoustic pressure field and a fluctuation of the shear layer oscillating at the same frequency as that of the

acoustic pressure field. The pressure disturbances were sustained by the shear layer deflecting into the cavity and impinging on the rear wall of the cavity. He considered as a necessary condition that the fluid within the shear layer stagnated on the rear wall of the cavity creating the pressure disturbance. The present investigation, as well as that of Miles (3), indicates that the restriction that the shear layer must impinge and stagnate on the rear cavity wall in order to sustain resonance must be modified to be applicable to acoustic resonance in circular cavities. Circular cavities provide no such bluff surface on which the shear layer can impinge and stagnate; instead, the shear layer oscillates about the sharp recompression edge. The abruptness of the stagnation process is mitigated somewhat by the curvature of the circular cavity walls which tend to change the direction of the flow rather than abruptly stagnate the fluid. Thus, the production of the resonant acoustic field can probably be more accurately described as being the result of an isentropic recompression of the fluid injected into the cavity rather than the consummate stagnation of fluid impinging on a bluff surface.

#### 5.6 Influence of Acoustic Resonance on Cavity Flow Field

Velocity profiles of the cavity wake taken with a hot-wire anemometer are shown in Figure 5-25. The data points on either side of the vertical diameter of the cavity were monitored with

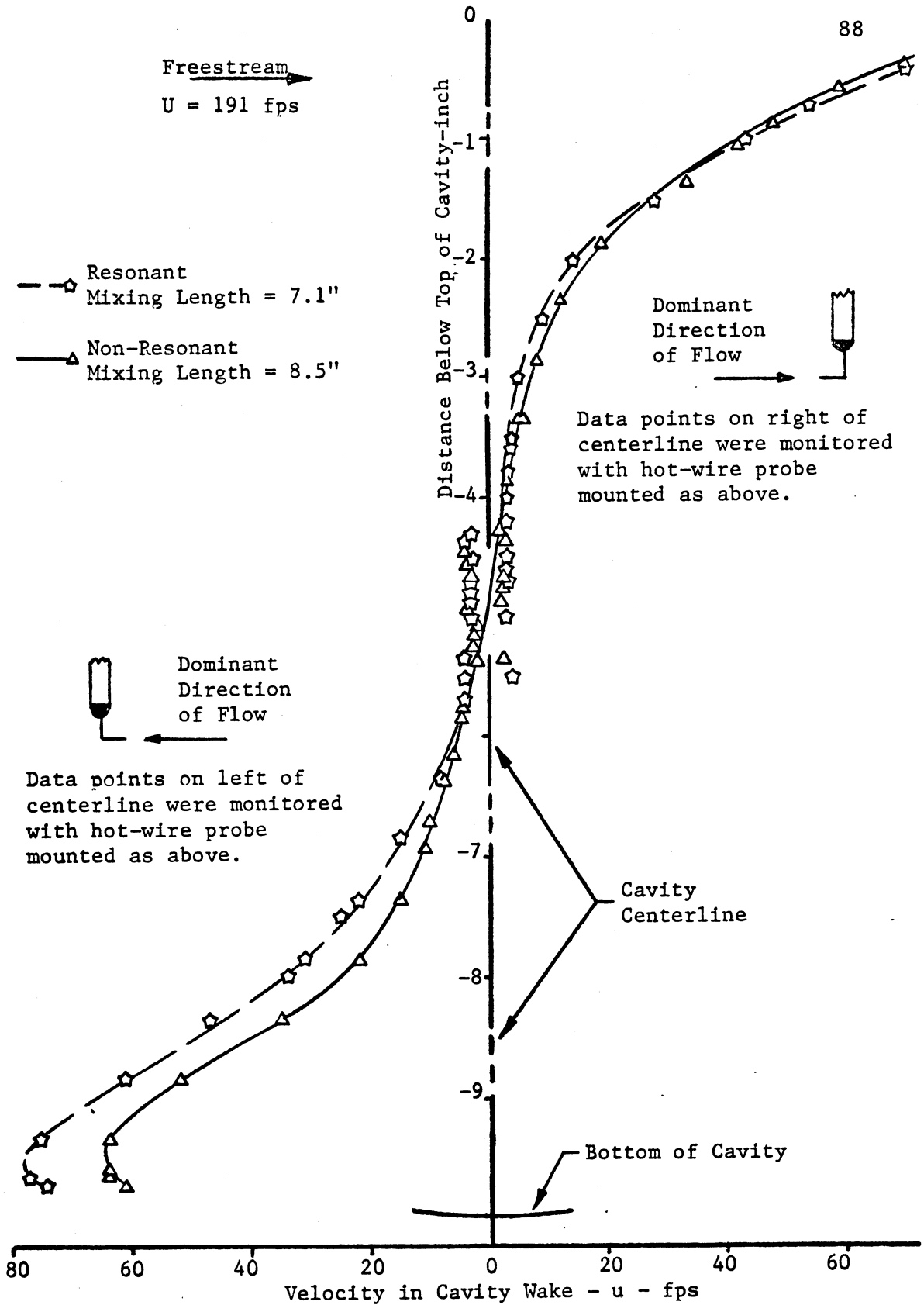


Figure 5-25. Comparison of velocity profiles along cavity centerline for resonant and non-resonant conditions.

the boundary layer hot-wire probe mounted in opposite sense and with the wire horizontally oriented. This was done in an effort to locate a point of zero velocity in the central region of the cavity. No point of zero velocity was monitored, but there apparently does exist a rather broad region, extending over approximately 25% of the cavity diameter, of very low velocity flow in the central portion of the cavity. The higher velocity flow is injected into the cavity near the cavity wall and is held there by centrifugal forces.

In Figure 5-25 the velocity profiles of the cavity wake are compared for resonant and non-resonant conditions. The length of the cavity opening was set at 7.1 inches in order to induce tuned acoustic resonance in the cavity. A reasonably comparable flow configuration was achieved by increasing the mixing length to 8.5 inches while holding the freestream velocity constant. As noted in Figure 5-25, the cavity wake velocities recorded during acoustic resonance were appreciably higher than those recorded during the non-resonant conditions. This is particularly significant in light of the fact that the length of the mixing region during the non-resonant condition was 20% longer than the mixing length required to achieve the resonant condition. The longer mixing region itself would have the effect of inducing higher wake velocities in the cavity because of the longer length over which fluid entrainment could take place. Evidently, the influence of

acoustic resonance on the momentum exchange between the cavity and the freestream is strong enough to more than compensate for the advantage of the longer mixing length used during the non-resonant condition. As mentioned in Chapter II, McGregor's work (11) also indicates that momentum exchange is augmented by acoustic resonance, inasmuch as measurements of cavity drag made by McGregor showed that the drag of resonating cavities was higher than the drag of non-resonating cavities subjected to comparable freestream conditions.

Coincident with the increase in momentum transfer caused by acoustic resonance is an increase in the mass flow rate between the cavity and the freestream. Evidence that the mass flow rate is increased by acoustic resonance is supported by Miles' (3) experimental work. The drop by 50% in the differential bulk temperature of the cavity fluid that Miles observed with the onset of acoustic resonance cannot be solely attributed to changes in the nature of the heat transfer between the cavity wall and the cavity fluid. Relatedly, Jackson et al. (29) and Eastwood et al. (30) have determined by means of some experiments that local convective heat transfer coefficients can be affected by an interaction between a standing acoustic pressure wave and the thermal boundary layer along an isothermal surface. Above a certain Reynolds number the resonant acoustic vibrations tended to suppress the overall heat transfer rate. But Purdy's and Eastman's work would

indicate that the overall insulating effect of a standing acoustic pressure wave is not substantial enough to produce the rather drastic drop in bulk temperature that Miles noted during acoustic resonance. The drop in the bulk temperature that Miles detected was evidently due to a major increase in heat transfer between the cavity and the freestream caused by appreciably more fluid being fed into and subsequently passed from the cavity due to shear layer oscillation than would occur by shear layer entrainment alone.

It is rather apparent that acoustic resonance does increase the fluid exchange rate between the cavity and the freestream. The mass exchange model proposed by Charwat (7) describes the basic nature of the contribution of acoustic resonance to fluid transfer between the cavity and the freestream; however, Charwat's model assumes the entire mass flow rate to be the result of the pulsating nature of the flow caused by oscillation of the free shear layer. However, mass flow rates are known to exist between cavities and the adjacent freestream when acoustic resonance is not present. Evidently, the mass flow mechanism during acoustic resonance is the sum of a steady state mass flow rate and a periodic, time-dependent mass exchange. The steady state mass transfer is due to the entrainment of fluid by the shear layer. The time dependent contribution is due entirely to oscillation of the shear layer and accounts for the increase in mass flow rates over those predicted by steady state models (3,4).

It is now mentioned in passing that the role played by the approaching boundary layer in stimulating the increase in mass flow between a resonating cavity and the freestream as deduced from experiments in the present investigation is in direct opposition to the influence which Charwat (7) proposed that the boundary layer should have. Charwat theorized that the mass flow rate, and consequently the heat transfer rate, between a cavity and its freestream was directly related to the thickness of the shear layer spanning the cavity opening and suggested that a thick approaching boundary layer would cause the shear layer to thicken, thereby enhancing heat transfer. However, the present investigation has demonstrated that a thin approaching boundary layer enhances acoustic resonance which in turn sustains oscillation of the shear layer and ultimately leads to increased mass flow and heat transfer rates. Thus, it would appear that Charwat's model for the heat transfer mechanism between a cavity and a freestream does not accurately reflect the influence of the approaching boundary layer.

No theory is advanced in this writing which would allow calculation of the magnitude of the oscillation of the free shear layer about the recompression edge. Some experimentally determined values for shear layer deflection have been presented in Section 5.5. The magnitude of the shear layer deflection



is needed in order to calculate the time-dependent contribution to mass flow rate between a resonating cavity and the freestream.

#### 5.7 Effects of Perturbations in Internal and External Flow Fields on Acoustic Resonance

During resonance the cavity wake flow is well ordered with the high velocity flow staying near the cavity wall and subsequently impinging, at a slight angle, on the approaching boundary layer of the freestream at the separation edge of the cavity. To determine whether the well ordered nature of the cavity wake flow is essential to sustaining acoustic resonance, radially-oriented baffles were placed along the cavity wall over the full width of the cavity so as to induce a disordered flow field in the cavity. The effect of location of the baffle on the acoustic response of the cavity was investigated by mounting a single baffle along three different cavity diameters during individual tests. The positions at which the baffles were mounted are depicted in Figure 5-26. Two baffles with heights of 2 and 4 inches were used separately during these tests in order to control, to some extent, the degree to which the cavity wake flow was disturbed. The effect of the level of the flow disturbance on acoustic resonance could then be observed.

The influence of the presence of baffles within the cavity on the different normal modes of resonance is of interest and was investigated. To accomplish this, the mixing length and

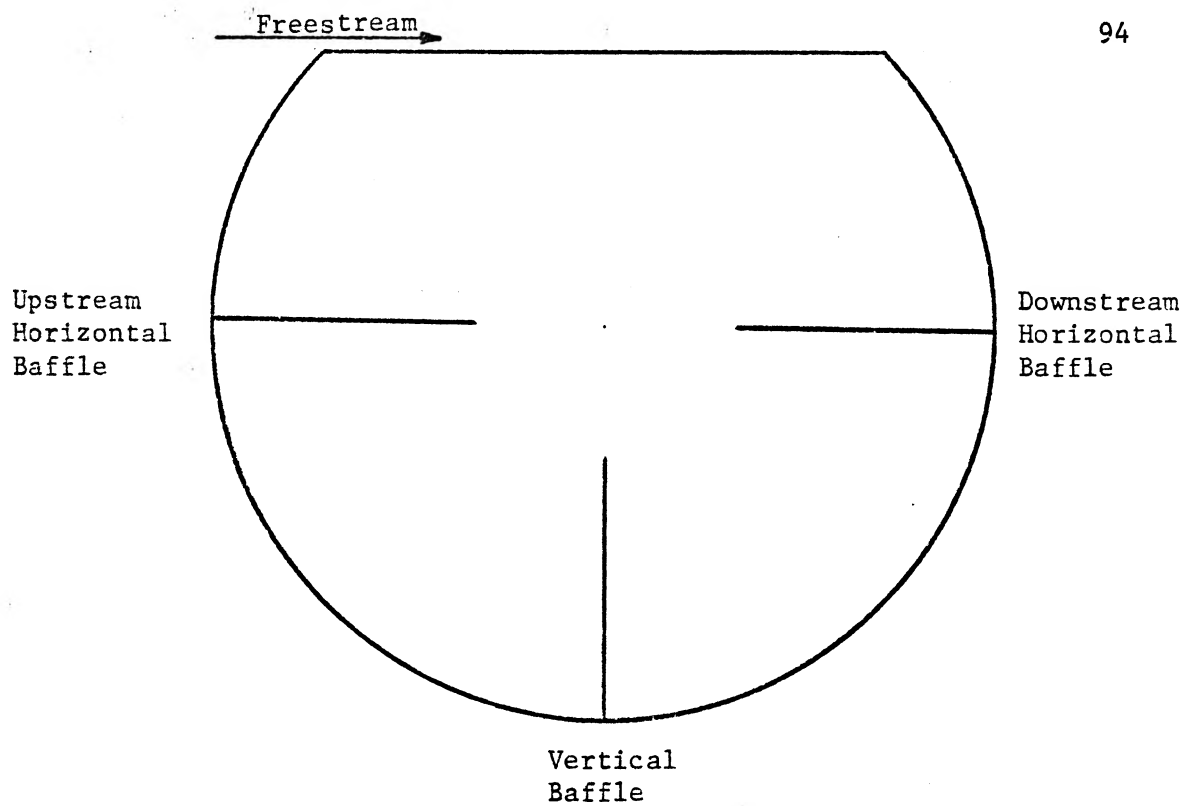


Figure 5-26. Orientation of baffles within cavity.

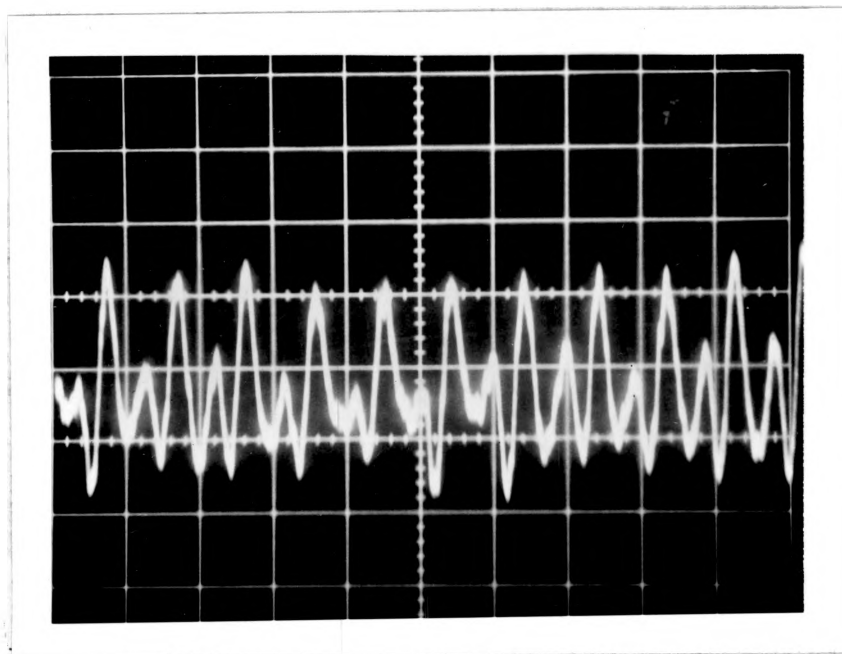


Figure 5-27. Kistler transducer signal as monitored when the 4 inch baffle was mounted vertically within the cavity. ( $U = 121$  fps; Mixing Length = 5.5")

freestream velocity were adjusted to achieve a tuned resonant condition for each mode and the frequency and maximum amplitude of the acoustic pressure wave were recorded. This procedure was followed for each of the three baffle orientations. Some typical data are presented in Tables 5-4, 5-5 and 5-6. The pressure amplitudes indicated in these tables were averaged over several periods. The 2 inch baffle was not mounted in the upstream horizontal position.

It is noted in Table 5-4 that the amplitude of the acoustic pressure wave in the Helmholtz mode of resonance is affected only by the location and not by the size of the baffle. The baffle damps the amplitude of the pressure wave less as the baffle is moved away from the recompression edge. It was also noted that the sinusoidal character of the pressure wave is impaired by the presence of a baffle. A photographic record of the acoustic pressure wave as monitored by the Kistler transducer is shown in Figure 5-27 for the case of the 4 inch baffle being mounted vertically within the cavity. As is indicated by the waveform of the pressure wave, there appears to be two waves of nearly equal frequency but different amplitudes superimposed on one another. This was typical for a number of resonant conditions when baffles were present in the cavity. The frequencies included in the tables for this type of resonant condition are the frequencies corresponding to the period as obtained between successive peaks

of the pressure signal, such as shown in Figure 5-27, regardless of the amplitude of the peak. This interpretation of the dominant frequency for these particular resonant modes provides frequencies which are similar to the normal frequencies recorded when baffles were not present in the cavity.

The half-wave mode of resonance, described in Table 5-5, could not be sustained when a baffle was present in the cavity; however, a low frequency and relatively strong resonant condition did supplant the half-wave mode. It is interesting to note that acoustic pressures of larger amplitude were attained when the 2 inch baffle was mounted vertically at the bottom of the cavity than when no baffles were within the cavity.

The full-wave mode of resonance (Table 5-6) was least affected by the presence of baffles. This is probably due to the fact that a relatively small mixing length was required to achieve this mode of resonance and consequently the fluid velocities induced in the cavity were not great. Thus, there is only slight stagnation of fluid against a baffle and the original resonant mode is not greatly affected by the presence of a baffle. The switch from the full-wave to the half-wave mode of resonance when the 4 inch baffle was mounted vertically was probably due to the fact that the acoustic characteristics of the cavity were changed by the baffle being so oriented (it is noted that the 4 inch baffle induces no change in the resonant mode when the baffle is mounted along the horizontal diameter).

Table 5-4. Effect of baffles on the Helmholtz mode of resonance (U = 121 fps, X = 6.9").

Baffle Size	Baffle Orientation	Resonant Frequency	Amplitude of Acoustic Pressure
inches	----	cps	psi
No Baffle	No Baffle	245	.075
4	Downstream Horizontal	176	.022
2	"	220	.022
4	Vertical	176	.027
2	"	230	.027
4	Upstream Horizontal	195	.038

Table 5-5. Effect of baffles on the half-wave mode of resonance (U = 121 fps, X = 5.5").

Baffle Size	Baffle Orientation	Resonant Frequency	Amplitude of Acoustic Pressure
inches	----	cps	psi
No Baffle	No Baffle	720	.055
4	Downstream Horizontal	245	.055
2	"	240	.038
4	Vertical	127	.044
2	"	196	.076
4	Upstream Horizontal	123	.050

Table 5-6. Effect of baffles on the full-wave mode of resonance (U = 132 fps, X = 1.1").

Baffle Size	Baffle Orientation	Resonant Frequency	Amplitude of Acoustic Pressure
inches	---	cps	psi
No Baffle	No Baffle	1150	.030
4	Downstream Horizontal	1150	.025
2	"	1150	.018
4	Vertical	600	.009
2	"	1150	.011
4	Upstream Horizontal	1030	.023

In general, the resonant mode sustained when baffles were mounted in the cavity was one of lower frequency than was sustained when the baffles were not present. The sinusoidal character of the wave form was generally not preserved; however, the flow disturbances caused by the presence of baffles do not completely suppress acoustic resonance as it was defined in Chapter III. It may then be concluded that the structure of the flow field internal to the cavity is not critical to sustaining resonance, but does influence the nature of the resonance.

The character of the flow field external to the cavity does have a rather pivotal effect on the occurrence and on the nature of acoustic resonance as is evidenced by the previously mentioned influence of the approaching boundary layer. The dependence of the occurrence of resonance on the nature of the freestream flow field was further investigated by means of an experiment discussed herein. Large scale, time-dependent perturbations in velocity were induced into the freestream flow field by hinging one side of a quarter-inch thick sheet of aluminum honeycomb to a rod mounted normal to the freestream and positioned within the converging section of the nozzle (see Figure 5-28). The sheet spanned the nozzle section and measured 1' x 3.5'. Interaction with the freestream caused the sheet to oscillate, which in turn resulted in low frequency (10 to 100 cps) disturbances in the freestream. A freestream flow field disturbed in the above manner will be referred to as a perturbed freestream.



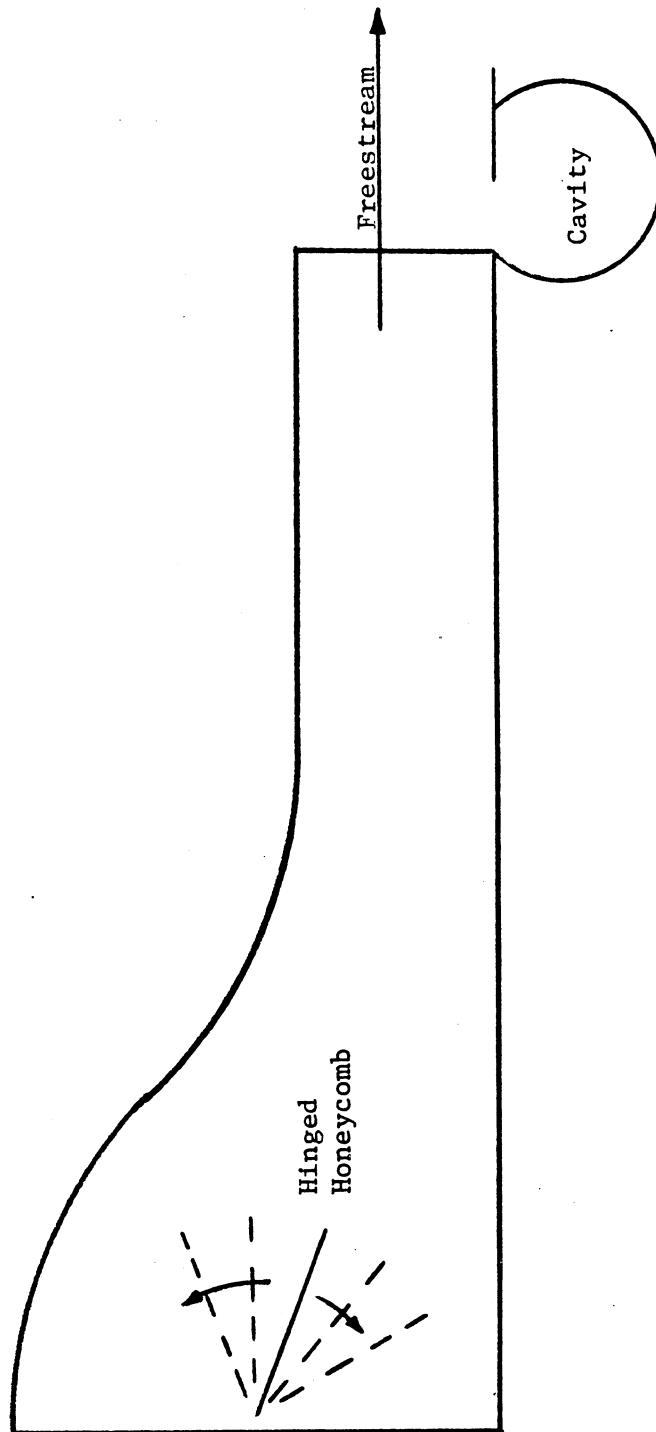


Figure 5-28. System used to generate a perturbed freestream.

It is interesting to compare the frequency spectrums of a signal from a hot-wire mounted in the middle of the freestream as monitored for a perturbed flow and for a freestream that is not perturbed (quiescent freestream). The comparison is shown in Figure 5-29. It is evident from Figure 5-29 that velocity perturbations in the quiescent freestream are at least an order of magnitude smaller than the velocity disturbances in the perturbed freestream.

The perturbed freestream was not able to induce acoustic resonance in the cavity throughout the entire range of velocities (40 fps to 180 fps) and mixing lengths (0 to 8.75 inches) even for the case of full boundary layer removal. Experiments carried out in this investigation have shown that only the quiescent freestream is able to induce resonance in the cavity.

The fact that a freestream must be relatively free of flow perturbations in order to induce acoustic resonance in cavities largely invalidates Plumbee's (19) contention that noise in the approaching boundary layer is the sustaining force for resonance. Evidently the cavity must be able to impose one of its own natural frequencies on the flow field in the vicinity of the cavity opening, which in turn sustains acoustic resonance in the cavity. If certain large-scale perturbations do exist in the freestream, the delicate timing of the feedback coupling between the acoustic

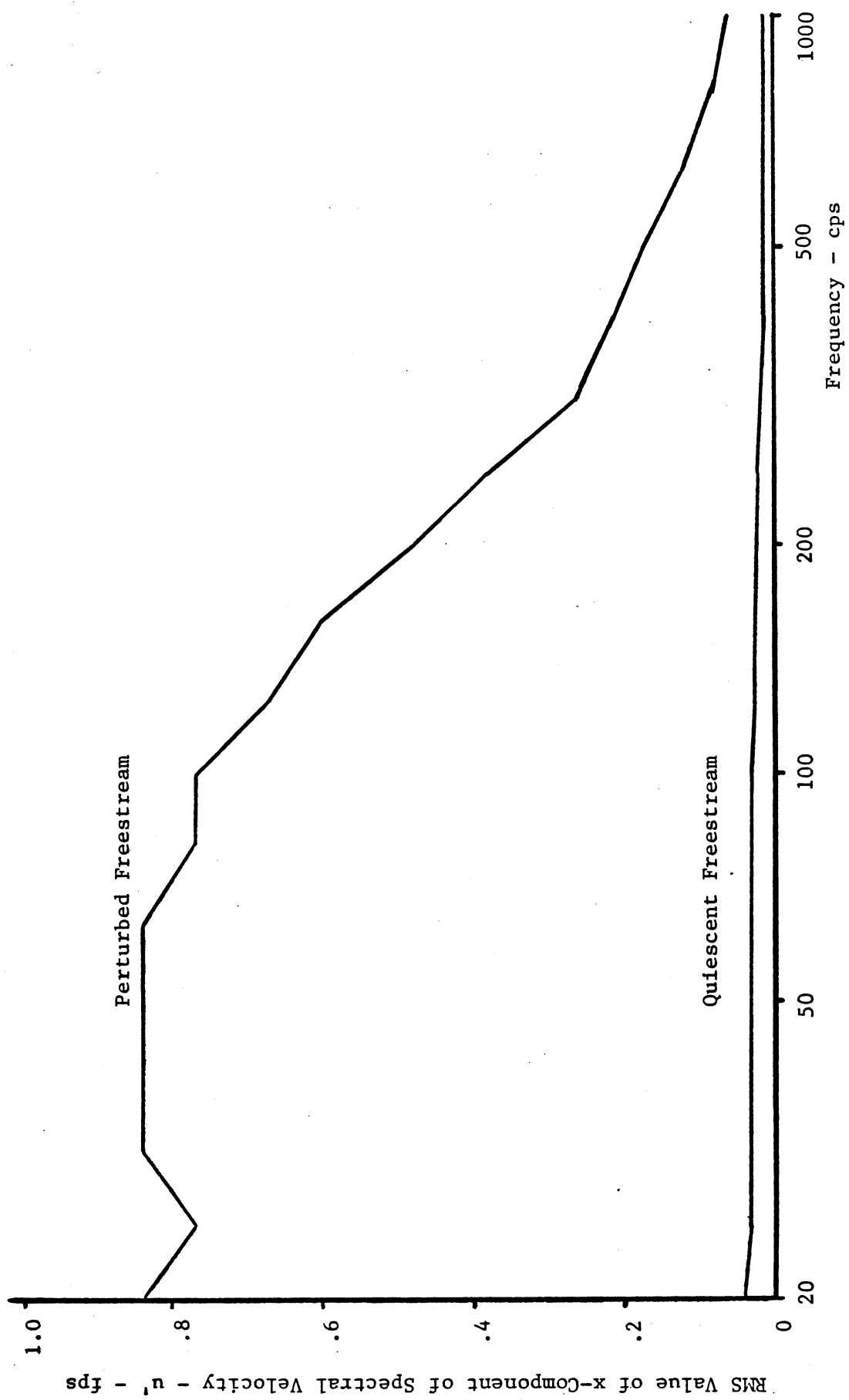


Figure 5-29. Comparison of frequency spectrums of hot-wire anemometer signals for perturbed and quiescent freestreams.

pressure wave and the oscillation of the shear layer is upset and acoustic resonance is not sustained.

#### 5.8 Effect of Reducing the Width of the Mixing Region on the Acoustic Response of the Cavity

As outlined in Chapter II, White's (20) theory for predicting acoustic resonance in cavities dealt with a characteristic time based on the rate of fluid entrainment by the shear layer. If his theory holds rigorously, the frequency of the acoustic field induced in the cavity should vary linearly with the rate at which fluid is pumped out of the cavity. The entrainment mass flow rate between the cavity and the freestream may be approximately linearly controlled by varying the width of the mixing region. A check on White's theory was effected by tuning the cavity to a given resonant condition and then recording any changes in the resonant response as the width of the cavity opening was decreased. The width of the mixing region was controlled by sliding "curtains" (1/16" aluminum sheeting) over the cavity opening from both sides of the cavity in such a manner that the "exposed" mixing region was situated over the center of the cavity. Some typical results of such a test are shown in Table 5-7.

It is seen that the amplitude of the acoustic pressure wave decreases somewhat linearly with the width of the mixing region.

Table 5-7. Summary of data which indicates the effect of reducing the width of the mixing region on resonance.

Freestream Velocity = 166 fps			Mixing Length = 6 inches	
Exposed Width of Mixing Region	% Exposed Width	Resonant Frequency	Amplitude of Acoustic Pressure	% of Maximum Pressure
inches	---	cps	psi	---
9.0	100%	720	.176	100%
4.5	50%	216	.11	62%
2.25	25%	172	.07	40%
1.125	12.5%	161	.042	24%
1.0	11.1%	159	.028	16%
0.5	5.5%	108	.07	4%

This might be expected because the momentum transfer from the freestream to the cavity is linearly decreased as the width of the mixing region decreases. It is also noted that the resonant frequency is decreased by a reduction in the width of the mixing region, and that the mode of resonance can be caused to switch to a lower other mode. A number of tests have shown that a reduction in mixing width invariably leads to a lower resonant frequency; however, the frequency of the acoustic field does not exhibit the linear dependence on mass flow rate as White has postulated. However, there does appear to be some relationship between the magnitude of the resonant frequency and the mass flow rate between

the cavity and the freestream as is indicated by the fact that the frequency continually decreases as the contact of the cavity flow field with the freestream is decreased, albeit not a linear dependence. Of course, the change in resonant frequency may be a result of a change in the normal resonant modes of the cavity due to the inherent change in geometry of the cavity caused by changing the area of the cavity opening. Also, the two-dimensional nature of the cavity is altered somewhat by the use of curtains to reduce the width of the cavity opening, which in turn may stimulate the sustaining of a three-dimensional wave within the cavity.

## CHAPTER VI

### CONCERNING METHODS FOR PREDICTING AND CONTROLLING ACOUSTIC RESONANCE

#### 6.1 Analysis of White's Prediction Theory

White's (20) theory for predicting acoustic resonance is based on matching a characteristic pumping time with one of the possible periods of the resonant acoustic field. The characteristic pumping time employed by White was originally defined by Ihrig et al. (21) and developed by Addy (22). This characteristic time, as it was used by Addy and Ihrig, was considered to be the time required to establish steady state flow conditions in a separated region by means of turbulent mixing, and resulting entrainment, with a primary stream. Such a system is quite similar to cavity flow. The volume of the cavity constitutes the separated region and the present freestream may be considered to be the primary flow field.

The characteristic pumping time for the cavity is defined by White as

$$t_c = \frac{M_c}{W_s} \quad \text{Eq. 6-1}$$

where

$$W_s = \frac{\rho (1 - C_r^2) \rho U}{\rho} I_{1j} \quad \text{Eq. 6-2}$$

$M_c$  is the mass of the fluid within the cavity, and  $W_s$  is the pumping rate due to fluid entrainment as calculated from Korst's mixing theory (10).  $I_{1j}$  is a mass flow integral tabulated by Korst (31) and  $\sigma$  is the single stream mixing similarity parameter. Korst presents  $\sigma$  as a function of the Mach number of the freestream:

$$\sigma = 12.00 + 2.76 M \quad \text{Eq. 6-3}$$

White's theory predicts that resonance will occur when

$$t_c = T$$

where  $T$  is the period of the resonant acoustic field.

White tested a model of a rectangular cavity on a water table at conditions which were known to induce acoustic resonance in cavities tested in transonic and supersonic wind tunnel experiments. During the water table experiments, a single dominant wave was seen to be traversing the cavity parallel to the direction of the main flow. White interpreted this wave motion to be equivalent to the dominant mode of resonance induced in cavities by the freestream in the wind tunnel tests. Accordingly, the resonant periods were calculated as being the time required for a pressure wave, moving at the acoustic velocity ( $c$ ), to traverse twice the length of the cavity opening.

$$T = \frac{2L}{nc} \quad \text{Eq. 6-4}$$

$L$  is the length of the cavity opening, and  $n$  is an integer allowing for the occurrence of multiple waves existing in the cavity opening.



Much of the data recorded in the present investigation regarding the orientation of the acoustic pressure wave within the cavity agrees with White's hypothesis that the wave is oriented parallel to the direction of the freestream. More precisely, the wave length of the acoustic wave is controlled by the internal dimensions of the cavity rather than by the length of the cavity opening as suggested by White. However, characteristic pumping times calculated from Equation 6-1 differ from the acoustic periods measured in the current investigation by at least two orders of magnitude. Further consideration of Ihrig's work shows that this result is not surprising. A simplified formulation of the characteristic response time for the adjustment of wake flow to a change in the rate of fluid entrainment by the shear layer over the separated region is given by Ihrig as

$$t_c = \frac{\sigma L}{U I_{1j}} \quad \text{Eq. 6-5}$$

The corresponding time required for adjustment to a pressure wave passing over the separated region is defined by Ihrig as being

$$t_a = \frac{L}{c} \quad \text{Eq. 6-6}$$

The ratio of the two characteristic times is

$$\frac{t_c}{t_a} = \frac{\sigma}{I_{1j}} \quad \text{Eq. 6-7}$$

It is apparent that  $t_a$  and  $t_c$  as defined by Ihrig are quite similar to the acoustic period and the characteristic pumping time, respectively, as defined by White. Using the formulation such as that presented in Equation 6-7, Ihrig calculated the ratio  $t_c/t_a$  to be roughly 30 for a freestream Mach number of unity. Within the Mach number range considered in the present investigation, the ratio of  $t_c$  to  $t_a$  (or  $t_c$  to  $T$ ) varies from 100 to 500. Thus, it cannot be expected that the period of the acoustic wave will match the characteristic pumping time for the cavity as defined by White, except possibly at very high Mach numbers.

By equating the characteristic time as defined in Equation 6-1 to the acoustic period, White had inadvertently imposed the requirement that the entire mass of the fluid within the cavity must be pumped out of the cavity during one acoustic period (or integral fraction thereof). This requirement is hardly realistic from a physical standpoint, particularly for the higher frequencies sustained in the cavity during the present investigation. For instance, the period of the acoustic field induced within a cavity with a 1.3 inch mixing length and sustained by a freestream velocity of 140 fps is .00084 seconds. In order to pump out the fluid within the cavity in .00084 seconds, the pumping rate due to fluid entrainment alone would have to be approximately 50 lbm/sec. Also, tests performed in this investigation as described in Section 5.7 have shown that acoustic resonance is not critically

dependent on the flow field within the cavity. Accordingly, it does not seem justified to base a theory for the prediction of resonance on the ability of the shear layer spanning the cavity opening to pump out the entire mass of the fluid within the cavity. Such a requirement causes the characteristic times calculated from White's theory to deviate by a considerable amount from the measured acoustic periods as is shown in Table 6-1.

Table 6-1 compares the measured acoustic periods of the resonant field with the characteristic pumping times as calculated from Equation 6-1 for flow conditions which are known to induce acoustic resonance in the cavity. Considering the cylindrical cavity used in the present investigation, the mass of fluid within the cavity per unit width is

$$M_c = \rho A \quad \text{Eq. 6-8}$$

where  $A$  is the area of the circular side of the cavity ( $A = 108 \text{ in}^2$ ).

Combining Equations 6-1 and 6-2, the characteristic time becomes

$$t_c = \frac{A \sigma}{X U I_{1j}} \quad \text{Eq. 6-9}$$

$C_r$  is essentially zero over the Mach number range used in the present investigation.

$\sigma$  may be obtained from Equation 6-3. Since the influence of Mach number on  $\sigma$  is quite small over the range of Mach numbers encountered,  $\sigma$  is taken as being equal to 12 for all freestream flows.  $I_{1j}$  is tabulated in reference 31. For isoenergetic flow

Table 6-1. Comparison of measured acoustic periods with White's characteristic pumping time for the cavity (boundary layer condition #1, full removal).

Freestream Velocity - U	Mixing Length - X	Measured Acoustic Period - T	Characteristic Pumping Time - $t_c$	$t_c/T$
fps	inches	seconds	seconds	—
210	8.75	.0015	.173	115
165	8.75	.0042	.22	52
191	7.1	.0014	.236	168
121	6.9	.0039	.382	98
234	6.4	.0014	.212	151
154	5.5	.0015	.377	250
194	3.3	.00082	.5	610
47	1.4	.006	4.85	810
140	1.3	.00084	2.05	2420
136	1.3	.00089	2.12	2830
183	.8	.00084	1.45	1730
135	.8	.00125	2.94	2350
141	.8	.0013	2.82	2170
137	.8	.0015	2.9	1930

as in the case in the present investigation, a value of .4 for  $I_{1j}$  is fairly representative for all the freestream velocities encountered.

Substituting numerical values for  $\sigma$  and  $I_{1j}$  into Equation 6-9 and using  $A = 108 \text{ in}^2$ ,  $t_c$  may be calculated for known values of mixing length (X) and freestream velocity (U) as follows:

$$t_c \text{ (seconds)} = \frac{270}{X \text{ (inches)} U \text{ (fps)}} \quad \text{Eq 6-10}$$

It is readily seen that the characteristic times based on Equation 6-1 differ from the measured acoustic periods by orders of magnitude as shown in Table 6-1. Thus, these characteristic times are evidently not related to the occurrence of acoustic resonance and refinements to White's theory are in order. Some modifications regarding the definition of the characteristic pumping time as it relates to acoustic resonance are suggested in the following section.

## 6.2 Significant Parameters for Improved Prediction Techniques

White's theory for the prediction of resonance was developed for a somewhat simplified model in that only two parameters, the freestream velocity and the characteristic dimension of the cavity, are considered to influence the characteristic pumping time for the cavity. The freestream velocity and the streamwise length of the cavity do provide sufficient information to calculate the pumping rate of the shear layer spanning in the cavity opening

and, since the cavity used by White was square, the length of the cavity alone was sufficient to define the mass of the fluid within the cavity. However, the characteristic times as calculated from Equation 6-1, do not reflect the influence of the approaching boundary layer or the influence of a variable mixing length.

Tests described in Section 5.7 have clearly indicated that the flow field external to the cavity has a controlling influence on the ability of a cavity to resonate. In particular, the flow within the approaching boundary layer has a decisive effect on the nature and occurrence of acoustic resonance. The driving mechanism for acoustic resonance is evidently located in the vicinity of the cavity opening, inasmuch as parameters which affect acoustic resonance, such as mixing length and approaching boundary layer thickness, are parameters which influence the flow field near the cavity opening. Consequently, any theory for the prediction of acoustic resonance should incorporate these parameters.

As is indicated by Table 6-1, the characteristic pumping times calculated from Equation 6-10 are much too large to be related to the acoustic periods recorded during the present investigation. This circumstance arises because the entire mass of fluid within the cavity has been used to establish the characteristic pumping time. In view of the fact that the driving mechanism for resonance appears to be an oscillation of the shear layer in the cavity opening, it would be more representative of acoustic

resonance to define the mass which must be pumped into and out of the cavity in order to sustain resonance in terms of the dimensions of the cavity opening. Thus, a "characteristic mass" might be defined which is contained within a volume setting in the cavity opening. The volume containing the characteristic mass would then be defined by the planform area of the cavity opening and a third dimension which must necessarily be oriented at right angles to the freestream. A characteristic mass defined in this manner would be somewhat analogous to the "mass slug" used in the calculation of the natural frequency of a Helmholtz resonator (24). The geometry and location of the characteristic mass with respect to the volume of the cavity are shown in Figure 6-1. The characteristic pumping time for this concept of cavity flow would be the time required for the characteristic mass to be pumped out of the cavity by the shear layer.

$$t_c = \frac{\text{characteristic mass}}{W_s} \quad \text{Eq 6-11}$$

In order to specify a unique value for the third dimension of the volume for the characteristic mass, it would be desirable to incorporate a quantity which is in itself descriptive of the approaching boundary layer, thereby integrating some property of the approaching boundary layer into a prediction technique for the occurrence of acoustic resonance. Analysis of the resonant conditions has shown that if the momentum thickness of the approaching boundary layer (Figure 5-10) is used to define the

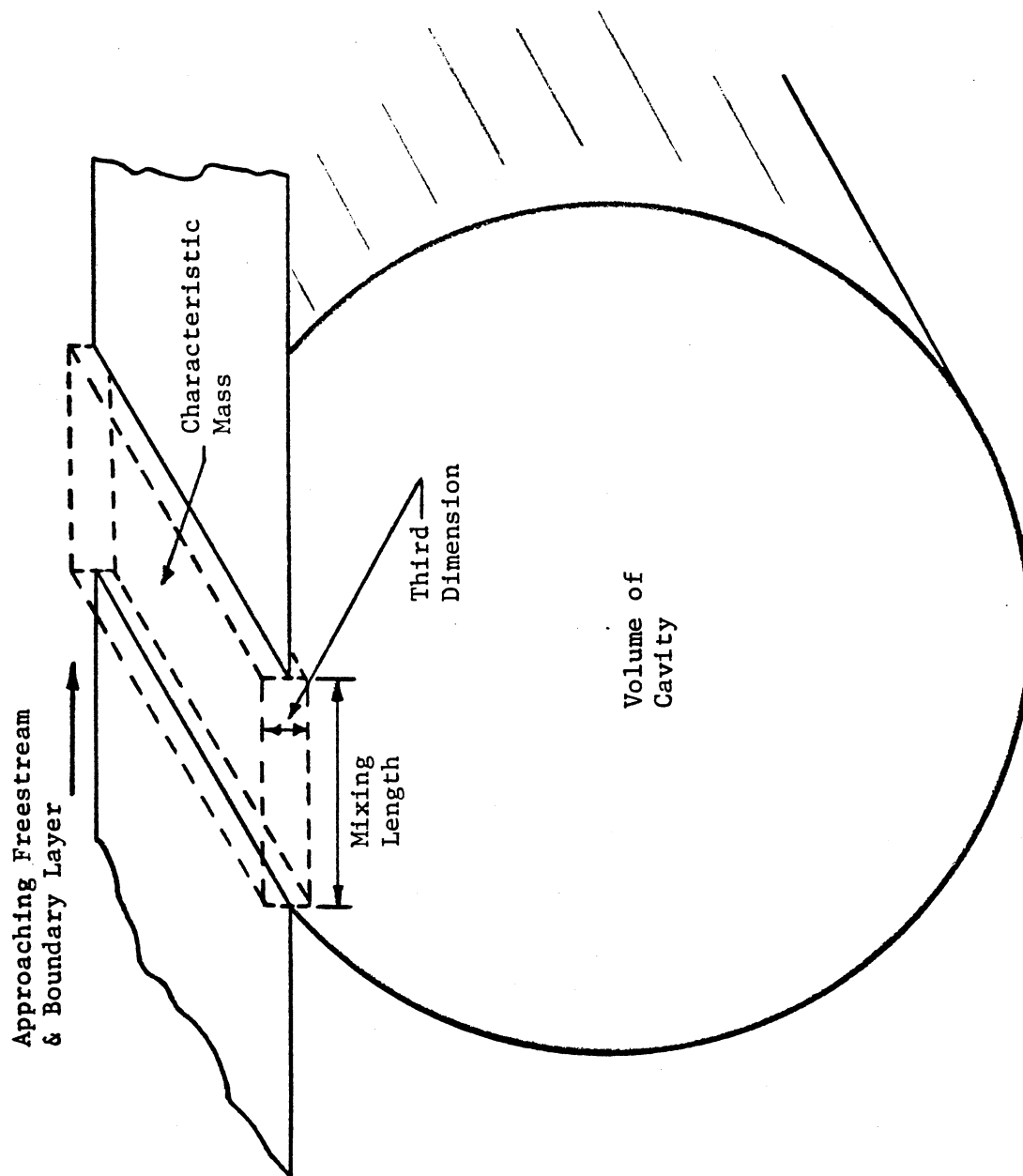


Figure 6-1. Relative size and position of the characteristic mass with respect to the cavity volume.



third dimension for the volume containing the characteristic mass, then characteristic times on the order of the acoustic periods recorded during resonance are obtained. Thus defined, the characteristic mass in terms of pounds per unit width is then expressed as

$$\text{characteristic mass} = \rho \cdot X \cdot \theta \quad \text{Eq 6-12}$$

and Equation 6-10 becomes

$$t_c = \frac{\rho \theta}{I_{lj} U} \quad \text{Eq 6-13}$$

Thus, longer characteristic times for thicker boundary layers are indicated by Equation 6-13, which is in agreement with the influence of the approaching boundary layer as discussed in Section 5.4. However, characteristic times predicted from Equation 6-13 are not entirely representative of the periods of the resonant acoustic fields induced in cavities because the influence of the mixing length is not included in this formulation for  $t_c$ . Experiment has shown that more than a single mode of resonance can be sustained by the same freestream flow field by merely changing the length of the cavity opening. Since mixing length cancels out of Equation 6-11, the influence of mixing length on acoustic resonance is not reflected in the above interpretation of the characteristic time.

Whereas the three-parameter prediction technique just outlined is a significant advance over White's two-parameter technique, ideally a prediction technique for resonance should show the effect

of the four parameters which are known to strongly influence the nature and occurrence of acoustic resonance. These parameters are the freestream velocity, the thickness of the approaching freestream boundary layer, the cavity mixing length, and the characteristic dimensions of the cavity (the cavity diameter for the present investigation). The internal dimensions of the cavity have been shown to define a number of normal resonant frequencies for the cavity which may be excited by certain external flow fields. Whether or not acoustic resonance is induced in the cavity and the mode of resonance excited is determined by the nature of the external flow field. Specifically, the parameters which influence the exciting of a given mode are the freestream velocity, approaching boundary layer thickness, and the mixing length. The manner in which these three parameters are interrelated for a given flow field determines whether one of the resonant modes of the cavity can be excited.

While a great deal of information concerning the parameters that influence acoustic resonance has been obtained in this investigation, the exact nature of their interrelationship with regard to the occurrence of resonance is not completely clear. Consequently, a highly refined prediction technique is not presented in this writing.

### 6.3 Use of Approaching Boundary Layer to Control Acoustic Resonance

Although no accurate prediction technique can be put forward, some general trends of the effects of the aforementioned parameters

on acoustic resonance have been identified and any subsequent use of these parameters to either enhance or suppress resonance may be guided accordingly. It is quite clear that a thick approaching boundary layer suppresses resonance. This is particularly evident in Figure 5-18 which shows the effect of the thickness of the approaching boundary layer on the acoustic intensity as calculated for some peak resonant conditions. It is noted that a substantial drop in acoustic intensity can be effected by a slight increase in the thickness of a thin boundary layer. This sensitivity of the magnitude of acoustic resonance to an increase in the thickness of thin boundary layers apparently exists because of the following circumstances. When the boundary layer is thin, the high speed flow in the outer portion of the boundary layer is readily ducted into the cavity supplying relatively larger amounts of momentum to drive the cavity during resonance. As the boundary layer thickens the fluid ducted into the cavity will have less momentum. Consequently, the intensity of resonance is suppressed which, in turn, leads to a less pronounced oscillation of the shear layer. Thus, a slight increase in the thickness of the approaching boundary layer can lead to potentially large drops in the momentum transfer between a resonating cavity and the freestream.

It has also been noted that the presence of flow disturbances in the freestream suppress resonance. As mentioned in Section 5-7, the presence of flow disturbances of arbitrary frequency within the

freestream flow field evidently disrupt the timing between the shear layer oscillation and the acoustic wave within the cavity.

Accordingly, effective means of controlling resonance might be to control the nature of the approaching boundary layer or to control the nature of the flow field over the cavity. Rossiter's (15) use of a baffle to disturb the flow upstream of the cavity essentially satisfied both of these criteria for suppressing resonance. The baffle thickened the boundary layer, thereby decreasing momentum transfer between the cavity and the freestream, and also it induced large scale perturbations in the flow field over the cavity which negated the occurrence of resonance. Preferably such a baffle should be placed within the approaching boundary layer in order to provide maximum disruption of the flow over the cavity and minimize any subsequent momentum losses to the freestream.

It has been noted in the present investigation (Section 5.4) that appreciable amounts of energy can be dissipated in the form of acoustic energy during resonance. McGregor's (11) work has shown that the drag of cavities is increased with the onset of acoustic resonance. Thus, acoustic resonance in cavities placed within aerodynamic surfaces is certainly to be avoided. For that matter cavities should be prevented from resonating in any flow field where the momentum of the freestream is to be preserved. It is suggested that acoustic resonance in cavities can be controlled if not completely eliminated by affixing a baffle in the boundary

layer upstream of the cavity. An investigation should be made to determine if the inherent momentum losses to the freestream caused by the baffle are greater than the momentum losses due to cavity resonance.

## CHAPTER VII

### CONCLUSIONS AND RECOMMENDATIONS

#### 7.1 Conclusions

Based on the results of the experimental investigations as discussed in Chapters V and VI, the following conclusions relating to flow induced acoustic resonance in cavities may be made:

1) The wavelength of the resonant acoustic field is determined by the internal dimensions of the cavity. The wavelength is generally more dependent on the streamwise dimension of the cavity in that the acoustic pressure wave tends to stand along the streamwise diameter of the cavity during a number of resonant conditions. The resonant response of the cavity may be broadly classified into modes of resonance based on the ratio of the wavelength of the resonant acoustic field to the cavity diameter. The most prevalent resonant conditions are grouped into the Helmholtz mode, the half-wave mode, and the full-wave mode.

2) The approaching boundary layer has a regulating influence on the intensity and occurrence of acoustic resonance. Thicker boundary layers tend to suppress the intensity of resonance, as well as to inhibit its occurrence.

3) The occurrence of acoustic resonance is not critically dependent on the nature of the flow field within the cavity.

4) Certain regular velocity perturbations in the flow field external to the cavity tend to prevent the occurrence of resonance.

5) Acoustic resonance is sustained by a feedback coupling between the acoustic pressure wave within the cavity and an oscillation of the shear layer spanning the cavity opening which, in the final analysis, is the mechanism by which energy is obtained from the freestream for the sustenance of resonance.

6) The oscillation of the shear layer due to acoustic resonance causes the momentum transfer and mass flow rates between a cavity and the freestream to be increased over steady-state values, which result solely from fluid entrainment.

7) White's prediction technique for the occurrence of acoustic resonance is based on a characteristic time for entrainment of the entire mass of fluid within the cavity and is evidently not directly related to the basic nature of the acoustic resonance studied in the present investigation. However, White's theory may be valid for higher Mach numbers.

8) Acoustic resonance in cavities induced by lower velocity freestreams is strongly influenced by the freestream velocity, the nature of the approaching boundary layer, the length of the mixing region, and the internal dimensions of the cavity. Accordingly, any prediction technique for the occurrence of acoustic resonance in cavities should reflect the influence of these four parameters.

## 7.2 Recommendations

The current experimental investigations have also uncovered some areas where future work related to flow induced acoustic resonance might be of benefit:

1) A rigorous mathematical analysis of the normal resonant modes of cavities would lead to more exact determination of the frequencies at which cavities may be expected to resonate. Such an analysis, which builds heavily on classical acoustics (13), has been carried out by Plumbee (19) for rectangular cavities. Future related analyses might consider cavities of different geometries such as the cylindrical cavity of variable closure used in the present investigation. Relatedly, provisions could be made in future experimental investigations to detect and describe three-dimensional acoustic waves induced within cavities.

2) An experimental investigation to determine the magnitude of the shear layer oscillation and its relation to the intensity of acoustic resonance, as outlined in Section 5.5, could lead to a mathematical model to predict momentum transfer and mass flow rates between a resonating cavity and the freestream.

3) Further study to determine the influence of the mixing length on acoustic resonance in cavities may furnish sufficient insight to allow the inclusion of the mixing length as a parameter in a prediction technique for resonance.

4) A study to determine the optimum size, geometry, and orientation of baffles used for the purpose of preventing acoustic resonance in cavities could yield valuable design information.



## BIBLIOGRAPHY

1. Krishnamurty, K., "Acoustic Radiation from Two-Dimensional Rectangular Cutouts in Aerodynamic Surfaces", NACA-TN 3487, 1955.
2. Krishnamurty, K., "Sound Radiation from Surface Cutouts in High Speed Flow", Ph.D. Thesis, California Institute of Technology, 1956.
3. Miles, J. B., "Stanton Number for Turbulent Flow Past Relatively Deep Cavities", Ph.D. Thesis, Department of Mechanical and Industrial Engineering, University of Illinois, 1963.
4. Bales, E. L., "On Heat Transfer Within and Across Nearly Circular Cavities Including the Effects of Variable Wall Temperature and Mass Bleed", Ph.D. Thesis, Department of Mechanical and Industrial Engineering, University of Illinois, 1967.
5. Roshko, A., "Some Measurements of Flow in a Rectangular Cutout", NACA-TN 3488, 1955.
6. Charwat, A. F., Roos, J. N., Dewey, F. C., and Hitz, J. A., "An Investigation of Separated Flows - Part I: The Pressure Field", Journal of the Aerospace Sciences, Vol. 28, No. 6, June 1961.
7. Charwat, A. F., Roos, J. N., Dewey, F. C., and Hitz, J. A., "An Investigation of Separated Flows - Part II: Flow in the Cavity and Heat Transfer", Journal of the Aerospace Sciences, Vol. 28, No. 6, July 1961.
8. Fox, J., "Flow Regimes in Transverse Rectangular Cavities", Proceedings of the 1965 Heat Transfer and Fluid Mechanics Institute, University of California Los Angeles, June 1965.
9. Burggraf, O. R., "A Model of Steady Separated Flow in Rectangular Cavities at High Reynolds Number", Proceedings of the 1965 Heat Transfer and Fluid Mechanics Institute, University of California Los Angeles, June 1965.
10. Korst, H. H., "A Theory for Base Pressures in Transonic and Supersonic Flow", Journal of Applied Mechanics, ASME, Vol. 23, 1956.

11. McGregor, O. W., "Aerodynamic Drag of Two-Dimensional Rectangular Notches in Transonic and Supersonic Turbulent Flow (With Emphasis on the Effects of Self-Induced Pressure Oscillations)", Ph.D. Thesis, Department of Mechanical and Industrial Engineering, University of Illinois, 1969.
12. Torda, T. P. and Patel, B. R., "Investigations of Flow in Triangular Cavities", AIAA Journal, Vol. 7, No. 12, December 1969.
13. Morse, P. M. and Ingard, K. U., "Theoretical Acoustics", McGraw-Hill Book Company, 1968.
14. Chanaud, R. C., "Aerodynamic Whistles", Scientific American, January 1970.
15. Rossiter, J. E., "Wind Tunnel Experiments on the Flow Over Rectangular Cavities at Subsonic and Transonic Speeds", RAE Tech. Report No. 64037, Oct. 1964.
16. Brown, G. B., "The Vortex Motion Causing Edge Tones", Proc. Phys. Soc., Vol. 49, 1937.
17. Spee, B. M., "Wind Tunnel Experiments on Unsteady Cavity Flow at High Subsonic Speeds", AGARD Proceedings No. 4, Separated Flows - Part II, Paris, France, May 1966.
18. Nyborg, W. L., "Self-Maintained Oscillations of the Jet in a Jet-Edge System", Acoustical Society of America, Vol. 26, No. 2, 1954.
19. Plumbee, H. E., Gibson, J. S., and Lassiter, L. W., "A Theoretical and Experimental Investigation of the Acoustic Response of Cavities in an Aerodynamic Flow", WADD TR-61-75, March 1962.
20. White, R. A. and McGregor, O. W. "Dynamics of Resonant Two-Dimensional Cavities in Aerodynamic Surfaces at Transonic and Supersonic Mach Numbers", Proceedings, Tenth Midwestern Mechanics Conference, Fort Collins, Colorado, August 1967.
21. Ithrig, H. K. and Korst, H. H., "Quasi-Steady Aspects of the Adjustments of Separated Flow Regions to Transient External Flows", AIAA Journal, Vol. 1, No. 4, 1963.

22. Addy, A. L. and Chow, W. L., "On the Starting Characteristics of Supersonic Ejector Systems", Journal of Basic Engineering, ASME, Vol. 86, No. 2, 1964.
23. Ingard, K. U., "On the Theory and Design of Acoustic Resonators", Acoustical Society of America, Vol. 25, 1953.
24. Randall, R. H., "An Introduction to Acoustics", Addison-Wesley Press, Inc., 1951.
25. Schlichting, H., "Boundary Layer Theory", McGraw-Hill Book Company, Sixth Edition, page 131, 1968.
26. Roshko, A., "On the Development of Turbulent Wakes from Vortex Streets", NACA Report 1191, 1954.
27. Hinze, J. O., "Turbulence, An Introduction to Its Mechanism and Theory", McGraw-Hill Book Company, Chapter 2, 1959.
28. Peterson, P. G. and Gross, E. E., "Handbook of Noise Measurement", General Radio Company, Sixth Edition, 1967.
29. Jackson, T. W. and Purdy, K. R., "Resonant Pulsating Flow and Convective Heat Transfer", Journal of Heat Transfer, ASME, Vol. 87, No. 2, 1965.
30. Eastwood, I., Jackson, T. W., Oliver, C. C., and Purdy, K. R., "Heat Transfer Threshold Values for Resonant Acoustic Vibrations in a Horizontal Isothermal Tube", ARL 62-326, Office of Aerospace Research, USAF, Wright-Patterson AFB, Ohio, April 1962.
31. Korst, H. H. and Chow, W. L., "Compressible Non-Isoenergetic Two-Dimensional Turbulent ( $Pr_t = 1$ ) Jet Mixing at Constant Pressure, Auxiliary Integrals", ME Tech. Note 392-4, Engineering Experiment Station, University of Illinois, January 1959.

## VITA

George Houston Watson was born in Casey, Iowa on February 24, 1942. He was graduated from Nora Springs High School of Nora Springs, Iowa in 1960. He entered Iowa State University in 1960 and was graduated with the degree of Bachelor of Science in Aerospace Engineering in 1964. He worked as an associate engineer in the aerodynamics department of the McDonnell Aircraft Corporation, St. Louis, Missouri in 1964 and 1965. He entered the Graduate School of the University of Missouri, Columbia in September 1965 and received a Master of Science degree in Mechanical Engineering in 1967.

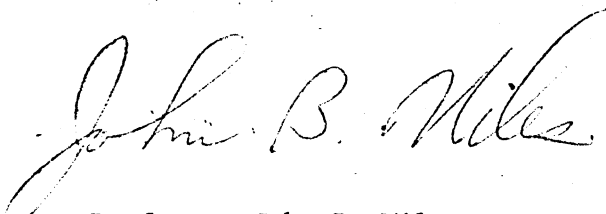
The undersigned, appointed by the Dean of the Graduate Faculty, have  
examined a thesis entitled

AN ANALYSIS OF FLOW INDUCED ACOUSTIC RESONANCE IN CAVITIES

presented by George H. Watson

a candidate for the degree of Doctor of Philosophy in  
Mechanical and Aerospace Engineering

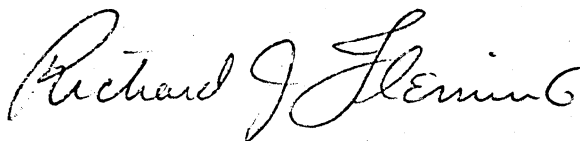
and hereby certify that in their opinion it is worthy of acceptance.



First Reader - Professor John B. Miles,  
Department of Mechanical and Aerospace Engineering



Second Reader - Professor John C. Lysen,  
Department of Mechanical and Aerospace Engineering



Digitization Information Page

Local identifier      Watson1970  
Source information

Format                Book  
Content type        Text  
Source ID            Gift copy from department; not added to MU Libraries'collection.  
Notes                Includes paste-in photographs

Capture information

Date captured        June 2023  
Scanner manufacturer Fujitsu  
Scanner model        fi-7460  
Scanning system software ScandAll Pro v. 2.1.5 Premium  
Optical resolution    600 dpi  
Color settings        8 bit grayscale  
File types            tiff  
Notes

Derivatives - Access copy

Compression        Tiff: LZW compression  
Editing software     Adobe Photoshop  
Resolution            600 dpi  
Color                 grayscale  
File types            pdf created from tiffs  
Notes                 Images cropped, straightened, brightened